1252

TRANSPORTATION RESEARCH RECORD

Design, Management, and Operation of Pavements

TRANSPORTATION RESEARCH BOARD
NATIONAL RESEARCH COUNCIL
WASHINGTON, D.C. 1989

Transportation Research Record 1252
Price: $9.00

mode
1 highway transportation

subject areas
24 pavement design and performance
25 structures design and performance
62 soil foundations
63 soil and rock mechanics
64 soil science

TRB Publications Staff
Director of Publications: Nancy A. Ackerman
Senior Editor: Edythe T. Crump
Associate Editors: Naomi C. Kassabian
Ruth S. Pitt
Alison G. Tobias
Production Editor: Kieran P. O'Leary
Graphics Coordinator: Karen L. White
Office Manager: Phyllis D. Barber
Production Assistant: Betty L. Hawkins

Printed in the United States of America

Library of Congress Cataloging-in-Publication Data
National Research Council. Transportation Research Board.

Design, management, and operation of pavements.
p. cm. — (Transportation research record, ISSN 0361-1981 ; 1252)
Includes bibliographical references.
ISBN 0-309-04973-3
1. Pavements—Design and construction. 2. Roads—Subgrades. 3. Soil freezing. 4. Soil moisture. I. National Research Council (U.S.). Transportation Research Board. II. Series.
TE7.H5 no. 1252
[TE251]
388 s—dc20
[625.7] 90-6179
CIP

Sponsorship of Transportation Research Record 1252

GROUP 2—DESIGN AND CONSTRUCTION OF TRANSPORTATION FACILITIES
Chairman: Raymond A. Forsyth, California Department of Transportation

Soil Mechanics Section
Chairman: Michael G. Katona, TRW

Committee on Subsurface Drainage
Chairman: Gary L. Hoffman, Pennsylvania Department of Transportation
Robin Bresley, George R. Cochran, Barry J. Dempsey, Gregory A. Dolson, Ervin L. Dukatz, Jr., Wilbur M. Haas, Donald J. Janssen, Larry Lockett, Donald C. Long, Robert H. Manz, Vernon J. Marks, Charles D. Mills, Lyle K. Moulton, Edwin C. Novak, Jr., Willard G. Puffer, Georges Raimbault, Hallas H. Ridgeway, Emile A. Samara, L. David Suits, William D. Trolinger, Walter C. Waidelich, David C. Wyant, Thomas F. Zimmie

Geology and Properties of Earth Materials Section
Chairman: C. William Lovell, Purdue University

Committee on Environmental Factors Except Frost
Chairman: Robert L. Lytton, Texas A&M University System
S. S. Bandy, Warren T. Bennett, Michael L. Bunting, Fu Hua Chen, Barry J. Dempsey, Donald G. Fohs, Donald J. Janssen, Badru M. Kiggundu, Amos Komornik, C. William Lovell, Said Ossama Mazen, R. Gordon McKeen, James B. Nevels, Jr., Zvi Ofer, Thomas M. Petry, Rogel H. Prysock, Albert C. Ruckman, Larry A. Scofield, Joe P. Sheffield, Malcolm L. Steinberg, Shiraz D. Tayabji, John L. Walkinshaw, William G. Weber, Jr., Gdalyah Wiseman

GROUP 5—INTERGROUP RESOURCES AND ISSUES
Chairman: William M. Spreitzer, General Motors

Committee on Low-Volume Roads
Chairman: Adrian Pelzner, Strategic Highway Research Program
Mathew J. Betz, Robert A. Cherveny, Santiago Corro Caballero, Earle F. Dobson, Ronald W. Eck, Martin C. Everitt, Asif Faiz, Jacob Greenstein, J. M. Hoover, Stuart W. Hudson, Kay H. Hymas, Lynne H. Irwin, John W. Kizer, Melvin B. Larsen, Ruth T. McWilliams, Thomas E. Mulinazzi, Andrzej S. Nowak, George B. Plikington II, Jean Reichert, Richard Robinson, Eldo W. Schornhorst, James Chris Schwarzhoff, Eugene L. Skok, Jr., Bob L. Smith, Walter J. Tennant, Jr., Alex T. Visser

G. P. Jayaprakash, Transportation Research Board staff

Sponsorship is indicated by a footnote at the end of each paper. The organizational units, officers, and members are as of December 31, 1988.

NOTICE: The Transportation Research Board does not endorse products or manufacturers. Trade and manufacturers' names appear in this Record because they are considered essential to its object.

Transportation Research Board publications are available by ordering directly from TRB. They may also be obtained on a regular basis through organizational or individual affiliation with TRB; affiliates or library subscribers are eligible for substantial discounts. For further information, write to the Transportation Research Board, National Research Council, 2101 Constitution Avenue, N.W., Washington, D.C. 20418.

Transportation Research Record 1252

Contents

Foreword

The five papers included in this Record are of interest to pavement, maintenance, and operations engineers.

Rutherford reports that reduction in the resilient modulus of the different layers of secondary roads, which is caused by the spring thaw, is responsible for increased deterioration and higher maintenance costs. Therefore, posting load restrictions during the thaw period benefits maintenance.

Barcomb reports on the use of thermistors to collect data. The data have justified the posting of restrictions on traffic over asphalt roadways during spring thaw periods in the Kootenai National Forest in Montana. According to the author, this approach has significantly reduced the cost of maintenance of these roads.

R. Alfelor and S. McNeil present a dynamic optimization approach for determining the optimum blading frequency for unpaved roads. The approach uses the principles of optimal control. They have formulated optimization equations for unpaved roads and have applied them to hypothetical cases.

An integrated model is being developed at Texas A&M University that can predict the effects of air temperature, sunshine percentage, wind speed, rainfall, frost, and thawing action on the performance of pavements. D. Chandra et al. present a computer model that accounts for temperature and moisture effects on granular base course materials. Liang and Lytton report on a computerized method which simulates rainfall patterns, the knowledge of which is needed for pavement analysis and design.

Pavement Response and Load Restrictions on Spring Thaw-Weakened Flexible Pavements

MARY S. RUTHERFORD

Agencies faced with maintenance of secondary roads in frost areas often choose to restrict vehicle or axle loads during spring thawing to minimize the detrimental effects of heavy loads on severely weakened pavements. Thirty-two summer pavement structures were defined to represent "typical" restricted pavements. Layered elastic analyses were performed for these pavements for different levels of reduction in resilient moduli at three different times during spring thawing, including (a) base thawing, (b) 4 in. of subgrade thawing, and (c) total thawing. Allowable loads for deflection, fatigue, and subgrade vertical strain were identified by comparing the spring thaw response to the summer response. It was found that many thin pavements [2 in. asphalt concrete (AC)] reached critical conditions by the time of base thaw, and asphalt tensile strain was the critical response parameter for the majority of these pavements in spring. Four-inch AC pavements did not experience strains or deflections in excess of those in summer until some subgrade thawing occurred; subgrade vertical strain was the critical parameter for these pavements. It was also found that deflections are not a reliable indicator of when critical conditions are realized in a thaw weakened pavement. Finally, a method of evaluating the relative benefits of applying various levels of spring load restrictions is presented.

During spring thawing the strength of the ground may be measurably weakened compared with its summer/fall state as a result of moisture migration into the soil during the preceding freezing period and, possibly, the development of excess hydrostatic pressure in base and subgrade materials as moisture is liberated during thawing.

Recognition of seasonal variation in material properties is necessary for realistic estimates of pavement performance. For primary road facilities it is necessary to minimize the detrimental effects of substantial thaw weakening because it is anticipated that these roads will perform at a high level of serviceability throughout the year under high traffic volumes. For many secondary roads with lower traffic volumes, however, it is not economically feasible to provide adequate frost protection throughout for spring thawing. Agencies faced with secondary road maintenance in frost areas often choose to restrict vehicle and/or axle loads during the critical period in the spring to reduce damage at this time.

Although the use of load restrictions is the only feasible pavement maintenance strategy for many secondary roads, restricting roadways is never a popular practice. As it is desirable to minimize load restrictions during periods of severe weakness, it is of some use to identify pavement response during the thawing period. The location of segments of roads to be restricted is generally selected on the basis of experience. Pavement sections where excessive rutting, fatigue failures, or extensive potholing have occurred in the past during spring thawing are likely to be candidates for restrictions.

Individuals who are responsible for restricting pavements during spring thawing have had very little information or guidelines available for selecting (a) the time to place spring load restrictions or (b) what magnitude of load restrictions would be beneficial without unduly restricting pavements (*1*). The purpose of this work was to identify guidelines in these two specific areas. Often pavements are not restricted until some visible fatigue cracking or potholing has occurred. This practice does not result in optimal use of load restrictions because some permanent damage has already resulted.

One of the first decisions made to perform the study was to select some criteria for evaluating allowable spring load levels. Some pavement design methods use deflection as a criterion for evaluating performance. Results from previous work on pavement response during spring thawing (*2–4*) suggested that tensile strain at the bottom of the asphalt concrete (AC) layer and/or maximum vertical strain at the top of the base or subgrade material reached high levels before the development of large deflections. This occurs when one or more weak layers are present between stiffer materials, which is the case when only a small amount of thawing has taken place. From these observations it was concluded that several pavement response parameters (deflection, δ; asphalt tensile strain, ε_t; and subgrade vertical strain, ε_{vs}) would be evaluated. Further, it was decided that comparisons would be made of these response parameters between a reference time in the summer and several times during spring thawing rather than use some absolute value of strain or deflection levels as criteria for the need for load restrictions. The summer reference time selected was when the asphalt concrete temperature was at 77°F and the unbound materials were performing optimally, with moderate moisture contents and saturation levels. This time was compared with three times during spring thawing when the greatest changes in resilient stiffness were occurring because of the movement of the thawing plane. Using this approach, the results obtained indicated the relative performance of the pavement sections analyzed at selected times during spring thawing and summer.

The analysis was performed by developing hypothetical pavement sections that represented typical pavements currently receiving load restrictions during spring thawing (*1*). Several different load configurations and load levels were

Department of Civil Engineering, Seattle University, Seattle, Wash. 98122.

applied to these pavements, and the pavement response was obtained from layered linear elastic analyses. The results obtained from the elastic analyses demonstrated how the hypothetical pavement cross sections responded with respect to deflection, asphalt tensile strain, and subgrade vertical strain. The pavement sections developed for the study were analyzed at three different times during thawing to evaluate (a) when pavement performance relative to summer was compromised and (b) how long the pavement was in a weakened condition.

The following questions are proposed to identify some of the issues to be addressed from the results of the analysis regarding the use of load restrictions and pavement response during spring thawing:

1. After thawing began, when were the pavement cross sections analyzed in a weakened condition relative to the summer reference condition?
2. To what extent was the load-carrying capacity of the weakened pavement compromised relative to summer?
3. How did pavement response change during the thawing period for the hypothetical pavements analyzed?
4. What response parameters resulted in the greatest reductions in allowable loads for the pavement cross sections analyzed?
5. How were deflections correlated with pavement weakening?
6. How did pavement response vary for different wheel and axle configurations during spring thawing?
7. Can we quantify the benefits of applying load restrictions on the pavements analyzed?
8. What can be concluded about "real" pavements from these results?

A description of the pavement cross sections and materials selected for the study, the analysis methods, and the results are presented next to provide some insights into these issues.

DESCRIPTION OF ANALYSIS

Hypothetical pavement cross sections were developed to represent, to the best extent possible, the types of road construction and subgrade materials existing in currently restricted pavements. Data obtained from a survey of pavement structures currently receiving spring load restrictions (*1*) were weighed heavily in the development of these sections. The data suggested that pavement cross sections on which load restrictions are currently being applied range as follows:

	Range	*Normal*
Asphalt surface, in.	1½–6	2–4
Aggregate base, in.	4–18	6–12

On the basis of this information 2- and 4-in. asphalt surface courses and 6 and 12 in. unbound aggregate base courses were selected for the cross sections for the analysis.

The predominant subgrade material present where load restrictions have reportedly been applied was clay. Silts, gravels, granular materials, and tills were also mentioned as subgrade types requiring restrictions in the survey of current practice (*1*). Because of this information, both fine and coarse subgrade materials were modeled in the analysis. The material properties required for the elastic analyses are the resilient modulus and Poisson's ratio. The resilient moduli selected to model fine subgrade materials for the summer reference condition were 8 and 12 ksi. The resilient moduli selected for coarse subgrade materials during summer were 15 and 25 ksi. These values were selected to represent low- to medium-range resilient stiffness properties of unbound fine and coarse materials. It was anticipated that unbound coarse and fine materials with low to average resilient stiffness properties would be the most likely candidates for significant reductions in resilient stiffness during spring thawing. Resilient modulus values for pavement subgrade materials compiled by Rada et al. (*5*) suggest that these values are reasonable. The values of Poisson's ratio assumed for the analysis were 0.45 and 0.40 for fine and coarse subgrades, respectively.

The hypothetical pavement sections were analyzed using ELSYM5, a layered elastic pavement analysis program developed at the University of California at Berkeley (*6*). The variation in pavement response during the spring thaw period was evaluated relative to the summer pavement response, as described earlier. Material properties for the layers in each pavement structure were selected to represent the behavior at three distinct times during the spring thaw period when the most significant changes in material properties were expected to occur. The times selected were the following: (a) when thawing reached the bottom of the base material, (b) when the thawing plane was 4 in. into the subgrade material, and (c) when thawing was complete. The total thickness of the frozen material was assumed to be 4 ft before the start of thawing.

The material properties for each pavement layer for the summer reference condition are given in Table 1. The resilient modulus (M_r) assumed for the asphalt concrete was 300 ksi. Two unbound base materials were included with assumed M_r values of 25 and 50 ksi. Four subgrade materials were assumed for the analyses with resilient moduli of 8, 12, 15, and 25 ksi in summer to represent a range of resilient response.

Tables 2 through 4 give the material properties for the three analysis times during spring thawing. The asphalt concrete resilient stiffness in spring was assumed to be 1,200 ksi. The change in resilient stiffness from summer to spring was based on a change in average temperature of the asphalt layer from 77°F in the summer to 40°F in spring (*7*). Base M_r values were reduced by 25 and 50 percent during early thawing and by 15 and 40 percent at total thaw (see Tables 2 to 4). The reduction in base course resilient stiffness from summer to spring assumed for the analysis was based on M_r values from nondestructive field evaluation of base course resilient stiffness (*5*) and laboratory results of the change in resilient behavior (S_r) for granular materials in dry ($S_r \leq 60$ percent) and wet ($S_r \geq 85$ percent) conditions (*8*).

Subgrade M_r values for fine-grained materials (8 and 12 ksi) were reduced by 75 and 90 percent relative to summer levels at early subgrade thawing and by 65 and 75 percent at total thaw. Coarse subgrade materials (15 ksi and 25 ksi) were reduced by 50 and 75 percent at early thaw and by 40 and 65 percent at total thaw. Many studies both in the laboratory and the field have been performed on the resilient response of frozen and thawed materials (*7*). The results have indicated that resilient stiffness may be reduced up to 99 percent depending on the material type, moisture content, saturation level, and other factors. The reductions in resilient stiffness

TABLE 1 PAVEMENT STRUCTURE MATERIAL PROPERTIES, SUMMER CASE

Layer	Material	Thickness (in)	Resilient Modulus (psi)
Surface	BST or ACP	2	300,000
	ACP	4	300,000
Base	Unbound	6	25,000; 50,000
	Unbound	12	25,000; 50,000
Subgrade	Fine-grained	<40	8,000; 12,000
	Coarse-grained	<40	15,000; 25,000
Bottom	Rigid	Infinite	100,000

TABLE 2 PAVEMENT STRUCTURE MATERIAL PROPERTIES, BASE THAW

Layer	Material	Thickness (in)	Resilient Modulus (psi)
Surface	BST or ACP	2	1,200,000
	ACP	4	1,200,000
Base	Unbound	6	50%, 75% summer
	Unbound	12	50%, 75% summer
Subgrade	Fine-grained	<40	50,000
	Coarse-grained	<40	50,000
Bottom	Rigid	Infinite	100,000

TABLE 3 PAVEMENT STRUCTURE MATERIAL PROPERTIES, 4 IN. SUBGRADE THAW

Layer	Material	Thickness (in)	Resilient Modulus (psi)
Surface	BST or ACP	2	1,200,000
	ACP	4	1,200,000
Base	Unbound	6	50%, 75% summer
	Unbound	12	50%, 75% summer
Subgrade	Fine-grained	4	10%, 25% summer
	Coarse-grained	4	25%, 50% summer
Subgrade	Frozen	<36	50,000
Bottom	Rigid	Infinite	100,000

TABLE 4 PAVEMENT STRUCTURE MATERIAL PROPERTIES, TOTAL THAW

Layer	Material	Thickness (in)	Resilient Modulus (psi)
Surface	BST or ACP	2	1,200,000
	ACP	4	1,200,000
Base	Unbound	6	60%, 85% summer
	Unbound	12	60%, 85% summer
Subgrade	Fine-grained	<40	25%, 35% summer
	Coarse-grained	<40	35%, 60% summer
Bottom	Rigid	Infinite	100,000

assumed for the study were selected to represent a range of resilient behavior for coarse and fine material types.

When an elastic analysis is performed on a pavement system with a stiff base course over a weak subgrade, tensile stresses may be obtained within the unbound base material. Such results are considered to be unrealistic in view of the lack of ability of unbound materials to sustain tensile stresses. Therefore, a limit on the ratio of base M_r to subgrade M_r of 4 was imposed, based on the work of Klomp and Dorman (*9*), to avoid developing unrealistic stress distributions in these materials.

The ELSYM5 program used for the analyses incorporates linear elastic material behavior. It has been demonstrated that resilient behavior of the layers within pavement systems is typically not linear. Stress-dependent resilient properties have been used to model response more accurately. Because hypothetical pavements were developed for this analysis, it was felt that it would be sufficient to identify resilient moduli and relative values of these moduli at the different analysis times in spring and summer. Adding more complexity to the analysis by introducing nonlinear behavior would not necessarily have resulted in improved results, given the nature of this analysis.

Three primary response variables used to evaluate flexible pavement performance are deflection, δ, maximum asphalt tensile strain, ε_t, and maximum subgrade vertical strain, ε_{vs}. These parameters were selected to observe the response through the spring thaw period. In addition, estimates of remaining life for fatigue using the equation developed by Finn et al. (*10*) and estimates of rut life using the Shell equation (*11*) were obtained. This was done (a) to assess the impact of spring thaw weakening on long-term pavement performance and (b) to compare the performance of different pavement structures.

The standard load used in the analysis was a single tire, single axle load of 20,000 lb. In addition, dual tire, single axle loads of 20,000 lb and dual tire, tandem axle loads of 34,000 lb were analyzed. Surface deflections and subgrade vertical strain were obtained for 20 percent and 100 percent of the total load for each load configuration for each hypothetical pavement cross section to develop load-deflection and load-strain relationships at each analysis time in the spring. The deflection and strain from the summer reference condition were then compared with the spring load-deflection or load-strain response at each analysis time in spring. Using this procedure the spring pavement response was identified in terms of the allowable spring load, which was the load that corresponded to the summer deflection or strain parameter level. The critical parameter at each analysis time in the spring was the response parameter that resulted in the greatest reduction in allowable load. This is shown schematically in Figure 1.

Asphalt tensile strain has been used as a pavement response parameter since it has been correlated with asphalt concrete fatigue failures in both the laboratory and field (*10*). In addition to obtaining primary response parameters (strains and deflections), estimates of remaining life for the hypothetical pavement cross sections were made to compare the pavement performance in summer and spring as well as that of different pavement sections. The equation for remaining fatigue life

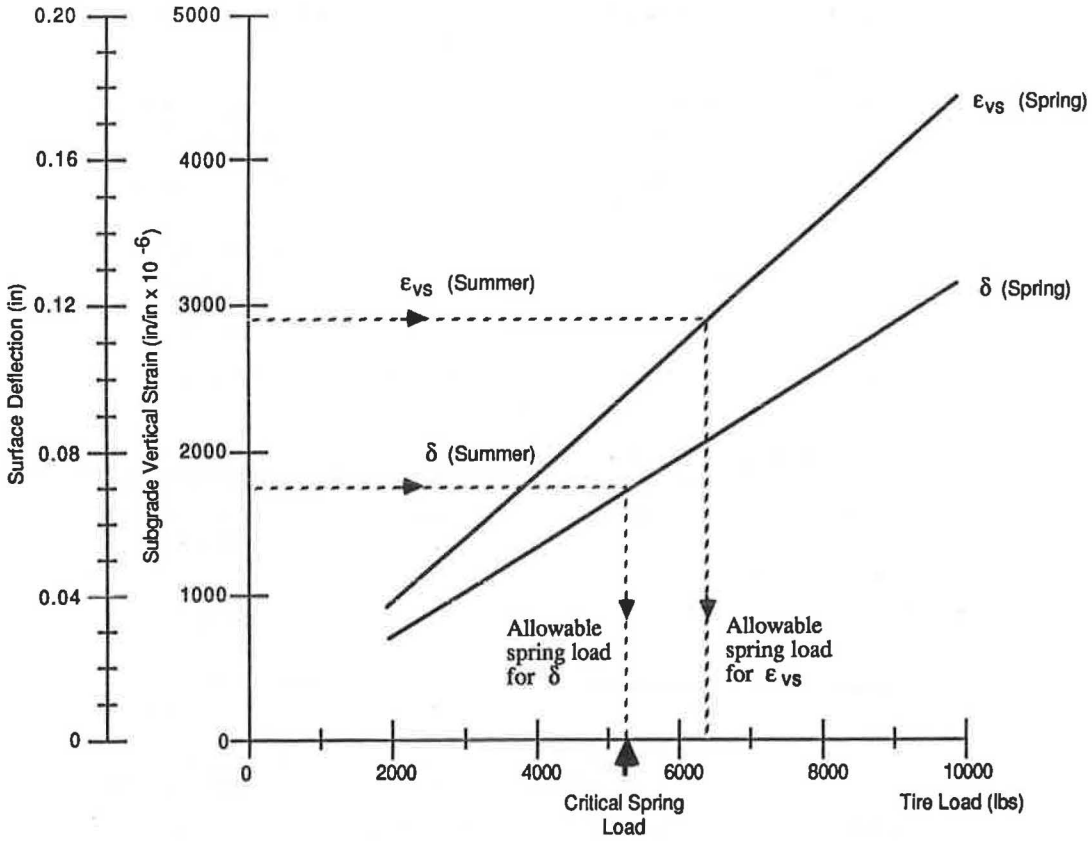

FIGURE 1 Selection of allowable spring load levels for deflection and subgrade vertical strain.

used for this study, developed by Finn et al. (*10*), is the following:

$$\log N_f = 15.947 - 3.291 \log (\varepsilon_t/10^{-6}) - 0.854 \log (E^*/10^3)$$

where

N_f = the number of load applications of constant stress to cause the initiation of fatigue cracking,
ε_t = the initial tensile strain for the applied stress, and
E^* = the complex modulus, in psi.

The form of this equation indicates that fatigue is a function of resilient stiffness (M_r) and maximum asphalt tensile strain, ε_t. In this analysis the asphalt concrete resilient modulus varied in spring and summer because of the variation in average pavement temperature at these times. Because asphalt tensile strain response was obtained to predict fatigue, it seemed more defensible to compare fatigue life in spring and summer than asphalt tensile strain directly. Therefore, allowable loads for asphalt tensile strain were actually based on fatigue life computed using the Finn equation with AC M_r values of 300 and 1200 ksi for summer and spring, respectively, as follows:

$$\log \frac{\varepsilon_{t\,su}}{\varepsilon_{t\,sp}} = \frac{0.854}{3.291} \left(\log \frac{M_{r\,sp}}{M_{r\,su}} \right)$$

The relationship of spring and summer fatigue life and asphalt tensile strain is shown in Figure 2.

RESULTS

The results described in this section are for a single tire, single axle loading. Results for other load configurations assumed for the analyses are presented later.

The results suggested that the 2-in. thick and 4-in. thick pavements modeled responded quite differently when spring and summer responses were compared. The majority of 2-in. pavements developed asphalt tensile strains that resulted in significant reductions in fatigue life by the time thawing had reached the bottom of the base course. Allowable loads were reduced up to 89 percent for all 2-in.-thick pavements, with an average reduction of 50 percent. The greatest load reductions were obtained for the pavements modeled with base materials with summer M_r values of 50 ksi (the stronger base material used for the study).

When thawing proceeded into the subgrade, asphalt tensile strains in all 2-in. AC pavements increased further. The average allowable spring load for asphalt tensile strain at this time was 47 percent of the maximum load, with allowable loads ranging from 0 to 84 percent for fatigue. Asphalt tensile strain was the critical parameter for the majority of the 2-in. pavements modeled for the study at early subgrade thawing. However, thin pavements (2 in. AC) with summer base M_r values of 25 ksi that were modeled with reductions in subgrade modulus of 75 to 90 percent at early subgrade thawing resulted in the greatest reductions in allowable loads from increases in subgrade vertical strain rather than asphalt tensile strain and fatigue.

At total thaw, AC tensile strain was the critical parameter for 42 of the 48 thin pavements analyzed. At this time, asphalt tensile strain and fatigue life were relatively unchanged compared with early subgrade thawing, whereas subgrade vertical strains decreased an average of 19 percent for these pavements. The change in allowable loads during the spring thaw period obtained from the analyses for deflection, asphalt tensile strain, and subgrade vertical strain for one of the 2-in. pavement cases is shown in Figure 3.

By comparison, the 4-in.-thick pavements modeled did not develop strains or deflections resulting in a reduction in allow-

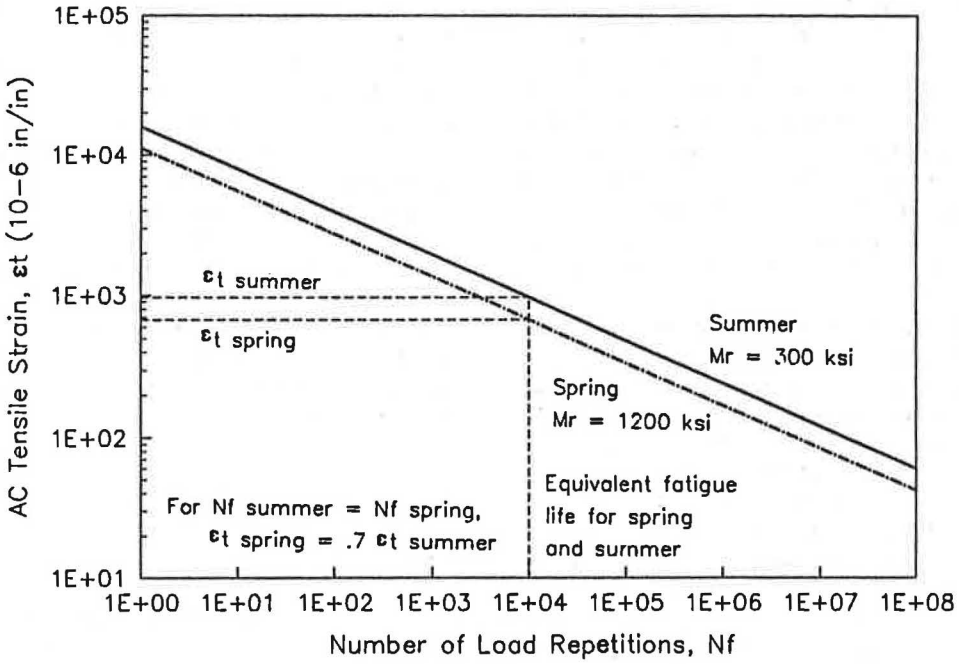

FIGURE 2 Comparison of spring and summer fatigue life using the fatigue model by Finn et al. (*10*).

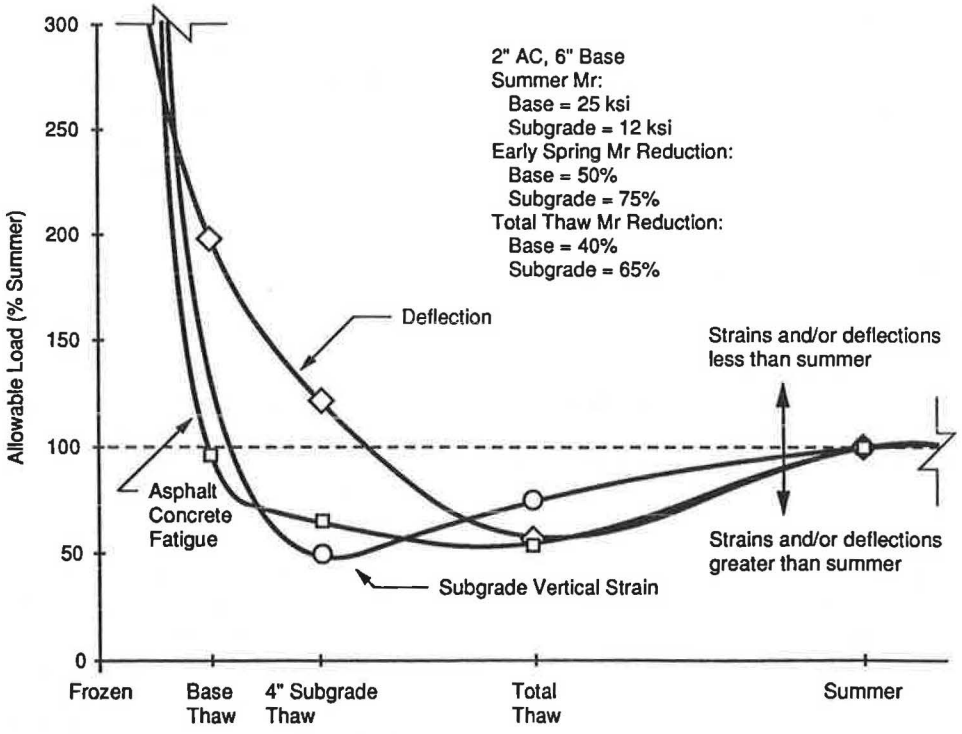

FIGURE 3 Allowable load versus time for a 2-in. asphalt concrete pavement.

able loads when thawing reached the bottom of the base material. It was not until some thawing of the subgrade material occurred that strains in excess of the summer levels were obtained. Not all of the 4-in.-thick pavements resulted in increased strains at this time. Those that did, however, resulted in the greatest calculated reductions in load-carrying capacity as a result of increased subgrade vertical strain leading to rut development. Allowable spring loads obtained at 4 in. of subgrade thawing ranged from 29 to 100 percent.

At the time of total thawing all 4-in.-thick pavements experienced a reduction in maximum subgrade vertical strain relative to the time of early subgrade thawing. This reduction ranged from 9 to 49 percent for the pavements that required some load reductions, with an average decrease in subgrade vertical strain of 25 percent since early subgrade thawing. The change in pavement response during spring thawing expressed in allowable load for one of the 4-in. pavements analyzed is shown in Figure 4. The results for allowable loads for all pavements modeled for the three analysis times in spring can be found elsewhere (*7*).

Many agencies have deflection testing capabilities that may be used for identifying the critical spring thaw period. It was found that, with the exception of the most severely weakened pavements, reductions in load-carrying capacity occurred before the time that deflections reached or exceeded summer levels. Figure 5 shows the deflection at the time of base thaw versus the allowable load for fatigue for all 2-in. pavements modeled. Deflections for 2-in.-thick pavements with accelerated fatigue consumption at base thaw (load reductions up to 89 percent were required for these pavements) ranged from 37 to 100 percent of summer deflection levels.

When thawing had advanced 4 in. into the subgrade, 2-in. pavements that experienced some reduction in load-carrying capacity due to fatigue or subgrade vertical strain (calculated load reductions up to 100 percent were obtained) had deflections that ranged from 66 to 279 percent of summer deflection levels, with the majority of these pavements resulting in deflections that were still less than in summer. Similar findings were reported by Stubstad and Connor (*2*) on actual pavements in Alaska and in Minnesota (*4*). These results were based on deflection measurements obtained during thawing using the Falling Weight Deflectometer (FWD).

The earliest time that calculated spring response for 4-in. pavements resulted in the need for load reductions due to deflection was at 4 in. of subgrade thawing. Deflections at this time for the 4-in. pavements that needed some level of load reductions because of fatigue or subgrade vertical strain ranged from 55 to 144 percent of summer levels.

As a result of the accumulation of strain in the weakened unbound materials with time in spring, all pavements resulted in calculated deflections equal to or greater than summer levels at total thaw in this analysis. For 4-in. AC pavements where subgrade vertical strain produced the greatest reduction in allowable load, a relationship between the allowable load needed to maintain subgrade vertical strains at their summer levels and deflection was obtained from a linear regression of the data from the analyses at total thaw. The relationship is the following:

$$P_{\varepsilon_{vs}} = 0.17 + 0.90\,(\delta_{summer}/\delta_{total\ thaw})$$

where

$P_{\varepsilon_{vs}}$ = the allowable load for subgrade vertical strain,
δ_{summer} = the deflection for the summer reference condition,
$\delta_{total\ thaw}$ = the deflection at total thaw.

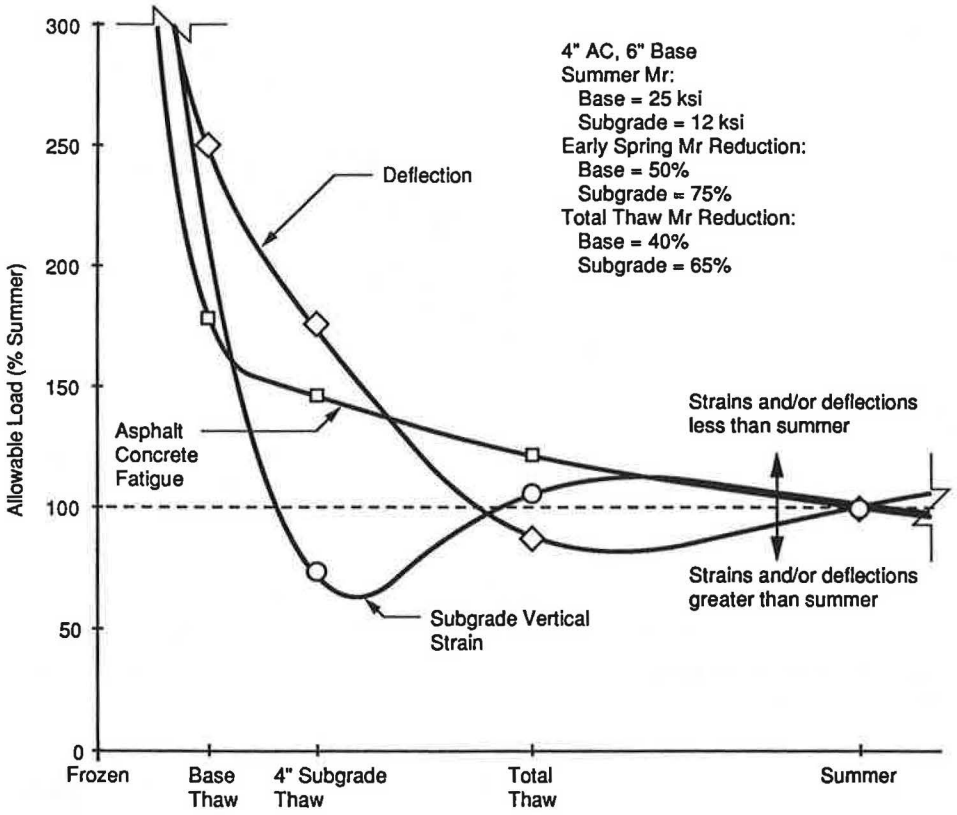

FIGURE 4 Allowable load versus time for a 4-in. asphalt concrete pavement.

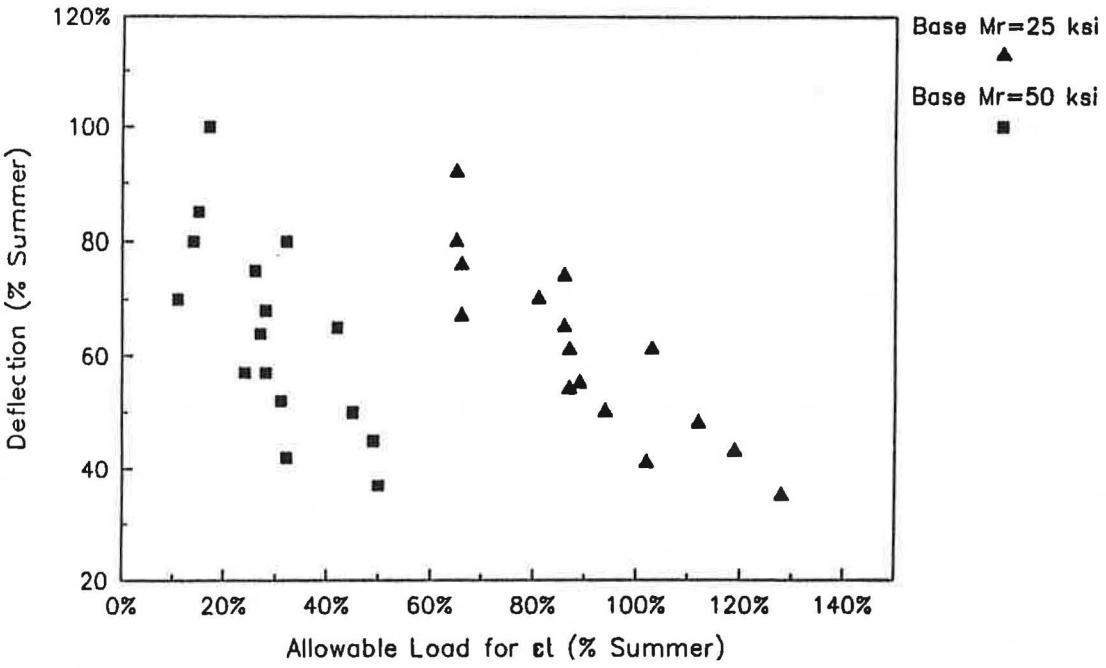

FIGURE 5 Deflection versus allowable load for asphalt tensile strain at base thaw, 2-in. AC.

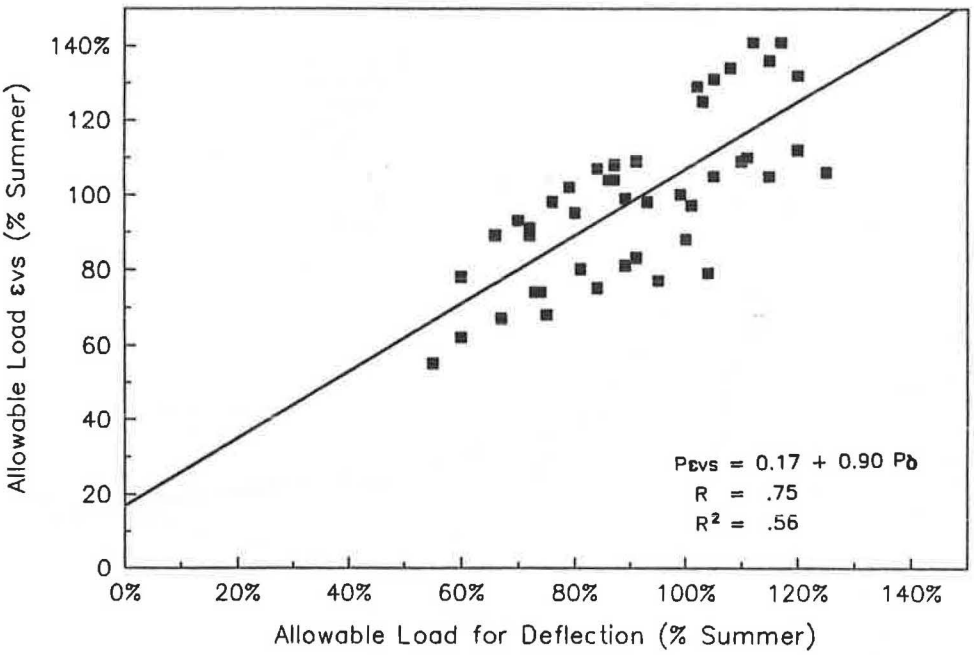

FIGURE 6 Allowable load for subgrade vertical strain versus allowable load for deflection at total thaw, 4-in. AC.

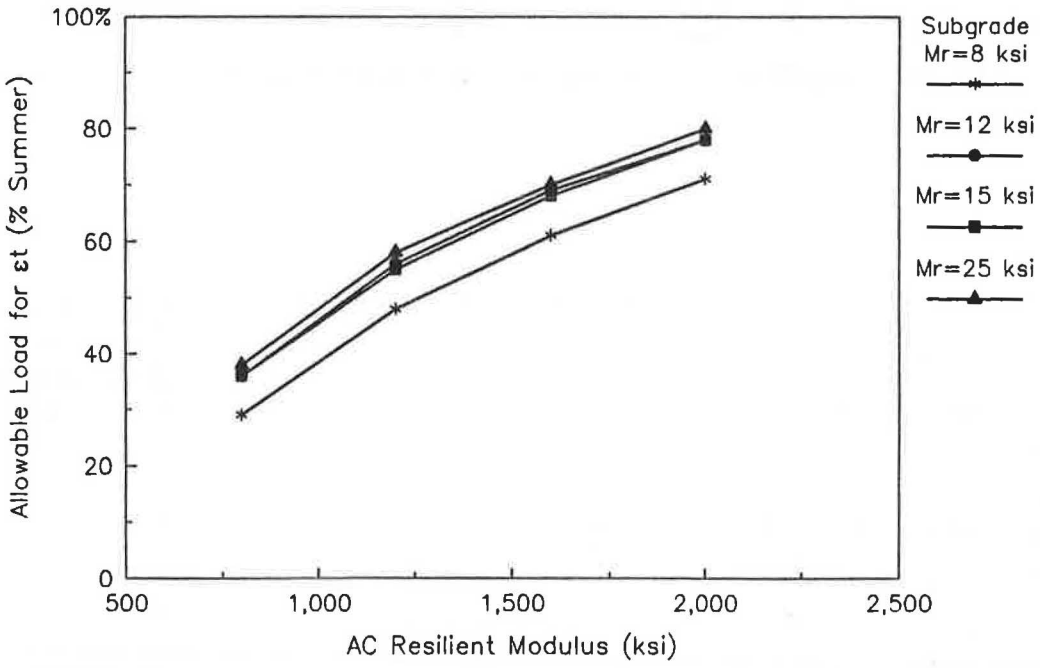

FIGURE 7 Allowable load for asphalt tensile strain versus spring AC M_r at total thaw.

The data points for the 4-in. pavements and the relationship obtained are shown in Figure 6. By comparison, the 2-in. pavements modeled resulted in the greatest calculated reductions in allowable loads at total thaw because of continued accelerated fatigue consumption. No useful correlation of allowable loads for fatigue and deflection at total thaw was found from the calculated response obtained for the 2-in. pavements.

Only one value of asphalt resilient modulus was assumed for the surface layer in the analysis. Because asphalt tensile strain was the critical parameter for thin pavements, the sensitivity of asphalt tensile strain to AC M_r was considered. A 2-in. pavement with a 6-in. base layer was selected as a reference case to consider the sensitivity of the results for different AC M_r values. The reduction in base resilient modulus assumed for the reference case was 50 and 40 percent for early and late thawing, respectively. The corresponding reduction in subgrade resilient modulus assumed was 75 and 65 percent. Summer AC M_r values selected for the sensitivity analysis ranged from 200 to 500 ksi. The corresponding spring M_r

values were four times the summer M_r values, as in the preceding portion of the analysis. The variation in allowable load for fatigue at total thaw (which was the critical parameter for these pavements) versus AC M_r is shown in Figure 7. A 42 percent variation in allowable load for fatigue resulted for the range of AC M_r investigated for the different subgrade cases. The effect of the variation in AC M_r on allowable loads for deflection and subgrade vertical strain was substantially less. The maximum variation in allowable spring loads for deflection and maximum subgrade vertical strain was 9 and 17 percent, respectively.

MULTIPLE LOAD CONFIGURATIONS

Heavy vehicles typically are configured with both single and tandem axles. Single axles are typically found on the steering axle on Class 8 heavy vehicles, and tandem axles often support the drive axle and the payload portion of the vehicle. In light of this, both axle configurations were included in the analysis.

The analyses for dual tires on single axles and dual tires on tandem axles were performed when thawing had proceeded 4 in. into the subgrade, because this was when allowable loads reached critical levels for all hypothetical pavements that required some load reductions for the single tire, single axle load case. It was found that for dual tire load configurations subgrade vertical strain was always the parameter that resulted in the greatest reduction in allowable load at this time. In the case of the single tire loads discussed previously, fatigue life (and asphalt tensile strain) was the critical parameter for the majority of 2-in. AC pavements.

Allowable loads for dual tire, single axle and dual tire, tandem axle loads were very close to the allowable loads for the same pavement structures loaded with single tire, single axle loads. The difference in allowable loads for the three load cases for a given pavement structure ranged from 0 to 11 percent. It was also found that the maximum subgrade vertical strain and maximum deflections for both dual tire cases always occurred between the tires during spring.

A comparison of the absolute value of maximum subgrade vertical strains when thawing was 4 in. into the subgrade showed that strains were consistently less for multiple load configurations compared with single tire loads. Figure 8 shows remaining rut life in a 2-in. AC pavement with a 6-in. base for the three load cases studied at early subgrade thawing. It can be seen that the calculated remaining rut life when spring thaw conditions prevailed was several times greater for dual tire loads for all cases of subgrade moduli included in the study.

EVALUATING THE BENEFITS OF APPLYING SPRING LOAD RESTRICTIONS

The results obtained from the analyses indicated that load restrictions up to 100 percent were required to maintain pavement performance during spring thawing at summer levels for the hypothetical pavement cross sections selected for the study. Current load restriction practices in the United States and Canada (*1*) indicate that agencies are currently imposing load restrictions that reduce allowable loads to 50 to 80 percent of the legal maximum loads. It is believed that the discrepancy in the allowable loads applied in practice and the allowable loads found for the hypothetical pavements is due to the fact that agencies do not intend to restrict pavements to the extent required to maintain summer performance levels. It is more likely that the objective in applying spring load restrictions is to reduce the need for major rehabilitation and/or to prolong serviceable life.

Based on these observations the calculated response from all of the analyses for fatigue and subgrade vertical strain was merged into two figures to evaluate the benefits of applying different levels of spring load restrictions for the hypothetical pavements. The remaining life for rutting was calculated for

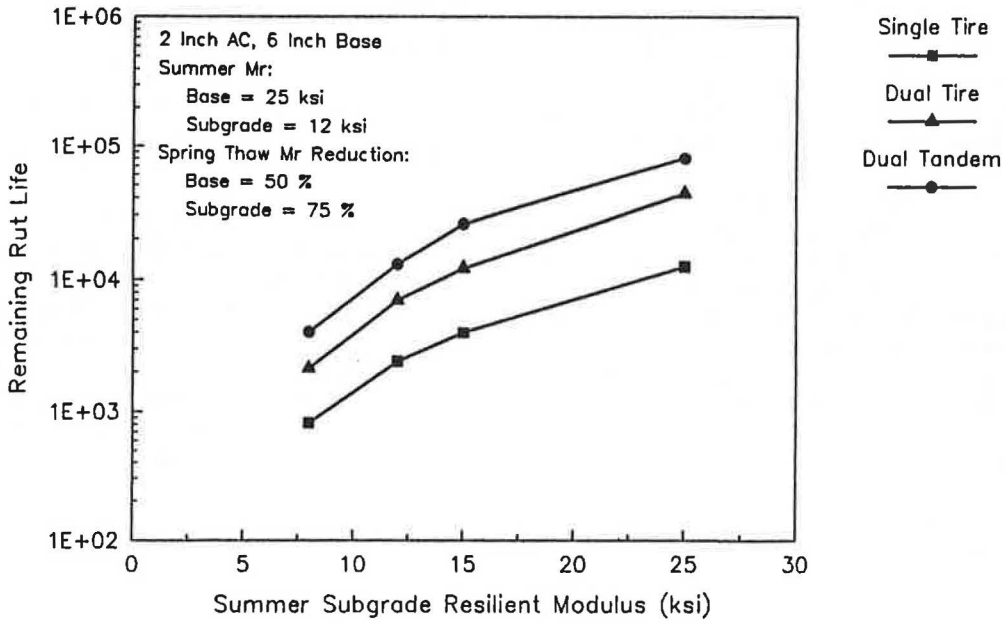

FIGURE 8 Comparison of remaining rut life for three load configurations at 4 in. subgrade thawing.

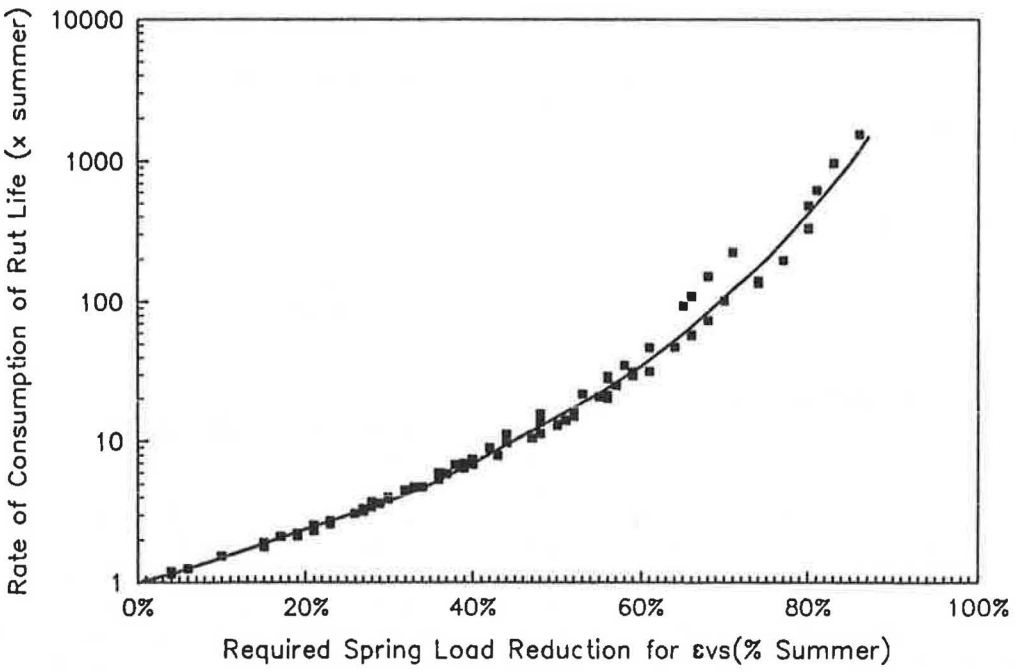

FIGURE 9 Rate of consumption of rutting life (relative to summer) versus required spring load reduction for subgrade vertical strain.

all pavement sections analyzed at 4 in. of subgrade thawing using the Shell equation (*11*). Figure 9 shows the rate of consumption of remaining rut life in spring compared with summer consumption as a function of the load reduction level required to maintain summer rutting levels. The benefits of applying some amount of load restrictions can be obtained from this figure for the pavements that require load restrictions based on subgrade vertical strains, which in this analysis was primarily the 4-in. AC pavements. For example, if an analysis of spring conditions suggested that the allowable spring load should be reduced to 40 percent of the legal maximum load to maintain summer conditions, the figure shows that the rut life consumption for this case with no load reduction would be about 7½ times as great as in summer. However, if a load restriction of 20 percent was applied, a load reduction of (40 − 20) or 20 percent would still be required. The rate of consumption of rut life for a required load reduction of 20 percent according to the figure is about 2½ times the summer consumption. Although this is clearly in excess of summer consumption, a considerable benefit has been realized by applying some level of spring load restriction.

Figure 10 presents the rate of consumption of remaining fatigue life as a function of load reduction for fatigue. This figure is used in the same way as the previous figure presented for rut life consumption; however, it should be used for pavements where asphalt tensile strain is the critical pavement response parameter during spring thawing, which typically was the case for the 2-in.-thick pavements analyzed.

CONCLUSIONS

The results obtained in this study suggest that single tire, single axle loads result in the greatest reduction in allowable spring loads compared with that in summer, as well as largest absolute values of strains and deflections. Therefore, the following conclusions are based on this load case. Further, it would appear to be reasonable to suggest that an agency might use this load case as a basis for formulating load restriction policies as most Class 8 heavy vehicles have steering axles that are configured with single tires.

The conclusions drawn from this study are the following:

1. Some thin pavements (2 in. AC) required load reductions at the time of base thaw to maintain the pavement at its summer response level.
2. All pavements that required some load reductions had reduced load-carrying capacity by the time of early subgrade thawing, and allowable loads were usually at their lowest levels at this time.
3. Four-inch pavements modeled typically experienced critical conditions as a result of maximum subgrade vertical strain during thawing.
4. Two-inch AC pavements resulted in load reductions at early subgrade thawing, usually because of asphalt tensile strain, but for many cases subgrade vertical strain was the critical parameter. At the end of thawing, however, asphalt tensile strain was the critical parameter for nearly all thin pavements analyzed.
5. A correlation was found between allowable loads for subgrade vertical strain and deflection for 4-in. AC pavements at the end of thawing.
6. In general it was found that deflections relative to summer were not a reliable indicator of the need for load restrictions during spring thawing. The results on the hypothetical pavements suggested that using summer deflection levels as a basis for when to apply load restrictions would generally be unconservative and would not result in the optimal use of spring load restrictions.
7. The most severe conditions with respect to fatigue and subgrade vertical strain occurred in the pavements analyzed during early thawing when deflections were less than summer levels.

Actual pavements will have their own unique material properties and relative changes in resilient response between sum-

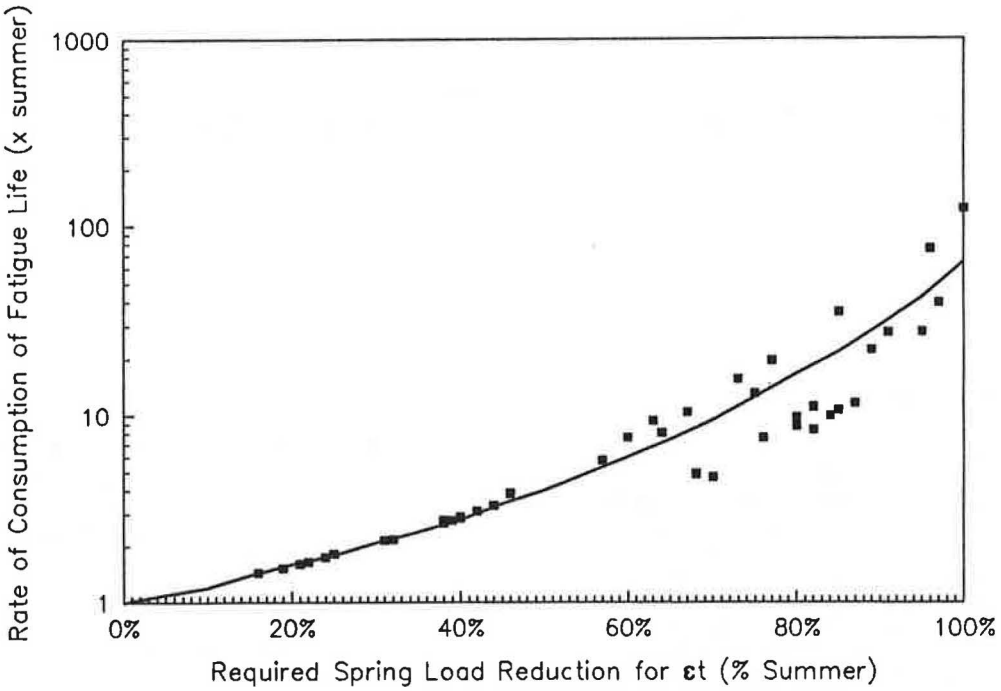

FIGURE 10 Rate of consumption of fatigue life (relative to summer) versus required spring load reduction for asphalt tensile strain.

mer and spring thawing. Further, the response of these pavements will vary from year to year because of variations in prevailing climatic conditions during the freezing and thawing period. The choices for layer thicknesses and resilient properties were intended to represent a broad range of resilient behavior that would be encountered in "real" pavements. If this has been accomplished, then the conclusions presented may be useful to individuals making decisions about the timing and magnitude of spring load restrictions. The assumptions made with respect to the change in resilient stiffness of materials from summer to spring conditions require further field testing and verification. This is clearly an area of further research.

In conclusion, it is important to recognize the need to rely on the judgment of experienced personnel in the decision-making process regarding the application of spring load restrictions. Site-specific topography, groundwater conditions, drainage, and annual variations in winter and spring climatic conditions result in considerable variation in the response of unbound materials underlying pavements. Observations by experienced individuals of the range of response of pavement sections that are particularly susceptible to damage during spring thawing should continue to be weighed heavily when making decisions regarding the application of spring load restrictions. It is intended that the research reported in this paper be used to enhance and not replace this experience.

REFERENCES

1. M. Rutherford, J. P. Mahoney, R. G. Hicks, and T. Rwebangira. *Guidelines for Spring Highway Use Restrictions*. Report WA-RD 80.1. Washington State Department of Transportation, Olympia, 1985.
2. R. N. Stubstad and B. Connor. *Prediction of Damage Potential on Alaskan Highways During Spring Thaw Using the Falling Weight Deflectometer*. Alaska Department of Transportation, Fairbanks, 1982.
3. J. A. Lary, J. P. Mahoney, and J. Sharma. *Evaluation of Frost Related Effects on Pavements*. Report WA-RD 67.1. Washington State Department of Transportation, Olympia, May 1984.
4. *Recommended Guidelines for Imposing and Lifting Springtime Restrictions*. Minnesota Department of Transportation, Minneapolis, 1985.
5. G. Rada, M. W. Witzcak, and S. D. Rabinow. A Comparison of AASHTO Structural Evaluation Techniques Using Nondestructive Deflection Testing. Presented at the 67th Annual Meeting of the Transportation Research Board, Washington, D.C., Jan. 1988.
6. G. Ahlborn. *Elastic Layered System with Normal Loads*. ITTE, University of California, Berkeley, 1972.
7. M. S. Rutherford. An Evaluation of Timing and Magnitude of Spring Load Restrictions for Flexible Pavements. Ph.D. dissertation. University of Washington, Seattle, 1988.
8. G. Rada and M. W. Witcsak. Comprehensive Evaluation of Laboratory Resilient Moduli Results for Granular Material. In *Transportation Research Record 810*, TRB, National Research Council, Washington, D.C., 1981, pp. 23–33.
9. A. J. G. Klomp and C. L. Dorman. Stress Distribution and Dynamic Testing in Relation to Road Design. *Proc., Australian Road Research Bulletin*, 1964.
10. F. Finn, C. Saraf, R. Kulkarni, K. Nair, W. Smith, and A. Abdullah. The Use of Distress Prediction Subsystems for the Design of Pavement Structures. *Proc., 4th International Conference on the Structural Design of Asphalt Concrete Pavement Structures*, Vol. 1, 1977, pp. 3–38.
11. J. M. Edwards and C. P. Valkering. Structural Design of Asphalt Pavements for Road Vehicles—The Influence of High Temperatures. Highways and Road Construction, Feb. 1974.

Publication of this paper sponsored by Committee on Low Volume Roads.

Use of Thermistors for Spring Road Management

JOE BARCOMB

The purpose of this paper is to discuss the use of subgrade temperature data, measured by permanently installed temperature sensors called thermistors, to administer spring road restrictions on asphalt surface roads within the Kootenai National Forest (northwestern Montana). The restrictions normally apply to logging trucks (three axles plus two axle trailers—approximately 80,000 lb gross). The interpretation of the data from the thermistor installations has provided an acceptable, rational approach to timing the spring restrictions. At present there are about 70 thermistor strings scattered over 300 miles of roads. Data are collected on the thermistor strings starting in December on a weekly basis, a schedule that is stepped up to daily readings as thaw conditions approach. The readings from just below the asphalt mat and the average reading for the whole string are analyzed with weather forecasts for use in predicting the need for load restrictions. The actual restrictions are placed when the thermistors located just below the mat on one or more strings indicate a thawed or nearly thawed condition. The success of the program can be attributed to the effort put into an information and education program aimed at the principal users and Forest managers. Problems with installations have been minor. Each thermistor string installation ranges in cost between $250 and $450; however, during the past 3 yr, surface maintenance repair costs have been reduced significantly (up to 50 percent annually on some roads).

The purpose of this paper is to discuss how the data collected from thermistor installations on the Kootenai National Forest are used to determine when road restrictions should be placed in the spring. It is a report on the effectiveness of the thermistor program that has been working since it was initiated in 1984. Those interested in the technical details on materials, equipment, testing, procedures, research, and installation should read the paper prepared by McBane and Hanek in 1986 (*1*). This paper minimizes the duplication of technical details covered in their paper.

The thermistor program on the Kootenai National Forest has provided road managers with a cost-saving tool. The idea to use thermistors on the Kootenai was brought to the Forest by Hanek and McBane in the early eighties. They were trying to find a way to lower road maintenance cost due to spring break-up. The success of the program on the Forest can be attributed to their information and education efforts.

Currently, there are nearly 70 installations on paved roads used by timber haulers (see Figure 1). These installations are monitored periodically during the winter months and the data are collected. The data are interpreted and used to determine when to apply haul restrictions on specific roads or road segments. The timeliness of the recent restrictions has resulted in reduced road maintenance costs. On the whole, the program has been very successful, with only a few minor problems.

U.S. Forest Service, Kootenai National Forest, 506 Highway 2 West, Libby, Mont. 59923.

BACKGROUND

The Kootenai National Forest is located in northwestern Montana, with a small portion occupying northeastern Idaho. On the north it is bounded by British Columbia, Canada. Figure 1 is a map showing the general location of thermistor strings on the Kootenai National Forest. In all, about 2.5 million acres (1.0 million hectares) of federal lands are managed by the Forest. These lands are intermingled with privately owned lands and are accessed by more than 6,600 miles (11,000 km) of Forest Service roads plus many county and private roads. Federal Routes 2 and 93 and Montana State Routes 37, 56, and 508 provide access to county and Forest Service roads. Elevations range from the lowest in Montana, about 1,800 ft, to over 8,700 ft (540 to 2650 m). Precipitation ranges from 14 in. to 120 in. (35 to 300 cm), with much of it falling as snow during the winter months. Frost penetration often exceeds 5 ft (1.5 m).

The Forest Service is in a unique situation to manage its road system because technically it is not a public road agency. It not only has the administrative authority to restrict size, weight, speed, and type of vehicle, but it can also close roads to all motorized vehicles. With the ability to close roads or severely restrict their use, the Forest Service very seldom designs roads to support traffic loads for all-season use because of the additional cost required to provide for the few weeks of worst subgrade conditions. Most low-volume roads elsewhere in the world are not built to provide all-season, full traffic load support for the same economic reason.

In addition to the 6,600 miles (11,000 km) of existing road under Kootenai National Forest's jurisdiction, about 180 miles (300 km) are added annually. Most of the roads were and are being built to accommodate timber hauling. The roads include narrow single-lane, native surfaced (5 to 15 mph—8 to 25 kph); single and double lane, aggregate surfaced (10 to 35 mph—17 to 58 kph); and single and double lane, asphalt paved (15 to 55 mph—25 to 92 kph). About 6 percent of the Forest's roads are paved. Pavements vary from a penetration treatment with a single chip seal to 4 in. (10 cm) of asphalt concrete mats.

Higher volume roads in the Kootenai National Forest may have seasonal daily traffic volumes of up to 300 vehicles, of which one third are log haul vehicles (typical five axle, 18 wheels with a gross weight of 80,000 lb, or 36 metric tons).

REASON FOR PROGRAM

The Kootenai National Forest has 420 miles (700 km) of asphalt-paved roads, of which only about 10 percent are capable of

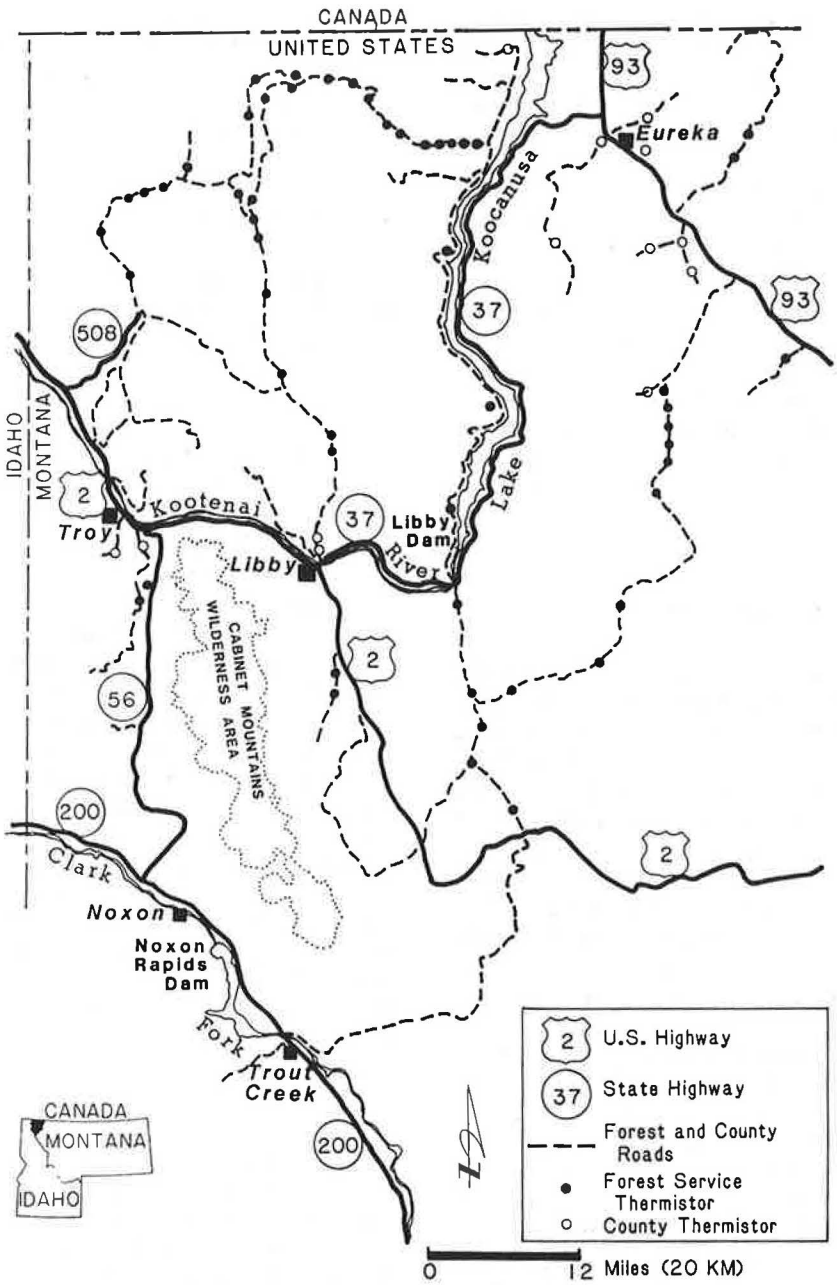

FIGURE 1 Thermistor locations on Kootenai National Forest.

handling year-round traffic. Those roads capable of handling year-round traffic were built by the Corps of Engineers in conjunction with the Libby Dam Project and were later turned over to the Forest Service. None of the roads has been designed to prevent frost heave. Roads can be constructed to prevent frost action if free draining aggregates are used, but the Kootenai National Forest could not economically justify the aggregate thicknesses needed. To protect roads during periods when thawing is occurring in the top few feet where the structural strength is weakest, haul restrictions have been applied for many years. In the past, decisions to restrict the roads were based on visual observations of the pavement surface and ambient air temperature conditions.

Visual observations normally detect damage only at the pavement surface. During break-up, initial damage that is not visible occurs to the underlying structure. In the past, there were disagreements with timber haulers when Forest Service management wanted to restrict road use, because the haulers were normally trying to build up their mill inventories in anticipation of haul restrictions. As a result, haul was most often allowed until visual surface damage was noted; therefore, maintenance costs for paved roads were excessive.

Reducing the maintenance costs for paved roads was deemed paramount. It was perceived that, by measuring the pavement structural capacity during the thawing period, Forest Service management would have better information from which to determine more accurately when to apply restrictions before serious damage occurred to the road structure. Actual measurements of the pavement deflection were either expensive, cumbersome, or untimely. It was decided that temperature

measurement of the base and subgrade could be used to establish in a timely manner when a road was thawing, and haul restrictions could be placed accordingly.

The road structure initially starts to weaken when the frost starts to leave the base just under the asphalt mat and before all the base and subgrade was thawed. At this time the moisture from the melting ice is trapped between the impervious frozen layer below, the edges of the pavement structure, and the asphalt mat above. Even the base, normally constructed of free draining rock, may become supersaturated as snow on the shoulders can insulate it, retarding thaw and thus preventing free water from escaping to the ditch line. The weakened condition often persists until the whole structure is totally thawed and the excess water can drain from the base and subbase. Several destructive conditions can occur when the road is in this weakened condition: contamination of the base, rutting of the base and subgrade, and cracking or breaking up of the asphalt mat.

INFORMATION AND EDUCATION PROGRAM

There was strong support for reducing the costs of maintaining paved roads, but there was no commonly understood, quantitative basis for consistently and fairly placing the necessary limits on timber hauling. The designers of the system, McBane and Hanek, performed their greatest service by developing an excellent informational and education program. Through their efforts in making presentations to Forest Service management, timber haulers, and county personnel, they were able to sell their concept and get a consensus on what measured conditions would cause administrative haul restrictions to occur. Cooperation was excellent when it came time to restrict roads in the spring on the basis of the thermistor readings.

The information and education program was primarily based on the narrated slide program but together by McBane and Hanek. In their program they covered past research, calibration testing of actual thermistors (ice water baths), laboratory testing of soils (determination of freeze-thaw temperature for typical soils in the area), typical installation of thermistor strings, use of the Benkelman beam (to correlate road structure strength and depth of thaw), and how the temperature data collected could be analyzed and interpreted. Their thorough explanation left little doubt in their audience's mind of the program's soundness.

Generally the cooperation has been good throughout the Forest Service and by users of the road system. There is, however, a continuing need to keep newcomers informed about the process.

GLOSSARY

Thermistor sensor is a small semiconductor where the electrical resistance varies with temperature fluctuations.

Thermistor string is a multistrand electrical cable with several thermistor sensors attached and sealed at specified intervals.

Thermistor installation consists of a thermistor string placed in a vertical hole below the road surface, lead cable, a thermistor sensor for air temperature, and a readout box to which the electric thermometer can be attached.

Electric thermometer measures electrical resistance in a circuit through a thermistor sensor and displays the correlated temperature reading.

INSTALLATIONS

A thermistor string used on the Kootenai National Forest is made of multistrand cable, eight or more thermistors, and an electronic box for taking data readings (see Figure 2). The thermistors are soldered and sealed to the last 3 to 5 ft of the cable. This portion is then inserted vertically into a core drill barrel after the inner barrel has been removed (cave-in is often a problem). The spacing of thermistors on a string has been standarized for preassembly; however, they are not spaced for all the varied conditions that could be found. At any specific site, spacing can easily be varied to meet the conditions that are determined to be necessary for monitoring.

The Kootenai National Forest has determined that reliable information can be obtained when the top thermistor is placed in the asphalt mat; the second is placed just below the asphalt mat; the third is placed 6 in. below the asphalt surface; the fourth, fifth, and sixth are placed 12, 18, and 24 in. below the surface; and the remaining are normally placed at 1-ft intervals below the sixth. One thermistor is mounted in the shade (referred to as #0 on figures) to record air temperatures near the readout box. Twenty to 40 ft of cable separate the thermistor from the data collection box.

At the present time there are 67 thermistor string installations on paved roads used by timber haulers. Thirteen of these are on county roads and the remainder on Forest Service roads. The installations have been placed only under bituminous surfaces. These are the Forest Serice heavy-use roads that are more often in the valley bottom where thawing first occurs.

With the lower elevation and heavy-use roads restricted, it was determined that the higher elevation and branch roads did not need to be monitored through the use of thermistors. There are several reasons why it was felt that branch roads and higher elevation roads need not be monitored. Investments in the branch roads are considerably less. Normally they are not paved, and excess moisture is readily visible on the surface, easily permitting a decision to restrict hauling to be made on these observations. When the higher elevations begin to thaw, timber harvest is normally curtailed as a result of excess moisture in the forest soils. Therefore, timber hauling normally ceases. The locations for individual thermistor installations have been selected with care. Normally, at least two sites are selected for each segment of road—one to try to match the earliest thaw and the other, the latest thaw. Elevation and the amount of exposure to the sun are major criteria in selecting locations. Often two sites are selected close together, one in a sunny spot and the other in a shaded area. This gives a better indication of how the overall road is thawing.

Initial restrictions are placed at the time thaw begins or shortly after thaw begins in the warmer sites. Sometimes the damage that occurs on the 200- to 400-ft (60- to 120-m) stretch of road around the warmest site is more acceptable than to restrict the entire road a few days earlier. After the subgrade

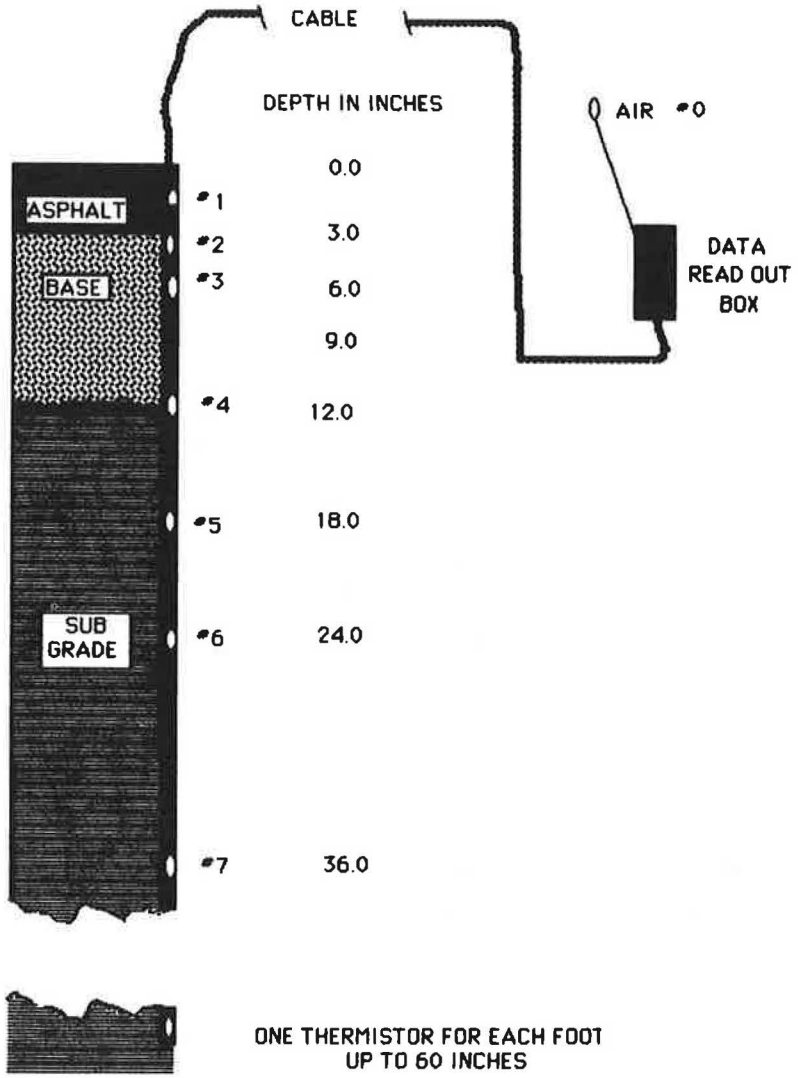

FIGURE 2 Typical thermistor string installations.

has thawed on the colder sites, consideration is given to lifting the restrictions.

DATA AND INTERPRETATION

Data readings of the individual thermistors normally start in December and continue through March. Higher elevation installations are read even later. Frequency of readings may start biweekly or weekly and then be increased to daily readings as weather conditions and thermistor data indicate that thaw conditions are imminent. A hand-held electric thermometer is plugged into the circuits, and individual sensor readings are taken and recorded manually. The collected data are then entered in a computer.

The temperature at which thawing starts is the critical information sought. This happens at around 31.7°F (– .2°C), because of the chemical consistency of pore water in the area soils (*1*).

The temperature data from individual sensors on a thermistor string are aggregated to produce a weighted average (*1*). Graphs of the average readings of individual installations are used for ease in spotting warming trends (see Figure 3). By putting a trend line on the temperature plots and projecting it through the thaw point, an estimate of the beginning of thawing at the site can be made. The interpreted trends, combined with the weather forecast, are used to make predictions on when break-up will occur. Typical data printouts are shown in Figures 4 and 5. The data readouts can be traced from December into March.

The actual decision to restrict a section of road is made when one or more strings show thawing temperatures in the sensor located just below the asphalt pavement. Figure 4 shows that thawing occurred just below the mat on 11 February (see box). Haul restrictions were placed starting 12 February on this road.

"THAW WEAKENING MONITORING RECORD—SITE NUMBER D6-36-2.8" has two thermistors not working (see Figure 5). It is still capable of supplying useful data, however. By adjusting the weightings for temperature readings to compensate for the missing thermistors, an average temperature can be calculated. This string would be consid-

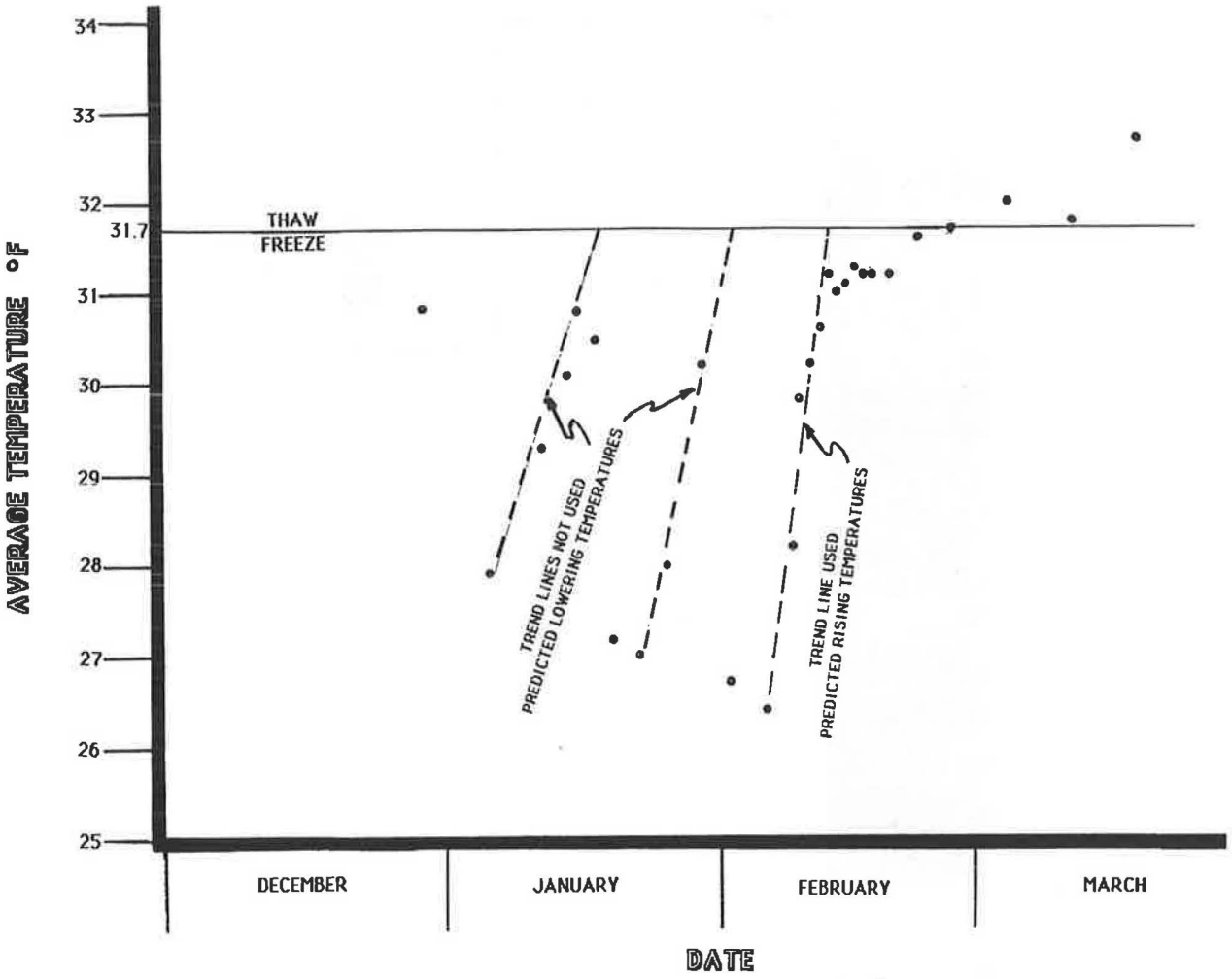

FIGURE 3 Average temperature graph for Site Number D6-763-0.95 used for predicting trends.

ered nonfunctional if the sensor just below the mat failed, or if any more sensors on the string failed.

When it appears that break-up is coming, notices are sent to personnel in the county, timber haulers, and Forest Service organizations. This can be related to the sequence that a racing starter goes through: "On your mark, get set, go." The "go" phase is when the haul restrictions are placed. Figure 6 shows a series of three messages that led up to restricting haul on certain roads.

BENEFITS

The benefits that the program has brought the Kootenai National Forest are a better basis for placing haul restrictions in the spring and a significant lowering of maintenance costs on paved roads. In addition, some of the timber haulers have become strong proponents of the thermistor program. They have seen annual maintenance costs of paved roads reduced (more dollars in their pockets in cases where they were the principal road maintainers). They now no longer pester the Forest management to keep roads open for "just another week."

The savings from reduced maintenance costs on one 17-mile (28-km) segment of road during the first year of operation paid for the development and installation costs. The savings amounted to about 50 percent of historical annual maintenance costs (see Figure 7). This convinced the Forest management team to expand the program to cover the remainder of the asphalt-paved roads in the Forest.

A typical thermistor string costs between $150 and $250 to construct or buy. This includes a readout box, 5 to 6 ft (about 1.75 m) of electrical conduit, 30 to 45 ft (9 to 13.5 m) of multistrand cable, 8 to 10 thermistors, and miscellaneous materials. Installation costs run between $100 and $200 for sawing the pavement, drilling the hole, installing the thermistor string, and sealing the saw cut and hole. The large variation in costs are due to the availability of different drilling equipment, site conditions, and skill and cost of labor.

PROBLEMS

There are some problems with the system as described. About 5 percent of the individual sensors fail annually. Whole strings are replaced when either a sensor just below the asphalt pave-

Enter TIME in military time
Enter TEMPERATURES in degrees F. to the nearest tenth of a degree
Average soil temperature will be automatically calculated
(([*,5]*1.5)+([*,6]*7.5)+([*,7]*12)+([*,8]*9)+(([*,8]+[*,9])*1.5))/33

DATE LV BLANK	TIME	0(AIR)	1(MAT)	2(BASE)	3(6.0)	4(18.0)	5(30.0)	6(42.0)	7(48.0)	8(54.0)	9(60.0)	AVE. TEMP.
NOV 18, 87	1232.0	24.7	30.1	30.3	32.8	38.2	42.4	45.3	46.5	47.5	48.4	38.3
DEC 08, 87	1120.0	31.3	31.3	31.4	34.3	37.1	38.7	40.3	41.4	42.4	43.3	36.9
DEC 15, 87	1312.0	26.0	28.4	28.0	30.9	34.2	37.1	39.4	40.6	41.6	42.6	34.3
DEC 29, 87	1142.0	21.9	23.5	23.1	25.5	31.4	34.2	36.7	37.9	39.1	40.1	30.8
JAN 05, 88	1142.0	9.9	15.1	15.7	20.7	28.5	33.0	35.5	36.7	37.9	39.0	27.9
JAN 11, 88	1255.0	35.3	27.6	26.3	26.2	28.4	32.0	34.5	35.8	37.0	38.1	29.3
JAN 14, 88	1302.0	36.8	31.1	30.1	28.6	29.0	31.8	34.2	35.4	36.6	37.7	30.1
JAN 15, 88	1345.0	37.3	31.8	31.0	30.1	29.8	31.8	34.1	35.3	36.5	37.5	30.8
JAN 17, 88	1109.0	29.5	25.8	27.1	29.1	30.3	31.8	34.0	35.1	36.3	37.3	30.5
JAN 19, 88	1308.0	25.3	22.5	19.0	20.3	27.8	31.8	33.9	35.0	36.1	37.2	27.2
JAN 22, 88	1144.0	26.2	22.2	20.2	21.4	26.7	31.3	33.7	34.8	35.9	36.9	27.0
JAN 25, 88	1235.0	34.2	28.5	25.2	24.2	27.3	31.1	33.5	34.6	35.7	36.7	28.0
JAN 29, 88	1306.0	43.7	33.7	31.0	29.7	29.4	31.0	33.1	34.3	35.3	36.3	30.2
FEB 01, 88	1332.0	21.7	16.1	14.7	19.1	23.3	31.2	33.1	34.1	35.1	36.1	26.7
FEB 05, 88	1245.0	24.1	24.0	22.4	22.1	25.7	29.8	32.8	33.9	34.9	35.9	26.4
FEB 08, 88	1246.0	39.7	30.8	28.3	26.2	26.3	30.3	22.6	33.7	34.7	35.7	28.2
FEB 09, 88	1131.0	37.0	31.4	30.7	29.6	28.9	30.4	32.5	33.6	34.6	35.6	29.8
FEB 10, 88	1155.0	37.3	32.0	30.3	30.1	29.6	30.6	32.5	33.6	34.6	35.5	30.2
FEB 11, 88	1119.0	46.3	35.0	31.6	30.7	30.0	30.8	32.5	33.6	34.5	35.5	30.6
FEB 12, 88	1433.0	58.1	44.9	39.2	31.1	30.3	31.0	32.5	33.5	34.5	35.4	31.2
FEB 13, 88	1115.0	41.2	34.9	33.0	31.2	30.5	31.0	32.5	33.5	34.5	35.4	31.0
FEB 14, 88	1324.0	40.4	33.1	31.6	31.4	30.6	31.1	32.5	33.5	34.4	35.3	31.1
FEB 15, 88	1154.0	39.0	38.7	35.4	31.4	30.7	31.2	32.5	33.5	34.4	35.3	31.3
FEB 16, 88	1056.0	32.5	31.0	31.2	31.5	30.8	31.2	32.5	33.5	34.4	35.2	31.2
FEB 17, 88	1023.0	36.5	31.3	31.0	31.5	30.8	31.3	32.5	33.4	34.3	35.2	31.2
FEB 19, 88	1104.0	31.5	31.3	30.7	31.5	30.9	31.3	32.5	33.4	34.3	35.2	31.2
FEB 22, 88	1335.0	46.8	44.6	35.5	31.6	31.1	31.4	32.5	33.4	34.3	35.1	31.6
FEB 26, 88	1330.0	49.9	47.0	36.7	31.5	31.2	31.5	32.6	33.4	34.3	35.0	31.7
MAR 04, 88	1310.0	43.7	46.5	41.0	32.1	31.2	31.6	32.6	33.4	34.2	34.9	32.0
MAR 11, 88	1240.0	43.2	45.7	35.7	31.8	31.4	31.6	32.7	33.4	34.1	34.8	31.8
MAR 18, 88	1252.0	55.7	54.7	45.6	33.3	31.5	31.7	32.7	33.4	34.1	34.8	32.7

NOTES:
1. Road haul restrictions were effective 12 February 88.
2. Thermistors 1 through 9 are followed by depth below road surface in inches.
3. There is an apparent error in the data entry of thermistor number 6 on 8 February of ten degrees.
4. Maximum frost depth at this site was beteen 30 and 42 inches (75 and 105 cm).

FIGURE 4 Thaw-weakening monitoring record (data printout), Site Number D6-763-0.95.

Enter TIME in military time
Enter TEMPERATURES in degrees F. to the nearest tenth of a degree
Average soil temperature will be automatically calculated
(([*,5]*3.7)+([*,7]*8.3)+([*,8]*6)+([*,9]*9)+([*,10]*6))/33.0

DATE LV BLANK	TIME	0(AIR)	1(MAT)	2(3.0)	3(6.0)	4(12.0)	5(18.0)	6(24.0)	7(36.0)	Ave. Temp.
NOV 18, 87	1404.0	27.4		29.5	18.5	34.0	36.5	39.1	43.2	37.0
DEC 8, 87	1146.0	32.1	-110.6	32.0	21.6	36.2	37.6	38.5	39.0	37.1
DEC 15, 87	1337.0	28.8		28.4	16.4	31.2	32.9	34.5	36.5	33.1
DEC 29, 87	1241.0	24.4		24.1		25.1	26.8	28.3	31.1	27.3
JAN 5, 88	1238.0	8.5		12.7		18.3	21.4	24.7	29.0	21.9
JAN 11, 88	1324.0	34.1		25.8		25.0	25.7	26.8	29.1	26.5
JAN 14, 88	1327.0	35.3		30.0		27.8	27.8	28.3	29.7	28.5
JAN 15, 88	1411.0	40.0		31.4		29.9	29.6	29.6	30.1	30.0
JAN 17, 88	1138.0	26.8		25.9		29.2	29.9	30.3	30.7	29.5
JAN 19, 88	1333.0	25.7		21.1		23.3	25.6	27.8	30.2	26.0
JAN 22, 88	1235.0	28.0		22.7		22.8	24.5	26.4	29.2	25.2
JAN 25, 88	1336.0	31.9		24.6		24.7	25.8	27.1	29.3	26.4
JAN 29, 88	1335.0	41.0		31.6		29.8	29.5	29.5	30.3	30.0
FEB 1, 88	1359.0	19.1		16.3		22.6	25.5	28.5	30.6	25.5
FEB 5, 88	1312.0	24.4		23.9		23.8	24.5	26.3	28.8	25.5
FEB 8, 88	1310.0	38.1		26.7		27.9	28.2	28.9	29.9	28.5
FEB 9, 88	1237.0	36.3		29.1		30.7	29.5	29.6	30.2	29.9
FEB 9, 88	1730.0	33.5		30.6		30.9	29.6	29.7	30.3	30.2
FEB 10, 88	1245.0	36.1		30.3		31.4	30.2	30.0	30.4	30.6
FEB 11, 88	1148.0	46.7		32.5		32.7	30.9	30.7	30.8	31.5
FEB 12, 88	1454.0	51.1		35.9		32.9	31.4	31.1	31.2	32.2
FEB 13, 88	1144.0	39.2		34.4		32.2	31.6	31.3	31.0	31.9
FEB 14, 88	1347.0	40.4		36.9		32.3	31.8	31.5	31.2	32.3
FEB 15, 88	1313.0	39.6		36.2		32.7	31.9	31.6	31.2	32.4
FEB 16, 88	1203.0	39.3		31.3		33.3	32.2	32.1	32.0	32.3
FEB 17, 88	1126.0	32.5		31.7		32.5	32.0	32.0	32.0	32.0
FEB 19, 88	1225.0	39.0		31.5		32.0	31.8	31.8	31.3	31.7
FEB 22, 88	1412.0	47.4		35.0		32.1	31.8	31.8	32.0	32.3
FEB 26, 88	1352.0	50.5		33.2		32.0	31.9	31.8	33.0	32.2
MAR 4, 88	1416.0	47.4		43.7		33.8	33.4	32.5	33.5	34.4
MAR 11, 88	1314.0	45.3		42.3		35.0	35.6	35.3	35.2	36.1
MAR 18, 88	1324.0	57.0		51.3		37.8	38.0	37.5	37.9	39.3

NOTES:
1. Road haul restrictions were effective 12 February 38.
2. Thermistors 1 through 7 are followed by depth below road surface in inches.
3. Thermistors number 1 (mat) and 3 (6.0) are not functioning but data from the string is still providing useful information.

FIGURE 5 Thaw-weakening monitoring record (data printout), Site Number D6-535-0.35.

ON YOUR MARK

Postmark: Feb 01,88 9:26 AM

The prerecorded phone message is up and running. The recorded message can be checked out by calling 293-7421. I sent the information to all interested parties and the papers in Libby, Eureka, and Kalispel. I'll give you copies of the news release that you can give to the purchasers. Mike

GET SET

Postmark: Feb 08,88 7:28 AM

Weather forecasts project days @ mid 40's and nights @ hi 20's for the rest of the week. Provided there is no change, current proposal is to post Fisher #1 @ 80,000# and Fisher #2 at 10,000# on Wed. 2-10; followed by Wolf Creek & Mc Killop @ 10,000 on Thurs. 2-11. We will be monitoring thermistors daily. If a cold spell sets in and the road subgrade firms up restrictions may be delayed. Larry

GO

Postmark: Feb 11,88 5:17 PM

Effective Friday 2-12, log haul will be restricted on entire Fisher River system (80,000 # weight on Fisher #1; 10,000# on Fisher #2, Mc Killop, and Wolf Creek). Message is on phone answering service. I have advised state, Champion, and purchasers. Information will be posted on the ground Friday morning. Restrictions will be lifted if colder weather sets in and the thermistors verify frozen road conditions. Larry

FIGURE 6 Copies of informational messages leading up to placing restrictions on Kootenai National Forest roads for spring break-up.

ment fails or too many fail on a single installation. Entire thermistor strings are being replaced at about 10 percent annually as a result of failure of thermistors, damage during road maintenance activities, and periodic reconstruction of roads. Also, a few strings have been discontinued in favor of a new location that is perceived to yield more reliable data. This past field season (1988) the Forest installed 14 strings. None were installed in the 1987 field season.

Initial acceptance of the thermistor program could be a major administrative problem if a good information and education program is not undertaken. Every change in management, whether Forest Service, timber hauler, or county, requires that the information and education program be repeated.

The biggest drawback to the thermistor program is that interpretation of the data cannot be used with all soil types to indicate when to lift the hauling restrictions. The Forest still uses visual observation of moisture conditions in the ditch line and cracks in the pavement. It has not been a significant problem on the Kootenai because the timber haulers do not usually want to resume hauling for approximately 2 to 3 months after initial restrictions. By then, the roads have had time to drain the excess moisture and regain strength. A study in Region 6 of the Forest Service (National Forests in Oregon and Washington) on different moisture-sensing devices may aid the Kootenai Forest in selecting a system to determine when pavement strength has returned and restrictions can be lifted.

APPLICATIONS FOR OTHERS

The Forest Service is unique in that it has the option of being able to place varied load restrictions, including total road closure. Most road agencies do not have that option and can only place haul restrictions that are much less stringent than those often used on the Kootenai National Forest. Initially, thermistor temperature data need to be correlated with either pavement deflections or other road strength tests to define the interaction of depth of thaw and road strengths. On the basis of pavement structure strengths at different thaw depths, agencies should be able to determine when to institute partial haul restrictions on their roads.

Many variations in the spacing and number of thermistor sensors on a thermistor string are acceptable. The Kootenai National Forest has tried to standardize spacing of sensors for its own use. Good temperature data are still available even after the failure of one or two sensors placed in the subgrade. Economically it makes more sense to place extra sensors at $10 each and allow for some failure than to replace a whole string for $300. The computer spreadsheet program used to

MACHINE AND HAND PATCHING YAAK VALLEY ROAD 92
MILE POST 12.5 TO 29.5

YEAR	AMOUNT IN $1,000
1981	54
1982	37
1983	34
1984	121
1985	35

USE OF THERMISTORS ON YAAK 92 AS A MANAGEMENT TOOL ESTABLISHED

1986	17
1987	16

FIGURE 7 Annual pavement maintenance costs.

develop a weighted average can easily be adjusted to account for the sensor spacing.

SUMMARY

Two individuals perceived a need and provided a cost-effective method for the Kootenai National Forest to prevent road damage and to lower asphalt road maintenance costs through timely restrictions at the beginning of the spring break-up period. The method involves installing thermistor strings in and below the pavement and monitoring the temperature changes before and during the spring break-up period. Success has been documented through on-the-ground field application. Information and education efforts were very important in establishing the new program. Information is continually sent to groups and individuals as it appears the roads are reaching a thaw stage. The data collected and interpreted provide a rational approach to restricting hauling on asphalt-paved roads.

The Kootenai Forest is still replacing thermistors and adding a few new installations each year. The problems encountered with the system have been fairly minor and the benefits, worthwhile. The program will continue until a better system can be found.

REFERENCE

1. J. McBane and G. Hanek. Determination of the Critical Thaw-Weakened Period in Asphalt Pavement Structures. In *Transportation Research Record 1089*, TRB, National Research Council, Washington, D.C., 1986, pp. 138–146.

Publication of this paper sponsored by Committee on Low Volume Roads.

Method for Determining Optimal Blading Frequency of Unpaved Roads

ROEMER M. ALFELOR AND SUE MCNEIL

Management systems for unpaved roads are often viewed as unwarranted because of the low levels of traffic normally found on these roads. However, unpaved roads in many developed and developing countries represent the larger portion of mileage in the network. Even at the low cost of maintenance per mile of unpaved roads, the total cost resulting from multiplying this value by the overall road mileage corresponds to a large financial outlay. Therefore, the efficient management of these roads is justified. Recognizing the need to optimize the blading and regraveling frequencies of unpaved roads, some agencies tried to develop methodologies for determining the appropriate maintenance strategies. The procedures vary from road classification-based maintenance to economic analyses of alternative maintenance frequencies. However, the general approaches used in solving the maintenance problem are unsatisfactory as they either require restrictive assumptions or do not give closed-form solutions. This paper presents a dynamic optimization approach for determining the optimum blading frequency for an unpaved road using the principles of optimal control. The model is based on a procedure developed for setting overlay frequency and thickness for paved roads. The optimization equations are formulated for unpaved roads and applied to hypothetical cases. A sensitivity analysis is performed to evaluate the parameters in the model. The study indicates this approach is appropriate for determining optimal blading strategies for unpaved roads. However, further research is required to develop suitable deterioration and user cost functions and to include the frequency of regraveling.

For low-volume unpaved roads, loose gravel or plain earth is the primary riding surface. These roads are designed to provide low-cost highways for accommodating low traffic volumes. They are found in many agricultural areas where access is needed for the transport of farm products. In many developing countries, unpaved roads constitute a significant portion of the total road mileage and play a major link in the overall economy. Some of the routes connecting major cities in these countries are unpaved, owing to the economic infeasibility of transforming these roads into hard-top, all-weather surfaces. Most third-world economies rely on farm-based industries, but several developed countries also have substantially extensive farming activities, giving rise to a large number of earth and gravel roads. The proportions of unpaved roads in representative developed countries in 1978 ranged from 5 to 63 percent, whereas for developing countries they are as high as 70 to 97 percent of the network (*1*).

Maintenance of unpaved roads involves blading using a motor grader or a modern tow-type blade to restore the shape and surface of the road to ensure drainage and enhance rideability. Regraveling is also performed for gravel-surfaced roads when the gravel thickness falls below a minimum value. The major difference between paved and unpaved roads with regard to maintenance is that the former, once built, will exist for a number of years with minimal or no maintenance whereas the latter deteriorate faster and require frequent maintenance.

Compared with that of paved roads, very little attention has been given to the maintenance of unpaved roads. As significant portions of the road network are unpaved in both developed and developing countries, even low-level maintenance consumes valuable resources. The development of management systems for unpaved roads aims at the efficient allocation of these resources. Existing systems either use unrealistic simplifying assumptions or do not give closed-form solutions.

This paper develops an analytical method to determine optimal blading frequencies for unpaved roads. The dynamic optimization technique optimal control is used. This procedure was applied by Tsunokawa (*2*) in solving for the optimum frequency and thickness of overlay in the rehabilitation of highway pavements. Tsunokawa's formulation, however, assumed that the performance of a pavement can be expressed in terms of a single measure, which is roughness, and that there is only one maintenance activity to correct for roughness at various levels. Deterioration of the pavement is manifested in many ways and is corrected or remedied by maintenance activities that vary with the extent and type of deterioration. For an unpaved road, roughness is the primary indicator of condition, and routine maintenance is limited to blading. Using performance functions derived from previous studies, a dynamic optimization model is formulated using roughness as the state variable and blading frequency as the decision or control variable.

The following section presents measures of condition for unpaved roads and reviews studies of performance and existing management systems. Then, the optimal control model for unpaved roads is developed and a case study, including sensitivity analysis, is presented. This research demonstrates the applicability of optimal control technique for determining blading frequencies and identifies areas for further research to determine its feasibility.

BACKGROUND

Previous research on the maintenance of unpaved roads has focused on measures of condition or deterioration, performance, and maintenance systems (*3*). Measures of condition and the performance of unpaved roads are fundamental elements of any maintenance management system as they are used to quantify the impacts of maintenance. The relation-

Department of Civil Engineering, Carnegie-Mellon University, Pittsburgh, Pa. 15213.

ships between condition and impacts have been developed in many of the existing maintenance management systems. A comprehensive review is presented in Alfelor (*4*). These relationships are briefly reviewed in this section as they are used in the determination of optimal blading frequencies. Some representative approaches to maintenance management are also described to illustrate the limitations of existing approaches.

Measures of Condition

Deterioration of unpaved roads is manifested and quantified in terms of the following measures of condition:

1. Surface roughness,
2. Gravel loss of the wearing surface,
3. Rut depth, and
4. Depth of loose surface materials.

Roughness is the primary component of serviceability of the road (*5*), and the way it is perceived by the road user is very important. In terms of profile, roughness can be defined as the summation of variations in the surface profile. For a gravel-surfaced road, traffic and environment act together to cause reduction in gravel thickness. This change in gravel height measured over a period of time is called gravel loss. Excessive gravel loss results in earth riding surfaces that become impassable during the rainy season. Ruts decrease the serviceability of the road because they cause vehicle displacements. The operating speed of the vehicle is substantially reduced because the vibration increases with speed. Loose material on the road leads to loss of traction and was found to increase fuel consumption for a wide spectrum of vehicles in the Kenya study (*6*). The present study focuses only on roughness because for unpaved roads, all other measures of condition contribute to surface roughness.

Roughness measures are classified as either profile numeric or summary numeric. For profile numerics, the longitudinal elevation profile of the road is measured and then analyzed to obtain one or more roughness indices. High-speed and manual profilometers are in use. The most popular measures of roughness using statistics from profiles are the root-mean square deviation (RMSD) and the Quarter Car Index (QI). The former was developed by the British Transport and Road Research Laboratory (TRRL) using an instrument for statically measuring profiles called the TRRL beam (*7*). The Quarter Car Index, on the other hand, was developed for the Brazil road cost study and was originally measured by the General Motors Surface Dynamics Profilometer. The research team in Brazil later adopted a simplified method of obtaining the index using rod and level.

Summary numerics are measured using instruments known as Response-Type Road Roughness Measuring Systems (RTRRMS). For these systems, a vehicle is instrumented with a road meter that produces a roughness reading as a result of the vehicle motions that occur while traversing the road. RTRRMS provide means to acquire roughness data using relatively low-cost equipment. The main disadvantage of these systems is that the roughness measure is intimately tied to the vehicle response, which varies among vehicles and likewise with time, vehicle condition, and weather. The quarter car model is a response-type system that produces the quarter car index and is used as a standard measure. The most popular RTRRMS in the United States is the Mays Road Meter because it is simple and cheap.

The condition measures just described are used in studies of the performance of unpaved roads and in the development of management systems.

Studies of Performance

The majority of research on unpaved roads was performed as part of a larger study that included paved roads. Hence, the focus of the study was not necessarily on unpaved roads themselves. These major studies were conducted in developing countries with the objective of establishing rational, quantitative bases for highway decision-making in those countries. The World Bank realized that situations in developing countries (i.e., economic, labor, and technology) are different from those of developed countries where pavement management systems exist, and concluded that those systems are not appropriate for use in entirely different environments. For this reason the World Bank initiated collaborative research with institutions in several countries, and took a share in funding this research. The original research was conducted in Kenya and included both paved and unpaved roads. This was followed by studies in the Caribbean, Brazil, India, and Bolivia, among others. The result is a large data base and empirical models that can be used for economic evaluation of unpaved roads. Included in the studies of performance are deterioration and vehicle operating costs as well as impacts of maintenance on condition. The result of this study was used in some of the existing management systems described next.

Existing Approaches to Maintenance Management

Maintenance management systems provide data for planning as they determine maintenance needs and the cost of executing a desired level of maintenance. Two types of management systems are currently used for unpaved roads—namely, the road-classification based and mathematical optimization techniques. Road classification is a simple way to assign maintenance to a road. The procedure is to divide the roads into different classes based on characteristics such as traffic volume. For each class a level of maintenance is defined. One example is the Ontario Road Classification System (*8*). In this system, roads are divided into three classes based on four quality-of-service characteristics: (a) average daily traffic, (b) visibility, (c) ease of passage, and (d) all-season travel. The main criterion used is the average daily traffic. The overlaps in the classification are taken care of by the other characteristics. The purpose of the classification is to establish a basis for distributing maintenance funds. A formula was developed that relates maintenance costs to each class in a linear manner. Given the ratios of maintenance costs among the classes, the portion of budget to be allocated to each class is computed. This system does not attempt to come up with optimal maintenance strategies, as it is designed only for allocating maintenance funds. It is also not clear how the other criteria (i.e., visibility and ease of passage) can be quantified as they are very subjective. The assumption on linearity of cost with average daily traffic is very unrealistic.

The more elaborate procedures applied in setting maintenance frequencies for unpaved roads consist of analysis of quantitative relationships describing the road's performance and determination of the most economic strategy using a certain objective function. Kerali and Snaith (*9*) proposed a simple analytical model that aims at minimizing the total costs involved after a road is constructed. The performance relationships are taken from the Kenya Study that predicts distresses on unpaved roads as functions of cumulative traffic and surfacing materials (*6*). The same study determined that roughness was the surface condition measure by which road user costs can be predicted. Assuming that the geometric and traffic characteristics of the road remain fixed, Kerali concluded that the vehicle operating cost incurred on a given road per vehicle-kilometer will change only if the road roughness changes. The relationship between unit vehicle operating cost and cumulative number of vehicles (and roughness) is graphed for a particular type of vehicle and surfacing material and a maintenance activity assumed to be repeated several times after a constant traffic interval. Assuming zero traffic growth, the cumulative increase in postconstruction cost (VOC + maintenance cost) is drawn against the cumulative traffic. Cost of maintenance is a fixed vertical line every time maintenance is performed. A Total Cost Line (TCL) connects the total cost coordinates for each maintenance cycle. The slope of the TCL will depend on the shape of the excess VOC curve and on the unit cost and interval of maintenance activity. The optimum maintenance interval is given by the TCL with the least gradient. The major flaw in the analysis is the assumption that roughness is brought back to the constructed value everytime maintenance takes place. Maintenance cost was also assumed fixed no matter how rough the road is before blading.

A model called Maintenance and Design System (MDS) that evaluates alternative regraveling and blading strategies for unpaved roads was developed by Visser (*1*) using the performance relationships estimated in the Brazil study but calibrated for South African conditions. The criterion used in the evaluation was total transport costs, including road maintenance and road user costs. The model generates blading alternatives expressed in number of bladings per year. Annual average roughness is computed by integrating the roughness-time relation for every grade/curvature combination and obtaining the weighted average over the road link using as weights the proportion of the road link in each grade/curvature combination. This annual average roughness is used in the user cost computations. The total costs of maintenance and vehicle operation are computed for each maintenance strategy. The program terminates by ordering the strategies in terms of increasing discounted total costs. The MDS model is one of the most comprehensive ever applied to unpaved roads. The main disadvantage of using the model is that it has no closed-form solution: the user has to define several alternatives, simulate each alternative, and pick the one with the least cost that is not guaranteed to be the optimal solution.

From the results of the Brazil study, the World Bank developed a comprehensive model for evaluating investments on highway design, construction, and maintenance in developing countries. The system is called Highway Design and Maintenance Standards Model (HDM) (*10*). It performs financial and economic analyses of user-defined alternatives for both paved and unpaved roads. In the present working model (HDM III), sets of design, construction, and maintenance options are input as alternatives and analyzed by calculating their life-cycle costs. For unpaved roads, maintenance options are entered as number of bladings per year (blading frequency). A steady-state roughness cycle is assumed that represents an equilibrium condition given a specific blading frequency. The analysis period used is equal to one regraveling cycle. The HDM model is designed to evaluate new construction instead of exclusively the costs involved after the road is constructed (which include maintenance and road user costs). Management systems are generally applied to already constructed highways, and HDM is not the appropriate tool for this purpose.

In general, the existing maintenance management systems applied to unpaved roads could be improved by applying a technique that generates the optimal blading frequency as a function of the road characteristics and their actual relationships with vehicle operating costs and maintenance costs. An ideal system is that which does not require the user to define alternatives, which is the more rigorous solution approach. In view of this, the optimal control technique is worth exploring.

OPTIMAL CONTROL MODEL

The maintenance of unpaved roads can be characterized as a dynamic system where both condition and performance change over time. For unpaved roads, dynamic optimization techniques have the advantage of giving a closed-form solution to the highway maintenance problem compared with a simulation model like the MDS, described previously. The interaction among maintenance, deterioration, and performance can also be modeled more realistically in the dynamic optimization framework, avoiding such restrictive assumptions as constant roughness after blading or constant maintenance cost, which were assumed in the graphical model.

A review of highway literature indicates extensive studies dealing with dynamic optimization of routine maintenance and rehabilitation of paved roads. Probabilistic dynamic programming was used by Carnahan and colleagues (*11*) in determining optimal maintenance decisions for a pavement system. Balta (*12*) formulated a dynamic control model using the principles of optimal control to compute the optimum time for rehabilitation of either flexible or concrete pavements. However, the jump in the performance function resulting from application of maintenance is difficult to model in the dynamic control framework because of the discontinuity over time of the state and control variables. This difficulty constrained Balta to consider only single overlay in his formulations. In a later study, Tsunokawa (*2*) proposed a procedure for approximating the discontinuous performance function by a continuous curve, and solved the maintenance problem using optimal control. This procedure is applied to determine the optimal blading frequency for unpaved roads.

In optimal control problems, variables are divided into two classes: state variables and control variables (*13*). The simplest form of the control problem is to choose the continuous control function $u(t)$, $t_0 \leq t \leq t_1$, to solve

$$\max \pi = \int_{t_0}^{t_1} f[t, x(t), u(t)]\, dt \tag{1}$$

subject to $x'(t) = g[t, x(t), u(t)]$

$$t_0, t_1, x(t_0) = x_0 \text{ fixed; } x(t_1) \text{ free} \quad (2)$$

The functions f and g should be continuously differentiable. The control function $u(t)$ is required to be piecewise continuous with time and affects both the performance function π through its own value and the change in the state variable $x(t)$. Equation 2 is called the state equation. Solution of this type of optimization problem involves forming the *Hamiltonian* function (H) as follows:

$$H[t, x(t), u(t), \Omega(t)] = f(t, x, u) + \Omega^* g(t, x, u) \quad (3)$$

where $\Omega(t) = dH/dg$ is called adjoint, auxiliary, or co-state variable. The Hamiltonian function is similar to the Lagrangian equation used in solving a nonlinear programming problem, with Ω as the Lagrangian multiplier or shadow price. This variable represents the marginal contribution of the change in the state variable to the performance or objective function. To determine the optimal control variable $u^*(t)$, the derivative of the Hamiltonian function with respect to u, dH/du, is equated to zero. The formulation presented in Equations 1 and 2 is equivalent to a formulation for determining the optimal maintenance strategy where the function f is the discounted user and agency costs, $x(t)$ is the condition of the road, and $u(t)$ is the maintenance strategy.

Roughness Trend Curve

The extension of the general control problem to highway maintenance poses some problems because of the discontinuity in state and control variables. Figure 1 shows the state variable (roughness) as a function of time under a maintenance strategy (blading). This problem may be overcome by the use of the concept of *roughness trend curve*, which is a continuous approximation to the roughness sawtooth curve shown in Figure 1. The times t_1, t_2, and t_3 represent the blading times. The reduction G in the roughness after the first blading is a function of the roughness before blading. To solve the problem using optimal control, the sawtooth roughness curve in Figure 1 is first approximated by a continuous *average roughness curve* that passes through all the midpoints of the spikes (line AB in Figure 1). Note that the time is in days, the reason being that deterioration of unpaved roads is relatively rapid. The difference between roughnesses (ΔAB) of the two points A and B on the midpoints of the spikes is equal to

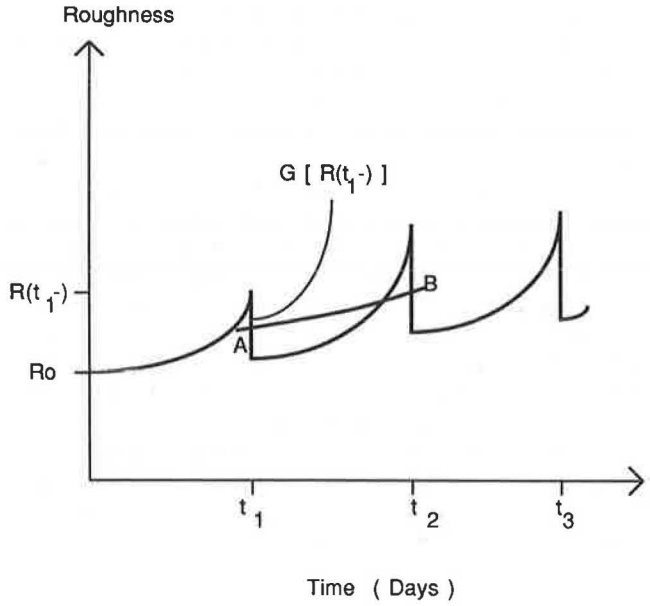

FIGURE 1 Sawtooth roughness trajectory curve.

$$\Delta AB = \int \dot{R}(t)\,dt - 1/2 * [\tilde{G}(R(t_{n+})) + G(R(t_{n-1-}))] \quad (4)$$

where

$\dot{R}(t)$ = deterioration rate of the road = $f(R(t))$,
$G(R(t_{n-1-}))$ = reduction in roughness due to blading at roughness $R(t_{n-1-})$, and
$\tilde{G}(R(t_{n+}))$ = inverse of G obtained from rewriting $x = y - G(y)$ as $y = x + \tilde{G}(x)$; equal to the reduction in roughness needed to bring roughness to condition $R(t_{n+})$.

The concept of maintenance application rate $h(t)$ is introduced such that

$$\int_{t_{n-1}}^{t_n} h(t)dt = 1 \quad (5)$$

This is simply a uniform rate of blading that has the equivalent of the impact on the average roughness in the period t_{n-1} to t_n as the average impact of blading at times t_{n-1} and t_n.

Using this relationship, the approximation of the average roughness curve by the roughness trend curve is derived as follows:

$$\int h(t) * \Delta AB\,dt \cong \int \dot{R}(t)dt - \int h(t)/2 * [\tilde{G}(R(t)) + G(R(t))]dt$$

$$\cong \int [\dot{R}(t) - h(t) * K(R)]dt \quad (6)$$

where

$R(t)$ = average roughness at time t, and
$K(R)$ = blading impact function, which
$= [\tilde{G}(R) + G(R)]/2.$ (7)

The slope of the average roughness curve is given by

$$h(t) * \Delta AB \cong \dot{R}(t) - h(t) * K(R)$$

$$\cong f[R(t)] - h(t) * K(R) \quad (8)$$

For a small interval dt, Tsunokawa (2) shows that the slope of the average roughness curve is approximated by the slope of a roughness trend curve (S) equal to

$$\dot{S} = dS/dt \cong f[S(t)] - h(t) * K(S(t)) \quad (9)$$

Problem Formulation

The rate of change in roughness for the roughness trend curve is substituted into the Hamiltonian function for a general objective function of the form

$$\min H = C(s(t)) + h(t) * M(S(t)) + z(t) * [f(S(t)) - h(t) * K(S(t))] \quad \text{subject to } h_1 \leq h \leq h_2 \qquad (10)$$

where

$C(S(t))$ = user cost function,
$h(t)$ = blading application rate,
$M(S(t))$ = agency maintenance cost function,
$z(t)$ = current value adjoint variable,
$f(S(t)) - h(t) * K(S(t)) = \dot{S}$ = $g(S,t,h)$, and
h_1, h_2 = minimum and maximum blading rates, respectively.

The necessary conditions for this minimization problem are

$$h = \begin{Bmatrix} h_1 \\ h \\ h_2 \end{Bmatrix} \text{ if } H_h = M(S) - z * K(S) \begin{Bmatrix} > \\ = \\ < \end{Bmatrix} 0 \qquad (11)$$

(12)

(13)

Equation 11 means that if the change in total cost with respect to the application rate $h(t)$ is greater than zero, then it is best to blade at the lowest frequency (h_1). Conversely, if the marginal value of the total cost decreases with the application rate (Equation 13), blading should be done as often as possible. The solutions defined by these two equations are called bang-bang controls. When the term H_h is equal to zero (Equation 12), h assumes values between h_1 and h_2 and is called a singular control solution. In practice the constraints h_1 and h_2 may be determined by resource constraints or manpower equipment, capital resource use, and minimum acceptable comfort levels.

The road deterioration equation used in the analysis is an approximation to the relationship derived from the Brazil study (*14*) and is given by

$$R = R_0 * \exp T(0.0034 + 1.3e-5 * Q) \qquad (14)$$

where R is the roughness at time T, R_0 is the initial roughness, and Q is the average daily traffic in passenger car units (pcu). Differentiating Equation 14 with respect to T yields

$$dR/dt = R_0 * \exp K_1 * T * K_1 = R * K_1 \qquad (15)$$

where K_1 is a constant term depending on the assumed value of Q. An equation predicting roughness after blading was estimated as follows:

$$RA = RB^{0.63} * \exp K_2 \qquad (16)$$

where RB and RA are the roughnesses before and after blading, respectively, and K_2 is a constant term defined by the input variables (i.e., width, plasticity index, traffic, surfacing material, etc.). The roughness values are in counts/kilometer.

Letting $K_3 = \exp K_2$, the improvement in road condition or decrease in roughness G as a result of blading is just equal to

$$G = RB - RA = RB - K_3 * RB^{0.63} \qquad (17)$$

For the continuous approximation, RB is equal to the roughness trend curve value S. The blading impact function is defined by Equation 7. The derivative of this function with respect to roughness is given by

$$K_s = \frac{1}{2} * (2 * G_s - G_s^2)/(1 - G_s) \qquad (18)$$

Differentiating Equation 16 with respect to S, substituting this to Equation 18 for K_s and finally integrating with respect to S results in the blading impact function

$$K = 0.58 * S^{1.37}/K_3 - 0.5 * K_3 * S^{0.63} \qquad (19)$$

Equations 15 and 19 can be used to define the state equation $\dot{S}$ that is required to solve the Hamiltonian function. This equation is written as

$$\dot{S} = K_1 * S - h(t) * (0.58 * S^{1.37}/K_3 - 0.5 * K_3 * S^{0.63}) \qquad (20)$$

For simplicity in calculation, the only component included in the vehicle operating cost function is the cost of fuel consumption. The analysis can be generalized by including other cost components. The expressions for vehicle speed and fuel consumption for a passenger car are taken from the Caribbean study (*15*). Cost of maintenance is influenced by the productivity of the motor grader, which is measured in terms of the number of kilometer-passes that a motor grader can blade for a given day depending on the roughness of the road to be bladed. An exponential approximation to the relationship derived from studies in South Africa (*1*) is used, which is given by

$$N(RB) = 60/\exp(0.009 * RB) \qquad (21)$$

where $N(RB)$ is number of kilometer passes/day and RB is the roughness before blading in counts/kilometer. For a road length of L kilometers and a daily cost of grader equal to CG, the maintenance cost is given by

$$M(RB) = L * CG * \exp(0.009 * RB)/60 \qquad (22)$$

This is the equation used in the optimization model, again substituting S to RB for the roughness trend curve. Given the expressions for vehicle operating costs, maintenance costs, and the differential equation representing the change in roughness trend curve with time, the general optimal control problem for unpaved roads is formulated using the Hamiltonian equation.

An upper limit is set for the frequency with which maintenance is applied. It is assumed that the most frequent interval of blading is every 25 days ($h_2 = 0.04$) or approximately once every month. To avoid the computational problems that arise when very low values of h are considered (2), a lower bound (h_1) for the application rate is defined, which is 0.005 or once every 200 days. Again, these bounds may be set to reflect resource constraints, resource use, and minimum comfort levels.

In summary, the optimal control model for unpaved roads has been developed using the deterioration and maintenance equations estimated in previous road studies. To be able to generate the components of the objective function (vehicle operating costs and maintenance costs) that will be minimized in the optimization problem, prediction equations for fuel consumption and number of days required to blade a road of certain roughness have been defined. The solution to the optimization problem using these equations is not expected to generate results that correspond to actual field experience because of the nature of equations used. For instance, fuel consumption is the only component of vehicle operating cost included. This cost function monotonically increases with speed. Because speed is inversely related to roughness, the cost function used decreases with roughness. This is not the case when other costs are included, such as vehicle depreciation, because this cost component increases with roughness. On the other hand, the cost of blading increases with the roughness of the road. The cost of maintenance then increases with the roughness. The functional equation used for maintenance cost is negative exponential, which simply means that extremely high blading costs are incurred at high roughnesses. This will offset the alternative to keep the road very rough and fuel consumption at its minimum, as the road needs to be bladed at least every year and the cost for blading an extremely rough road is extremely high. The following case study is intended to illustrate the application of the model and its sensitivity to changes in parameters based on the cost components used. The results should not be compared with real field solutions but are intended to demonstrate the applicability of the solution method.

CASE STUDY

Two *hypothetical* cases with different levels of traffic are used to test the preceding models. The volumes are 30 pcus/day and 250 pcus/day, respectively. Table 1 shows the parameters assumed for both cases. These parameters were assumed constant in the solution.

TABLE 1 VARIABLES USED IN CASE STUDY

Cost of Grading	$ 200 / day
Rise	5 meters/km.
Fall	5 meters/km.
Interest Rate	8 % per annum
Fuel Cost	28 ¢ / liter
Curvature	5º / km.
Type of Surface	lateritic gravel
Plasticity Index	5 %
Length of Road	10 kms.
% Passing 0.075 mm Sieve	15 %
Width of Road	10 meters

Results

The analysis begins by plotting the two curves $H_h = 0$ and $\dot{H}_h = 0$ on the S-z plane, as shown in Figures 2 and 3. The intersection of the two curves represents the singular control solution that also satisfies the steady-state conditions ($\dot{S} = 0$ and $\dot{z} = 0$). At steady states, S and z both attain time-invariant values corresponding to the coordinates of the intersection of the two curves defined by the following parameters:

Case 1: $Q = 30$ pcus/days	Case 2: $Q = 250$ pcus/day
$S = 150.5$ QI	$S = 266$ QI
$z = 1.26$	$z = 1.52$
$h = 0.0056$ (every 180 days)	$h = 0.0074$ (every 136 days)

The singular controls found in the two cases are between the minimum and maximum frequencies set for the problem, hence there are no bounded control solutions for this problem.

Because the initial roughness of the road differs from the steady-state roughness, a roughness trajectory curve (2) is constructed for each case. Assuming a range of roughness values within which the initial roughness is assumed to fall, it is determined whether all values in this range actually converge to the steady-state solution. The curves defined by such roughness values are called stable branches. Stable branches are derived by integrating the canonical equations $\dot{S} = 0$ and $\dot{z} = 0$ with respect to t and solving for the appropriate terms in the expressions $S(t)$ and $z(t)$ such that when both terms are differentiated, both S and z are time invariant. However, the expressions for S and z in the unpaved roads problems do not allow such calculations to be made. Hence, the stable branches are determined by calculating S and z at different points on the S-z plane and drawing the curves that converge to the steady-state solutions. Figures 4 and 5 show the minimum roughnesses (70 for Case 1 and 230 for Case 2) that exist for the stable branches. A maximum roughness value of 300 for the roughness trend curve was arbitrarily assumed. These extreme values are the ranges to be used in the analysis.

The roughness trend curves are drawn assuming an initial roughness within the ranges defined. Such curves are shown on Figures 6 and 7 for Case 1. Equation 5 is used to convert the roughness trend curve to the true sawtooth curve that is also shown on Figures 6 and 7. The discrete blading times (t_n) are determined from the sawtooth curve. For the first blading, the roughness trend curve passes through the midpoint of the first spike.

To check if the given solutions are the true minima, the total costs of the steady-state solutions are compared with the

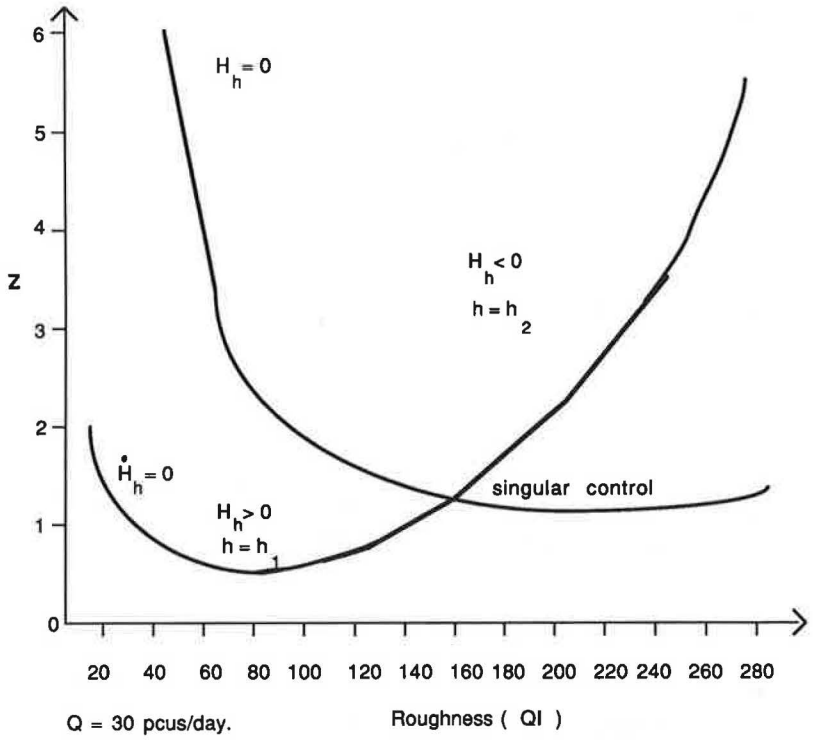

FIGURE 2 Graph of $H_h = 0$ and $\dot{H}_h = 0$ for Case 1.

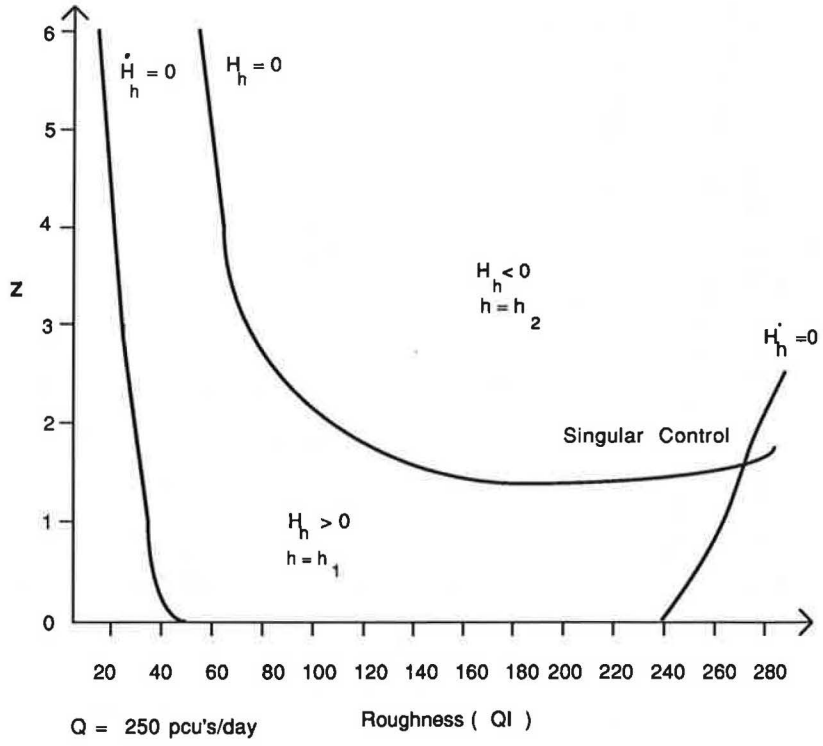

FIGURE 3 Graph of $H_h = 0$ and $\dot{H}_h = 0$ for Case 2.

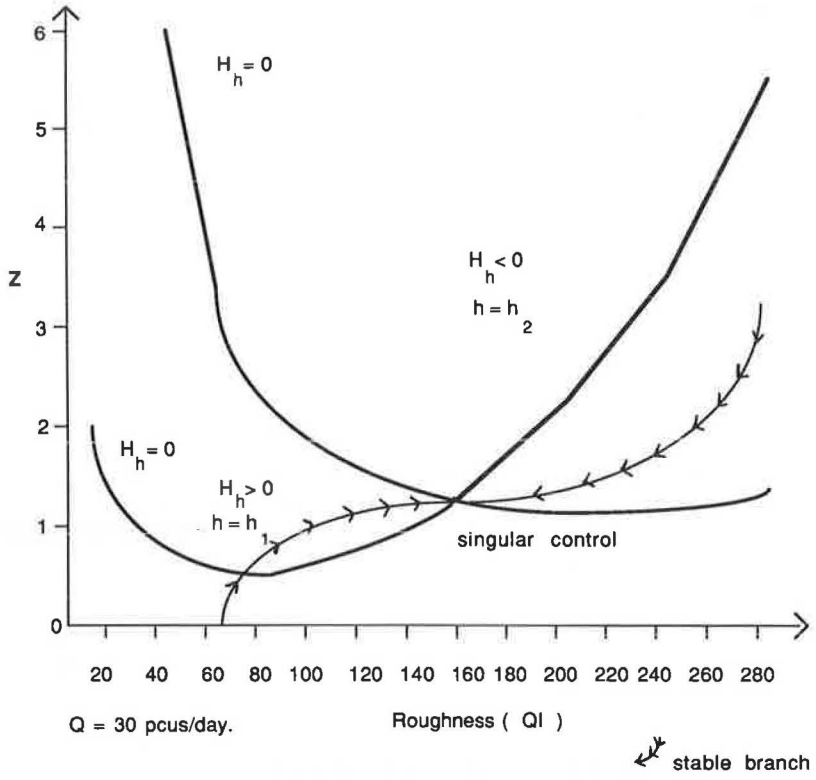

FIGURE 4 Stable branches for Case 1.

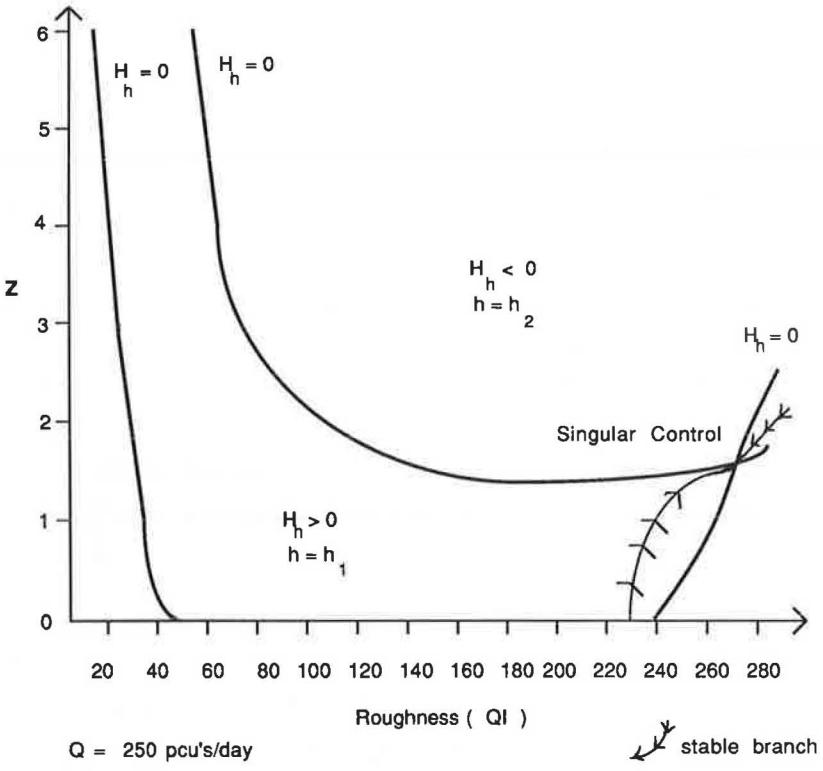

FIGURE 5 Stable branches for Case 2.

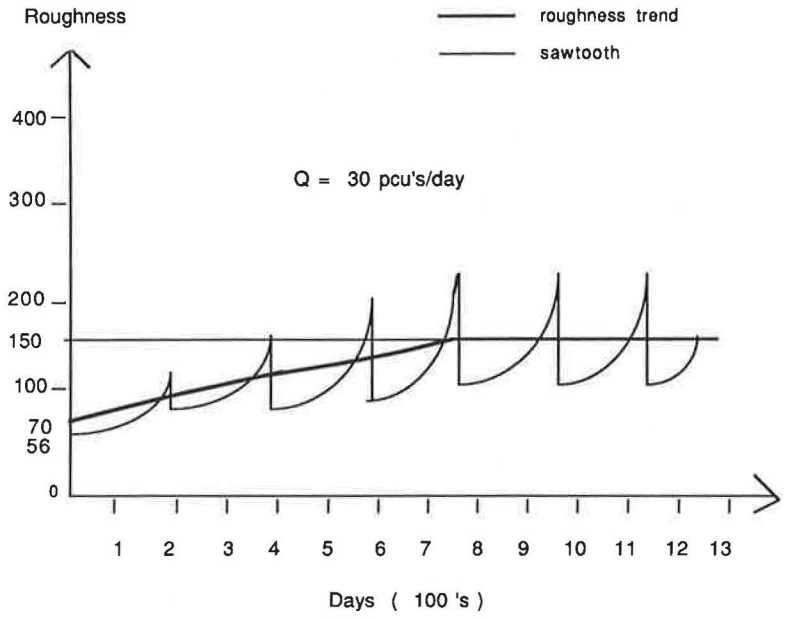

FIGURE 6 Roughness trend curve and sawtooth curve for Case 1 with initial roughness = 70 QI.

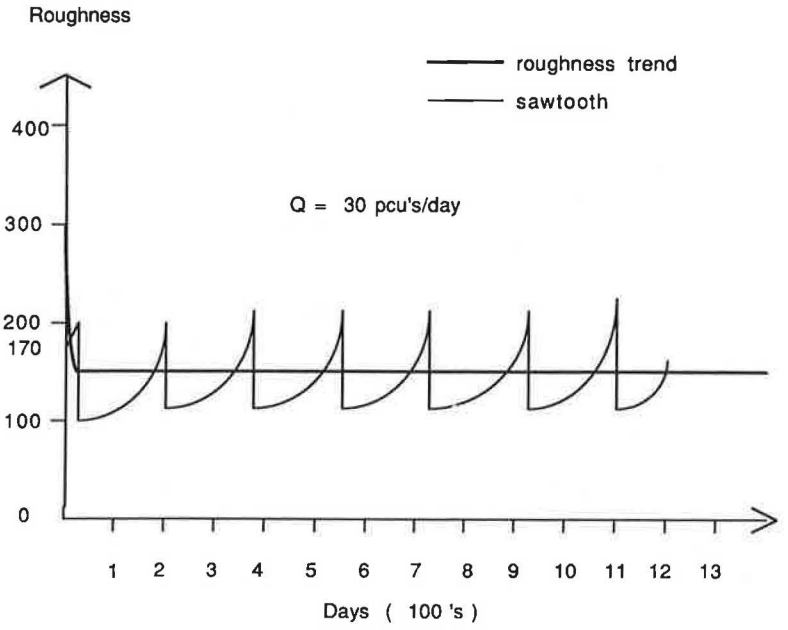

FIGURE 7 Roughness trend curve and sawtooth curve for Case 1 with initial roughness = 300 QI.

costs associated with other blading frequencies. The results are shown on Table 2. The values shown are not significantly different from each other. However, note that the case study is only for a 10-km road. If the same analysis is made for the entire unpaved road network, say, in Bolivia, which has a total length of 36,155 km, the amount that represents the difference in blading interval of 30 days (every 150 days instead of 180 days) for Case 1a is equal to $6.25 million for the entire planning horizon or $0.5 million annually using an interest rate of 8 percent. If traffic were to increase to 250 pcus/day as in Case 2, the amount corresponding to a difference in blading interval of 36 days (100 instead of 136) is equal to $17.8 million for an infinite planning horizon, or $1.42 million annually. For a developing country like Bolivia, these amounts represent significant improvement in the overall highway economy. The impacts are emphasized by comparing the total costs for the optimal solutions in both cases when applied to the total road network in Bolivia. Table 3 gives us some idea of the order of costs associated with a system of unpaved roads in a developing country like Bolivia.

TABLE 2 TOTAL COSTS IN DOLLARS FOR OPTIMAL AND NONOPTIMAL SOLUTIONS

		FREQUENCY	
	optimum		
Case 1a	every 180 days	every 150 days	every 200 days
Ro = 56 QI	37,234	38,963	43,105
Case 2a	every 136 days	every 100 days	every 150 days
Ro = 132 QI	287,496	292,426	298,782

TABLE 3 TOTAL COSTS (OPTIMAL) WHEN EITHER SCENARIO APPLIES IN BOLIVIA

	for a 10 km. road	for the whole network
Case 1a	$ 37,237	$ 134.6 B (entire horizon)
		$ 10.8 M (annually)
Case 2a	$ 287,496	$ 1039 B (entire horizon)
		$ 83.2 M (annually)

Sensitivity Analysis

The objective of this exercise is to see how the solution shifts from the optimal solution of the base problems when other variables are changed and determine whether the shifts make sense intuitively on the basis of the relationships between maintenance and vehicle operating costs used in the formulation. It is the direction of the changes that are important, not the absolute change. For example, if the traffic level is higher then it is expected, that blading will be required more frequently. Table 4 shows the results of these tests. The optimum frequency of blading is indeed a function of the different variables, notably the volume of traffic and the cost of fuel. For the base case with an average daily traffic of 30 pcus, it can be observed that increasing the fuel cost results in less frequent optimum blading (therefore higher steady-state roughness) because fuel consumption increases with speed; therefore, it is better to keep the road rough to reduce the vehicle speeds. On the other hand, if the daily cost of grading is doubled, the optimal solution is to blade more frequently so that the steady-state roughness declines. Because the maintenance cost increases with roughness before grading, it is more economical to keep the average roughness low, reducing the cost per blading and the user costs. Interest rate is found to be insignificant in the optimal solution.

Increasing the average daily traffic to 250 pcus raises both the frequency of maintenance and the steady-state roughness. This makes sense intuitively because doing more frequent maintenance in this case does not stop the average roughness from attaining a high value as a result of the traffic. When the fuel cost is increased to $1 per liter and the traffic remains the same, no optimum is found. However, decreasing the price of gasoline to $0.1 per liter shifts the optimum blading frequency to a higher value. With lower fuel prices, the vehicle speeds may be increased without considerably increasing the vehicle operating costs. The optimum solution is to blade the road more frequently so that the average roughness (and therefore the cost of maintenance) can be lowered. Further increase in the traffic volume (900 pcus daily) results in no optimal solution because of the exponential form of the deterioration function that predicts extremely high roughness for this volume.

The preceding sensitivity analysis is made to test how the model responds to changes in the different parameters and whether the results of applying it to different scenarios correspond with the expected results on the basis of the equations used in the formulation. The results that will be generated by using a different set of deterioration and cost functions will be different.

Computer Implementation

The amount of computation involved in solving the optimal control problem requires the use of a computer. For this reason, a program was written that gives the values of the roughness (S) and the adjoint variable (z) that were plotted on the S-z graphs. The steady-state solutions (singular and bounded controls) are also calculated by the program. In determining stable branches, however, manual computation was made, although this could have been done with the computer as well. Finally, the path traced by the roughness trend curve from the initial roughness was computed using a numerical approach. Cost computations were done using numerical integration.

SUMMARY AND RECOMMENDATIONS

The application of dynamic optimization in setting optimal blading frequencies for unpaved roads is shown to be useful in the maintenance of unpaved roads. A review of the existing systems used to manage unpaved roads indicates that the classification-based types of maintenance systems are popular in developed countries. Some mathematical optimization and simulation techniques have been applied. These systems, however, either suffer from very restrictive assumptions to solve the problem or do not give closed-form solutions. The dynamic optimization approach solves both problems. It has the advantage of being more realistic than the graphical anal-

TABLE 4 SENSITIVITY ANALYSIS

PARAMETERS	CASES										
	1*	2	3	4	5	6	7	8	9	10	11
No. of PCUS.	30	250			900		250	250	250	250	250
Fuel Cost ($/liter)	0.28					1	1	1	1	0.1	
Cost of Grading ($/day)	200		400								400
Length (km.)	10										
% passing 0.0075 mm sieve	15										
Plasticity Index	5										
Interest Rate (%)	8			20					20		
Width of Road (m)	10										
Surfacing T1 T2	0 0										
Rise (m/km)	5										
Fall (m/km)	5										
Blading Season	wet										
Curvature (deg/km)	5										
No. of Bladings /year	2	2.7	2.4	1.97	—	1.8	—	—	—	3.4	3.1
Steady State Roughness	150	266	124	158		175				182	208
Adjoint Variable (z)	1.26	1.52	2.79	1.24		-1.1				1.32	2.68

— no solution

* value for block with no entry same as that for Case 1

ysis. Likewise, the user does not have to define possible maintenance strategies because the solution is explicitly defined by the problem. The optimization technique chosen is optimal control, because the condition (roughness) curve is not constant between blading and this is very difficult to model in the dynamic programming framework. However, the discrete jumps in the condition function due to application of maintenance make the optimal control solution infeasible. This was overcome by approximating the sawtooth condition curve by a continuous curve, following Tsunokawa's approximation.

The results of this research must be interpreted carefully as the prediction equations and performance functions used in the analysis with which the optimization formulation was made are just approximations to the existing models and are in functional forms that may not represent the true relationship between deterioration, maintenance, and vehicle operating cost. The existing models have very poor explanatory power and functional forms not suitable for the optimization formulation. Hence, the research is basically an exploratory analysis of the solution to the optimization problem. Further research is needed on (a) developing equations predicting highway deterioration, vehicle operating costs, and maintenance costs with functional forms suitable for optimization and estimated from actual data; (b) solving the more general case of varying traffic volume that was assumed constant in the model; (c) incorporating other components of vehicle

operating costs, such as lubrication costs, tire wear, and parts consumption; and (d) including regraveling in the maintenance decision problem.

ACKNOWLEDGMENT

This research was sponsored by the National Science Foundation through a Presidential Young Investigator Award to Sue McNeil. The authors would also like to acknowledge the people who reviewed this paper for their valuable advice and comments.

REFERENCES

1. A. T. Visser. *An Evaluation of Unpaved Roads Performance and Maintenance*. Ph.D. dissertation. University of Texas at Austin, Feb. 1981.
2. K. Tsunokawa. *Optimization Models for Comprehensive Transportation Infrastructure Maintenance: Highway Pavement Maintenance Case*. Ph.D. thesis. Northwestern University, Evanston, Ill., Aug. 1986.
3. W. O. Paterson. *Road Deterioration and Maintenance Effects*. World Bank; Johns Hopkins University Press, Baltimore, 1987.
4. R. M. Alfelor. *Optimal Maintenance Frequencies for Unpaved Roads*. SM thesis. Massachusetts Institute of Technology, Cambridge, May 1988.
5. J. P. Guilford. *Psychometric Methods*. McGraw-Hill, New York, 1954.
6. T. E. Jones. *Kenya Maintenance Study on Unpaved Roads: Research on Deterioration*. TRRL Report 1111. Crowthorne, Berkshire, England, 1984.
7. M. W. Sayers, T. D. Gillespie, and C. V. Queiroz. The International Road Roughness Experiment: Establishing Correlation and Calibration Standards for Measurements. Technical Paper 45. World Bank, Washington, D.C., Jan. 1986.
8. E. F. Dobson and L. J. Postill. Classification of Unpaved Roads in Ontario. In *Transportation Research Record 898*, TRB, National Research Council, Washington, D.C., 1983, 36–47.
9. H. R. Kerali and M. S. Snaith. *A Simplified Method of Determining Optimum Maintenance Frequencies for Roads in Developing Countries*. Sixth IRF African Highway Conference, Cairo, 1985.
10. *Highway Design and Maintenance Standards Model (HDM III). Model Description and User's Manual*, Vol. IV. World Bank, Transportation Department, Washington, D.C., March 1985.
11. J. V. Carnahan, W. J. Davis, M. Y. Shahin, P. L. Keane, and M. I. Wu. Optimal Maintenance Decisions for Pavement Management. *Journal of Transportation Engineering*, Vol. 113, No. 5, Sept. 1987.
12. W. S. Balta. *Optimal Investment Policies for Maintenance and Rehabilitation of Highway Pavements*. SM thesis. Massachusetts Institute of Technology, Cambridge, 1982.
13. M. Kamien and N. Schwartz. Dynamic Optimization: The Calculus of Variations and Optimal Control in Economics and Management. Vol. 4. Elsevier Science Publishing Co., New York, 1981.
14. GEIPOT. Research on the Interrelationships Between Costs of Highway Construction, Maintenance and Utilization. Vol. 7. Empresa Brasileira de Planejamento de Transportes, Brasilia, Brazil, 1981.
15. H. Hide, G. Morosiuk, and S. Abaynayaka. Vehicle Operating Costs in the Caribbean. In *Transportation Research Record 898*, TRB, National Research Council, Washington, D.C., pp. 65–72.

Publication of this paper sponsored by Committee on Low Volume Roads.

Effects of Temperature and Moisture on the Load Response of Granular Base Course Material in Thin Pavements

DJAN CHANDRA, KOON MENG CHUA, AND ROBERT L. LYTTON

Theoretical models to account for temperature and moisture effects on granular base course materials are developed. The models, based on a micromechanical approach that treats the granular materials as elastic spheres in contact, can be used to formulate temperature and seasonal adjustment factors for low-volume roads and to estimate when and where seasonal load restrictions are required. The thermal model relates the volumetric expansion caused by temperature increase to the increase of confining pressure, which results in an increase in the pavement modulus. The moisture model is based on thermodynamic laws and considers the granular materials as a two-phase system. One phase represents the soil particles, and the other phase represents an air-water mixture surrounding the soil particles. To verify the models, pavement layer temperatures and Falling Weight Deflectometer deflection readings were taken at hourly intervals throughout the day on two pavement test sections at the Texas Transportation Institute Research Annex. In addition, six farm-to-market roads in different regions of the state of Texas were monitored. Deflection readings, rainfall data, and pavement temperature and suction readings were collected over a 10-month period. A comparison of the predicted moduli at different temperatures and moisture conditions with the backcalculated moduli from deflection basins is made to verify the models. An example problem of the application of the models for the predictive purpose is also presented.

Nondestructive testing devices have been extensively used to evaluate the structural integrity of pavements by measuring pavement surface deflections. These deflections are known to vary with the temperature and season at the time when testing is conducted. A common method to account for the temperature and seasonal variations is to develop adjustment factors based on observed data. The shortcoming of this approach is that although it can provide reasonable predictions for the location in which the observations were made, it does not explain the phenomenon behind these variations.

The structural integrity of pavements over any period of time (even within the day) can be affected by (a) the variation of moisture content caused by rainfall, temperature gradients, rise and fall of the water table level; (b) daily temperature fluctuations; and (c) freeze-thaw cycles. The fundamental mechanism of temperature and moisture effects on granular materials must be understood to improve the interpretation of surface deflection data. In this study, the models to account for temperature and moisture are theoretical in approach.

D. Chandra, Leighton and Associates, Walnut, Calif. 91789. K. M. Chua, University of New Mexico, Albuquerque, N.M. 87131. Robert L. Lytton, Texas A&M University, College Station, Tex. 77843.

Rather than formulating empirical relationships, the objective of this paper is to identify the various mechanisms by which the pavement will respond to temperature and moisture changes. The thin pavements considered here are the two-layer surface-treated type. The surface treatment is for waterproofing and also serves as a wearing course. The main load-bearing layer is the granular base course layer.

BACKGROUND

The nondestructive testing device and the backcalculation program used in this study are briefly discussed. Published works on methods of modeling temperature and seasonal effects on pavements are also reviewed.

Nondestructive Methods of Pavement Evaluation

In nondestructive testing of pavement, the deflection basin resulting from a static or dynamic load is recorded and then analytical methods are used to predict or match this basin. The material properties that give this matching basin are assumed to be those of the materials in the field. There are numerous nondestructive testing devices capable of applying dynamic load and recording deflections at various distances from the loading plate. The Falling Weight Deflectometer (FWD) is one of the more popular of these devices that are reported to be able to simulate pavement response under moving load (*1–3*). The FWD imposes an impulse load of between 2,500 lb and 24,000 lb, which is transmitted to the pavement through a 300-mm-diameter circular loading plate; at the same time, surface deflections are recorded by geophones at seven different locations. The loading period roughly corresponds to a wheel speed of 40 to 50 mph. The FWD used in this study was the Dynatest 8000 FWD.

A number of computer programs have been developed to backcalculate layer elastic moduli from deflection basins obtained by nondestructive testing. Most of these programs were developed on the basis of layered elastic theory or the finite element method. A detailed comparison of these programs for backcalculating layer moduli of low-volume roads has been presented by Chua (*4*). In this study, the LOADRATE (*5*) program was used. LOADRATE considers only surface-treated types of pavement. It uses regression equa-

tions based on results generated from a finite element program, ILLIPAVE. The equations were developed to relate the nonlinear elastic parameters of the bulk stress model (for the base material) and the deviator stress model (for the subgrade material) with the deflections at the load point and at some distance away from the load. Layer moduli were then calculated from these parameters. This program was developed to analyze vast amounts of deflection bowls very quickly and was written for evaluating farm-to-market roads.

Monitoring Moisture Presence in Soils

Soils just beneath the base course layer are usually unsaturated. Kersten (*6*) monitored moisture conditions of the upper 6 in. of the subgrade beneath flexible pavements in six states and reported that the degree of saturation of the subgrades averaged 73 percent. In the same study, Kersten also found that only 15 percent of the tests showed a saturation value of 90 percent or greater. Unsaturated soil is different from saturated soil in that it is a three-phase system consisting of solid, water, and air.

Soil suction has been used to characterize the effect of moisture on the volume and strength properties of unsaturated soils. Soil suction is defined as the free energy present in soil water with respect to a pool of pure water located outside the soil at the same elevation (*7*). It is made up of two components, the osmotic, which is due to dissolved salts, and the matrix suction, which is a negative pressure that exists in the soil water as a result of the capillary tension in the water. The soil suction can be measured by several methods, including a psychrometer, which measures the total suction, and a thermal moisture sensor, which measures the matrix suction. The use of the psychrometer is limited to soils with suctions lower (more negative) than -1 bar (-14.51 psi), while the moisture sensor is used for suctions higher than -1 bar.

Methods of Modeling the Effects of Temperature and Seasonal Variations

Pavement surface deflections have been found to vary with temperature, especially for flexible pavements. For the thick asphaltic concrete type of flexible pavement, higher temperatures are generally associated with larger deflections. Various temperature models have been formulated to simulate temperature in a pavement system. Most of the models have been developed to estimate temperature distribution with depth. One widely used empirical method to predict temperature at depth in an asphaltic concrete pavement has been developed by Southgate and Deen (*8*). This method estimates the temperature at any depth in a flexible pavement up to 12 in. thick provided that the surface temperature, the 5-day mean air temperature, and the time of the day are known. The analytical type of solution uses the Fourier diffusion equation for determining conductive heat transfer in a pavement system (*9, 10*).

There are two approaches to account for the effects of temperature on a pavement system. The first approach involves assigning incremental deflections for each degree of temperature difference between the pavement temperature and the reference temperature (*11–13*). The second method involves the use of a dimensionless multiplicative factor that is applied to a measured deflection at some known mean temperature of the pavement. This type of adjustment factor has been developed for the Benkelman beam (*8, 14*), Road Rater (*15*), and Dynaflect (*16*).

Other empirical formulas have been developed to estimate seasonal variations of pavement strength. From laboratory test results, Thompson and Robnett (*17*) developed a correlation between resilient modulus and degree of saturation for different soil types. Bibbens et al. (*1*) developed laboratory-determined resilient modulus versus moisture content curves. Cumberledge et al. (*15*) monitored five field test sites in Pennsylvania to collect temperature, engineering properties of subgrade soils, and Road Rater deflections. Multilinear regression analysis was performed to relate variations in surface deflections to changes in moisture content, percent of material passing a no. 200 sieve, thickness of pavement, liquid limit, and dry unit weight. Among the variables, changes in moisture content were found to be most influential on pavement surface deflections.

SIMPLIFIED MODEL FOR THERMAL EFFECTS ON GRANULAR SOILS

There are two main approaches for modeling soil behavior: the phenomenological approach and the micromechanical approach. The phenomenological approach treats the soil as a continuum that may include thousands to millions of soil grains and pores, and it analyzes the mechanism of the continuum as a whole. The micromechanical approach observes the behavior of soil at the grain level and considers the forces and deformations at contact points between individual particles.

Most micromechanical models seeking to describe analytically the mechanical behavior of granular soils are based on the Hertzian contact theory that deals with a pair of homogeneous, isotropic, elastic spheres in contact, compressed statically by a normal force (*18*). Other models include an extension of the theory by Mindlin (*19*) and Mindlin and Deresiewicz (*20*) that considers tangential force at contacts. The micromechanical approach has been successful, at least, in the qualitative predictions of the behavior of granular aggregates (*21, 22*).

Modeling Approach

The model developed here views the granular soil as an assemblage of soil particles that are in contact and subjected to temperature changes. Two different packing configurations that represent the densest and loosest arrangement of equal spheres are considered. The packings and the corresponding unit elements are shown in Figure 1. When unit elements are put together, they will form a regular array without addition or subtraction of spheres. The unit element of the simple cubic packing (SC) has a porosity of 47.64 percent, whereas that of the face-centered cubic (FCC) has a porosity of 25.95 percent. For typical granular soils, Ottawa sand, for example, the simple cubic array and the face-centered cubic array will have dry unit weights of 87.23 pcf and 123.4 pcf, respectively. Because

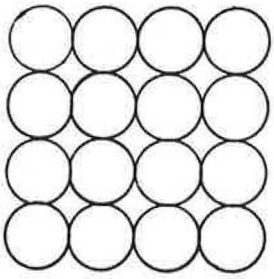

(a) Plan View of Simple Cubic Packing.

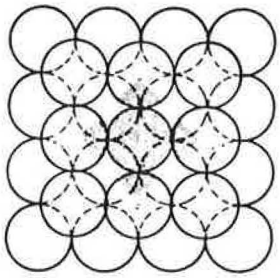

(b) Plan View of Face-centered Cubic Packing.

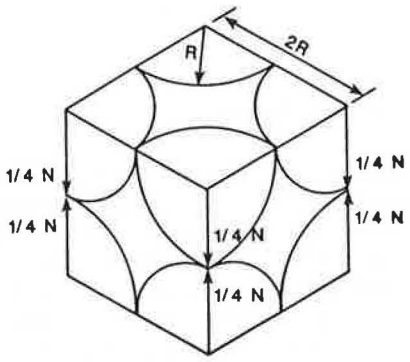

(c) Unit Element of Simple Cubic.

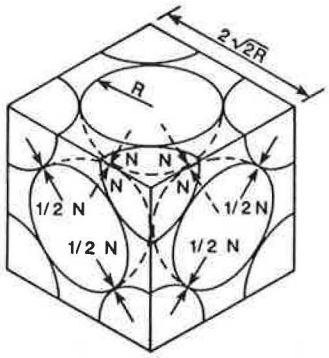

(d) Unit Element of Face-centered Cubic.

FIGURE 1 Modes of packing of equal spheres.

the model is developed for two packing configurations, the states between the loosest and densest condition are obtained by statistical estimates.

Granular base course soil particles in the field are subjected to overburden pressure and residual stresses. In this model, the soil particles are assumed to be confined in all directions. As such, owing to the inability of the particles to expand because of the confinement, a rise in temperature will cause an increase in the contact forces between particles. The contact pressures that are related to the confining pressure will then affect the stiffness of the soil. The resilient modulus is assumed to be related to the confining pressure in the following manner:

$$E = K_1 \theta^{K_2} \tag{1}$$

where

E = resilient modulus,
θ = bulk stress (sum of the three principal stresses), and
K_1, K_2 = constants.

It should be noted that other nonlinear models for resilient modulus where changes of confining pressure can be implemented can be used instead of Equation 1. The change of modulus with respect to the change of bulk stress is obtained by taking the derivative of Equation 1, which yields

$$\Delta E = K_1 K_2 \theta^{K_2 - 1} \Delta\theta \tag{2}$$

It can be seen that a rise in temperature will result in an increase of the stiffness, which will of course depend on the initial level of confining pressure and on the material properties.

Development of the Simplified Model

According to Hertzian contact theory, the centers of two spheres in contact under a normal force N will approach one another by an amount z given by

$$z = 2\left[\frac{\omega N}{R^{1/2}}\right]^{2/3} \tag{3}$$

in which

R = radius of the spheres,
$\omega = \frac{3}{4}[(1 - \nu^2)/E]$ is a property of the material,
E = elastic modulus, and
ν = Poisson's ratio.

The volumetric strain of the sphere is given by

$$\frac{\Delta V}{V} = \frac{3\Delta L}{L} = 3\frac{Z}{2R} = \frac{3}{R}\left[\frac{\omega N}{R^{1/2}}\right]^{2/3} \quad (4)$$

Referring to Figure 1c, when a uniform pressure p_{sc} acts on the unit element of the simple cubic (SC) array, the normal force N is related to p_{sc} by

$$N = 4R^2 p_{sc} \quad (5)$$

and substituting N into Equation 4 gives

$$\frac{\Delta V}{V} = 3\,(4\omega\, p_{sc})^{2/3} \quad (6)$$

Similarly, for the face-centered cubic (FCC) array,

$$N = \sqrt{2}R^2 p_{FCC} \quad (7)$$

and substituting N into Equation 4 gives

$$\frac{\Delta V}{V} = 3(\sqrt{2}\omega\, p_{FCC})^{2/3} \quad (8)$$

When the unit elements are subjected to temperature increase, ΔT, the volumetric strain in Equations 6 and 8 can be expressed as

$$\frac{\Delta V}{V} = \alpha_v\, \Delta T \quad (9)$$

where α_v = cubical thermal coefficient, which is approximately three times the linear thermal coefficient, α.

According to Smith et al. (*23*), an assembly of randomly packed like spheres may be regarded as an arrangement of separate clusters of simple cubic array and face-centered cubic array, each present in a proportion to yield the observed porosity, n_{obs}, of the assembly. Thus, if x represents the fraction of close-packed spheres, then

$$n_{obs} = x\, n_{FCC} + (1 - x)\, n_{sc} \quad (10)$$

Similarly, the hydrostatic pressure, p, acting on a granular medium with a porosity n can be approximated by

$$p = x\, p_{FCC} + (1 - x)\, p_{sc} \quad (11)$$

The pressures for the two different cubic arrays can be obtained from Equations 6 and 8, and Equation 11 becomes

$$p = \left(\frac{x}{\sqrt{2}\omega} + \frac{(1 - x)}{4\omega}\right)\left(\frac{1}{3}\alpha_v \Delta T\right)^{3/2} \quad (12)$$

The hydrostatic pressure in Equation 12 is caused by a change of temperature. If the initial bulk stress is θ, the pressure from the preceding equation is the change of the bulk stress, $\Delta\theta$, due to temperature variations. The new modulus can then be calculated by adding the change of modulus from Equation 2 to the original modulus.

Material Properties

The elastic modulus and thermal coefficient that appear in the equations shown earlier are for the individual soil particles and not for the soil mass. For their micromechanical model, Ko and Scott (*22*) assumed that the sand grains are the same material as silicon glass, and used the elastic modulus of 10×10^6 psi and Poisson's ratio of 0.17. Yong and Wong (*24*) reported that the elastic modulus and the Poisson's ratio of Ottawa sand grains is 12.5×10^6 psi and 0.17, respectively. Willis and De Reus (*25*) designed and constructed an apparatus that mainly consisted of a temperature control box with optical lever to measure the linear thermal coefficient of different types of rocks. These results are shown in Table 1, which lists the properties, namely, elastic modulus and linear thermal coefficient, of different types of materials.

MODEL FOR MOISTURE EFFECTS ON GRANULAR SOILS

Lamborn (*26*) formulated a micromechanical model to represent the load-deformation behavior of a partly saturated soil using the thermodynamic laws. The model consisted of

TABLE 1 MATERIAL PROPERTIES OF ROCKS (*25*)

Material	Elastic modulus ($\times 10^6$, psi)	Linear thermal coefficient ($\times 10^{-6}$)
Chert	3.1-18.0	6.0-7.2
Quartzite	3.8-10.2	6.2-6.9
Sandstone	2.9- 4.0	6.3-6.6
Basalt	11.4-13.9	3.9-5.9
Granite	7.6- 9.8	2.8-5.3
Limestone	5.1-12.6	1.8-5.4
Dolomite	2.5-10.0	4.0-5.0

equal spheres in contact, surrounded by an air-water mixture, each considered as a different phase. Both phases were modeled as homogeneous, isotropic, linear elastic materials. An equation that relates the mean principal stress acting on the system to the Helmholtz free energies per unit initial volume of the two phases, and the strain tensor was developed. The equation is given as

$$\bar{\theta} = C_s \frac{\partial \bar{F}_s}{\partial \bar{\varepsilon}_{kk}} + C_w \frac{\partial \bar{F}_w}{\partial \bar{\varepsilon}_{kk}} \tag{13}$$

where

θ = mean principal stress,
C_s, C_w = initial volume fractions for solid and water, respectively,
F = Helmholtz free energy, and
ε_{kk} = $\Delta V/V$ = volumetric strain.

The overbar denotes the average values of the quantities, and the subscripts s and w represent the solid and water phase, respectively. A change in suction will alter the Helmholtz free energy of the water phase, but not the solid phase. Thus, the first term on the right-hand side of the preceding equation is equal to zero because of suction change. The change in the mean principal stress, $\Delta\theta$, is obtained by taking the derivative of Equation 13 with respect to the volumetric strain, and yields

$$\Delta\theta = C_w (\Delta P_w) \tag{14}$$

where ΔP_W equals the change in mean principal stress of the water phase, which is equivalent to the change in suction. Thus,

$$\Delta\theta = -\Delta(\text{suction}) (V_w/V_T) \tag{15}$$

where V_w equals the volume of water and V_T equals the total volume.

Equation 2 can then be rewritten to include the change of the bulk stress caused by the temperature and the suction change,

$$\Delta E = K_1 K_2 \theta K_2 - 1 (\Delta\theta_T + \Delta\theta_s) \tag{16}$$

where the subscripts T and s denote temperature and suction, respectively.

FIELD STUDIES

Test Sites and Instrumentation

Two field studies were made. The first part involved taking FWD deflection readings on two surface-treated pavement sections at the TTI Research Annex at various temperatures. The tests were conducted at hourly intervals throughout the day several times in a year. The tests were conducted at different temperatures in the same day in an attempt to eliminate seasonal effects.

The second field study involved collecting data from six farm-to-market road sections located in different regions of the state of Texas. Monthly FWD readings as well as monthly subgrade soil suctions and temperatures at different depths were collected for 10 months. The locations of the test sites were selected on the basis of different climatic zones and subgrade soil types. The characteristics of the test sites are summarized in Table 2.

Wooden roods with thermocouples attached at different depths were inserted into the pavement sections. Thermal moisture sensors were installed in Districts 11 and 21 and measure matrix suction. As for District 8, psychrometers, which measure the total suction, were used because this area is dry. Base and subgrade materials were also retrieved from all of the test sections for laboratory testing.

TABLE 2 CHARACTERISTICS OF TEST SITES

Site	Closest weather station	Annual rainfall (in.)	Base course				Subgrade			
			Thickness (in.)	%passing #200	Classification AASHTO	Classification Unified	LL/PL	%passing #200	Classification AASHTO	Classification Unified
Annex 10	Easterwood	39.1	16	-	-	-	-	-	-	-
Annex 11	Easterwood	39.1	16	-	-	-	-	-	-	-
D8/FM1235*	Abilene	23.26	8	3	A-1-a	GP	43/31	58	A-7-6	CH
D8/FM1983	Roscoe	23.35	8	5	A-1-b	SW	25/16	27	A-2-6	SC
D11/FM2864	Nacogdoches	39.7	8.5	11	A-1-b	SW-SM	43/33	58	A-7-6	CH
D11/SH7	Nacogdoches	39.7	9.5	7	A-1-b	SP-SM	18/-	5	A-2-4	SP-SM
D21/FM491	Raymondville	27.48	8	4	A-1-a	GW	26/17	43	A-6	SC
D21/FM497	Raymondville	27.48	8.5	7	A-1-a	SP-SM	31/20	32	A-2-6	SC

* D denotes district

Observed Temperature Variations

The results of the tests obtained from the TTI Research Annex are discussed in this section. Figure 2 shows a plot of air temperature, base course temperature, and subgrade temperature variations within a day as obtained in September for Test Section 11. The base course temperature followed the same pattern as the air temperature except that there exists, as expected, a time lag between the two. In the afternoon, the base temperature reached its highest point approximately 2 hr after the air temperature. At night, the heat trapped in the pavement dissipated slowly, causing the temperature of the base course to be higher than the air temperature. This is illustrated in Figure 3. From Figure 2, it appears that the subgrade temperature did not fluctuate much within a day.

Two deflection basins obtained at the highest and lowest base course temperatures of the day are plotted in Figure 4. Even though the base course modulus is higher at 104°F, it does not necessarily imply that the deflection at every sensor location is lower at 104°F than at 84°F. As such, the deflection change at any individual sensor cannot be used as an indication of the variations of the pavement moduli. It is partly for this reason that in this study the changes of the pavement moduli, rather than the deflection at any one sensor, are used to determine the temperature effects.

Observed Moisture Variations

Monthly data were collected from the farm-to-market roads, and these include temperature and suction for both base course and subgrade, rainfall from the closest weather stations, and FWD deflection readings. There were problems in obtaining the suction readings at FM1983 and FM2864. The psychrometers in FM1983 gave only base course suction readings for several months, while the moisture sensors in FM2864 did not produce any readings at all. For the rest of the test sections, however, both the psychrometers and moisture sensors gave reasonable readings. For suction readings, a larger negative value corresponds to a drier soil and usually indicates a drier month.

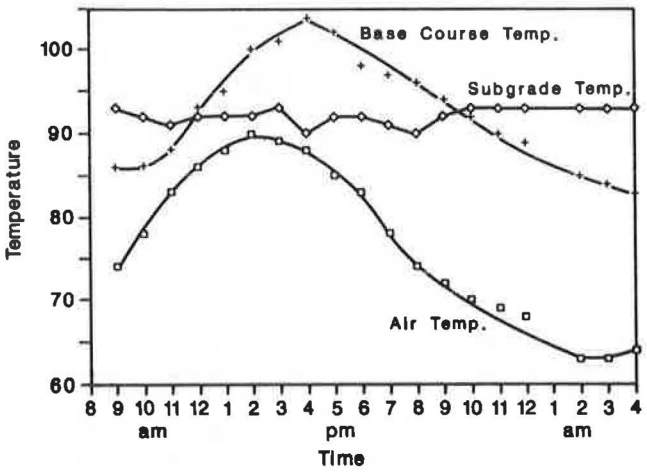

FIGURE 2 Typical variation of temperature within a day (Section 11 TTI Annex).

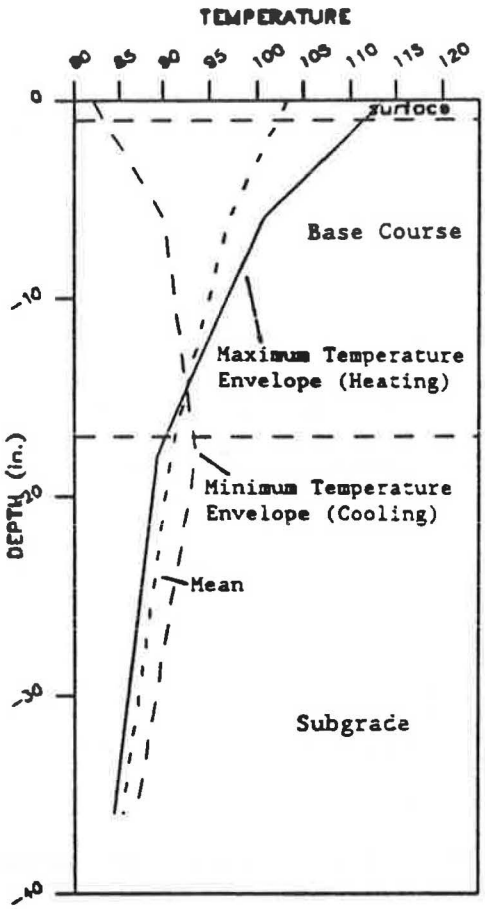

FIGURE 3 Temperature variation with depth.

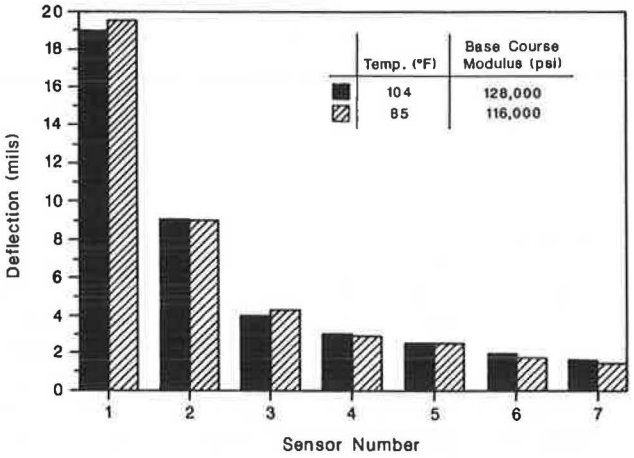

FIGURE 4 Comparison of deflection basins at two different temperatures.

COMPARING PREDICTED AND MEASURED RESULTS

The base course moduli backcalculated by the program are compared with the predicted results from the simplified model. The moduli from LOADRATE are referred to as "measured" moduli because they are calculated from the deflection basins.

Typical results from the September tests are discussed. For that test, the base course temperature varied from 85°F to

104° Fahrenheit in the same day. For the model to predict moduli at different temperatures, a reference modulus at a known temperature is required as one of the inputs. The base course mean temperature for the day, which was 94°F, is selected as the reference temperature. As the system can be expected to come to equilibrium at the mean daily temperature, the reference modulus was chosen to correspond to this temperature. The reference modulus is obtained by calculating the modulus values at 94°F from each modulus at different temperatures and then averaging them. The material properties used are those of limestone, with an elastic modulus of 10×10^6 psi, Poisson's ratio of 0.17, and linear thermal coefficient of 5×10^{-6}°F. Other factors needed are the values of K_1 and K_2 in Equation 2. The constant K_1 can be obtained from LOADRATE and K_2 is 0.33, which was the value used when the program was developed.

The results of the prediction are plotted in Figure 5. The predicted moduli and the measured results showed a similar trend of increase as the temperature increases. The prediction results of other tests were also plotted against the measured results (Figure 6). The points cluster along the 45-degree line, which indicates that the model predictions and the actual values are in agreement. The standard deviation of 5200 psi is made up of random errors due to measurement, systematic errors due to the backcalculation procedure used, and errors due to the effects of suction change that are not accounted for in the predictions.

To isolate the moisture effects on the base course moduli, deflection data with identical base course temperatures were analyzed. The result is presented in Table 3. Because the range of moisture content variations of granular materials is small, the initial volume fraction (C_w) is assumed to be 0.13 for all of the calculations. It can be seen that for all the test sections, the base course moduli in different months but with the same base course temperature varied by less than 7 percent. Thus, the effects on the modulus of the base course due to changes of suction were too small to be measured reliably by the backcalculation method used.

However, when the fluctuation of the suctions is large, as in the case of FM1235, the effects of suctions on the modulus values are apparent. In Figure 7, the month of October is used as the reference, and all the other moduli are predicted from the October modulus. The deflection readings were collected from different months in which there was a wide spread of base course temperatures. The base course modulus for each month was the mean value of the moduli backcalculated from 10 deflection basins taken at the same spot. The solid line in the figure denotes the predicted moduli without considering the suction effects. The dotted line, calculated by considering both temperature and suction variations, yields a much better prediction.

The same method is used to fit the base course moduli of SH7, where the suction readings were obtained by thermal moisture sensors. The result is plotted in Figure 8, which shows a good agreement between the predicted and measured results.

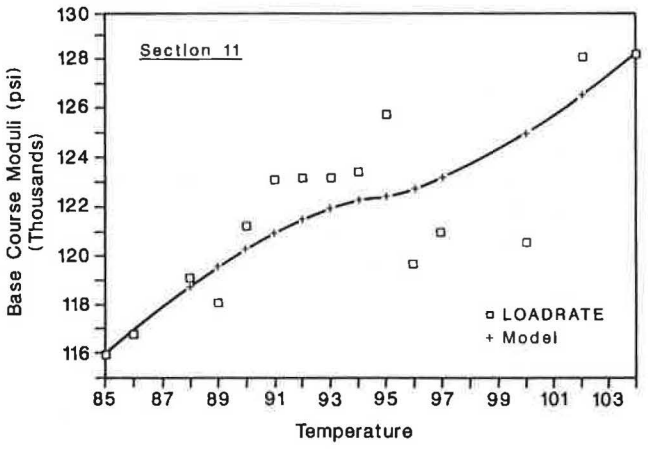

FIGURE 5 Comparison of base course moduli from LOADRATE and the model (Section 11 TTI Annex).

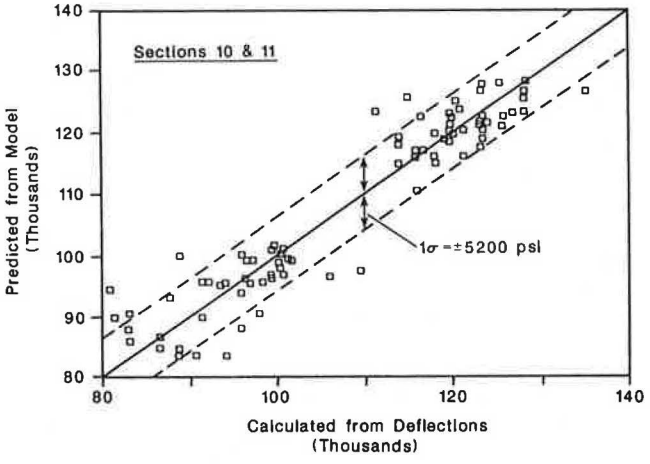

FIGURE 6 Predicted versus backcalculated results (TTI Annex).

TABLE 3 MOISTURE EFFECTS ON BASE COURSE ELASTIC MODULI

Site	E (psi)	K_1	θ (psi)	Δsuction (psi)	$\Delta\theta$ (psi)	Measured change of modulus	Predicted change of modulus
FM1235	110,000	33,700	34.8	-59	+7.7	+7,000	+8,032
FM1983	74,000	21,800	39.1	-15	+2.0	-2,900	+1,261
SH7	110,000	36,000	28.5	-2	+0.25	+5,000	+321
FM491	46,000	15,300	27.8	-10	+1.3	-3,000	+717
FM497	49,000	17,700	21.1	-1	+0.13	-3,400	+101

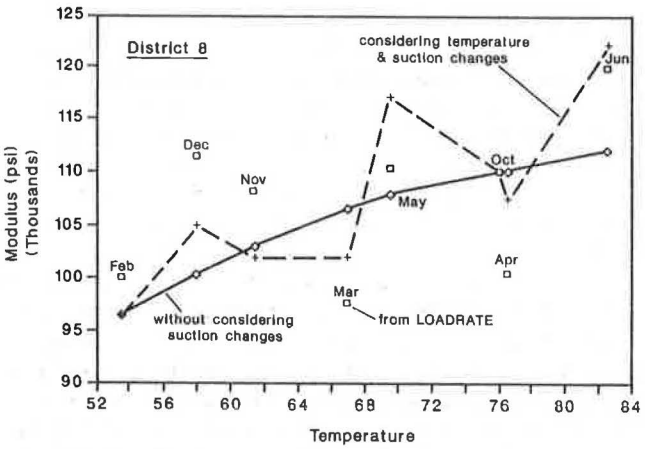

FIGURE 7 Comparison of base course moduli from LOADRATE and the model (FM1235).

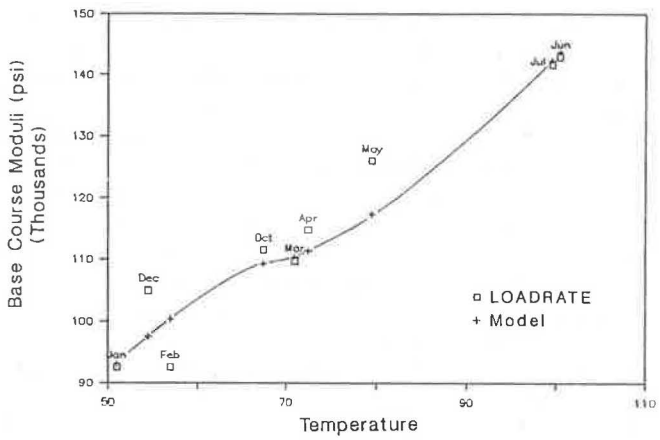

FIGURE 8 Comparison of base course moduli from LOADRATE and the model (SH7).

COMPARATIVE STUDY

In this section, an example is presented to illustrate the application of the thermal and moisture models. The models are used to convert the base course moduli at different temperatures and suctions to those at a reference condition so that a comparative study can be performed.

Consider two low-volume roads, A and B. The base course modulus of road A backcalculated from a deflection basin is 60,000 psi. The temperature and suction of the base course when the deflection data were taken were 50°F and −10 psi, respectively. The base course modulus of road B is found to be 70,000 psi at 110°F, and the suction was −100 psi. The properties of the base course materials are summarized in Table 4. The problem is to find out which pavement is stronger by comparing the base course modulus.

The temperature of 70°F and suction of −10 psi are selected as the reference condition. Assuming that the dry unit weight of the base course for both roads is 120 pcf, the porosity, n_{obs}, can be calculated. The fraction of the total volume representing face-centered cubic arrays, obtained from Equation 10, is used in Equation 12 to obtain the change of bulk stress caused by temperature variation. The change of bulk stress due to suction is obtained from Equation 15. Equation 16 is used to calculate the change of modulus. The equivalent moduli at the reference condition are calculated for both roads. At first glance, it seems that road B is stronger than road A because the base course modulus is higher. However, because the base course temperatures and suctions at the time the moduli were obtained were not the same, a comparative study cannot be performed unless the equivalent moduli are calculated. It turns out that the modulus of road A is slightly higher than that of road B at the same temperature as shown in the table.

CONCLUSION

Theoretical solutions to model temperature and moisture effects on granular materials are presented in this paper. The thermal model requires the properties of the soil particles and the modulus at the reference temperature as the input, whereas suction values are required in the moisture model. The variations of base course moduli due to temperature and suction

TABLE 4 COMPARISON OF BASE COURSE MODULI

Road	Base Course			Base course material	Material properties	Calculated modulus at 70°F and 10 psi suction
	temperature (°F)	modulus (psi)	suction (psi)			
A	50	60,000	-10	Limestone	K_1 = 10,000 psi K2 = .45 μ = .17 α = 8x10^{-6} /°F E = 8x10^{-6} psi	61,400
B	110	70,000	-100	Crushed stone	K_1 = 15,000 psi K2 = .40 μ = .21 α = 6x10^{-6} /°F E = 10x10^{-6} psi	59,400

NOTE: The values of K_1 and K_2 are from Rada and Witczak (27).

changes predicted by the models agree well with the back-calculated moduli. Instead of using empirical temperature adjustment factors, the models can be used for comparative studies as illustrated in the example. Because the solutions are developed theoretically, the models are applicable to other problems in which the effects of temperature and moisture on granular soils are of concern.

The following conclusions can be drawn from this study:

1. The granular base course moduli of low-volume roads showed a trend of increase as temperature rises and suction becomes more negative, which can be explained as the result of an increase of the contact pressure between particles due to thermal expansion and suction changes.
2. The theoretical models presented in this paper predict very well the changes of the moduli of granular base course layer due to the changes of temperature and moisture.
3. The models can be applied to adjust the base course moduli of low-volume roads for temperature and moisture effects. They can also be used for comparative study of pavement conditions, as illustrated in the example. Furthermore, the moisture model can be used to predict pavement conditions at a certain time of year so the application of seasonal load zoning can be determined as early as possible.

ACKNOWLEDGMENT

This paper presents partial results of a three-year study on the effects of overweight vehicles on farm-to-market roads, sponsored by the Texas State Department of Highways and Public Transportation. The authors are extremely grateful for this support.

REFERENCES

1. R. F. Bibbens, C. A. Bell, and R. G. Hicks. Effect of Season of Year on Pavement Response. In *Transportation Research Record 993*, TRB, National Research Council, Washington, D.C., 1984, pp. 1–15.
2. M. S. Hoffman and M. R. Thompson. Comparative Study of Selected Nondestructive Testing Devices. In *Transportation Research Record 852*, TRB, National Research Council, Washington, D.C., 1982, pp. 32–41.
3. O. Tholen, J. Sharma, and R. L. Terrel. Comparison of Falling Weight Deflectometer with Other Deflection Testings Devices. In *Transportation Research Record 1007*, TRB, National Research Council, Washington, D.C., 1985, pp. 20–26.
4. K. M. Chua. *Evaluation of Moduli Backcalculation Programs for Low-Volume Roads*. First International Symposium on Nondestructive Testing of Pavements and Backcalculation of Moduli, ASTM, Baltimore, Md., June 1988.
5. K. M. Chua and R. L. Lytton. Load Rating of Light Pavements Structure. In *Transportation Research Record 1043*, TRB, National Research Council, Washington, D.C., Jan. 1984.
6. M. S. Kersten. Survey of Subgrade Moisture Conditions. *HRB Proc.*, Vol. 24, 1944.
7. G. D. Aitchison. *Moisture Equilibria and Moisture Changes in Soils Beneath Covered Areas*. A Symposium in Print, Butterworth, Australia, 1965, pp. 9.
8. H. F. Southgate and R. C. Deen. Temperature Distribution Within Asphalt Pavements and Its Relationship to Pavement Deflection. In *Highway Research Record 291*, HRB, National Research Council, Washington, D.C., 1969, pp. 116–128.
9. H. N. Schenck Jr. *Fortran Methods in Heat Flow*. Ronald Press, New York, 1963.
10. A. L. Straub, H. N. Schenck, Jr., and F. E. Przybycien. Bituminous Pavement Temperature Related to Climate. In *Highway Research Record 256*, HRB, National Research Council, Washington, D.C., 1968, pp. 53–77.
11. J. B. Cox. Use of the Benkelman Beam in Design and Construction of Highways over Soft Clays. In *Transportation Research Record 572*, TRB, National Research Council, Washington, D.C., 1976, pp. 71–84.
12. R. I. Kingham and T. C. Reseigh. A Field Experiment of Asphalt-Treated Bases in Colorado. *Proc., Second International Conference on Structural Design of Asphalt Pavement*, University of Michigan, Ann Arbor, pp. 909–930.
13. G. Y. Sebastyan. The Effect of Temperature on Deflection and Rebound of Flexible Pavements Subjected to the Standard CGRA Benkelman Beam Test. *Proc., Canadian Good Roads Association*, 1961, pp. 143–161.
14. *Asphalt Overlays and Pavement Rehabilitation*. MS-17 Asphalt Institute. Riverdale, Md., Sept. 1977.
15. G. Cumberledge, G. L. Hoffman, A. C. Bhajandas, and R. J. Cominsky. Moisture Variation in Highway Subgrades and the Associated Change in Surface Deflections. In *Transportation Research Record 497*, TRB, National Research Council, Washington, D.C., 1974, pp. 40–49.
16. S. S. Bandyopadhyay. Flexible Pavement Evaluation and Design. *Transportation Engineering Journal, ASCE*, Vol. 108, No. TE6, Nov. 1982, pp. 523–539.
17. M. R. Thompson, and Q. L. Robnett. Resilient Properties of Subgrade Soils. *Transportation Engineering Journal, ASCE*, Vol. 105, No. TE1, Jan. 1979, pp. 71–89.
18. S. P. Timoshenko and J. N. Goodier. *Theory of Elasticity*. McGraw-Hill Book Co., New York, 1951, pp. 403–415.
19. R. D. Mindlin. Compliance of Elastic Bodies in Contact. *Journal of Applied Mechanics*, Vol. 16, 1949, pp. 259–268.
20. R. D. Mindlin and H. Deresiewicz. Elastic Spheres in Contact under Varying Oblique Forces. *Journal of Applied Mechanics*, Vol. 20, 1953, pp. 327–344.
21. J. C. Armstrong and W. A. Dunlap. The Use of Particulate Mechanics in the Simulation of Stress-Strain Characteristics of Granular Materials. Research Report 99-1. Texas Transportation Institute, Texas A&M Univ., College Station, Aug. 1966.
22. H. Y. Ko and R. F. Scott. Deformation of Sand in Hydrostatic Compression. *Journal SMFD, ASCE*, 93, SM3, 1967, pp. 137–156.
23. W. O. Smith, P. D. Foote, and P. F. Busang. Packing of Homogeneous Spheres. *Physical Review*, Vol. 34, Nov. 1, 1929, pp. 1271–1274.
24. R. N. Yong and C. W. Wong. Experimental Studies of Elastic Deformation of Sand. Proc., 3rd Southeast Asian Conference on Soil Engineering, Asian Institute of Technology, Bangkok, Thailand, 1972, pp. 323–327.
25. T. F. Willis and M. E. De Reus. Thermal Volume Change and Elasticity of Aggregate and Their Effect on Concrete. *ASTM Proc.*, Vol. 39, 1939, pp. 919–929.
26. M. Lamborn. *A Micromechanical Approach to Modeling Partly Saturated Soils*. Master's thesis. Texas A&M University, College Station, Dec. 1986.
27. G. Rada and M. W. Witczak. Comprehensive Evaluation of Laboratory Resilient Moduli Results for Granular Material. In *Transportation Research Record 810*, TRB, National Research Council, Washington, D.C., 1981, pp. 23–33.

Publication of this paper sponsored by Committee on Environmental Factors Except Frost.

Rainfall Estimation for Pavement Analysis and Design

HUI SHANG LIANG AND ROBERT L. LYTTON

An integrated model that is being developed under contract to the FHWA combines three different completed environmental effects models: the CMS Model, CRREL Model, and the TAMU ID Model. It will be a comprehensive model that predicts the effects of air temperature, sunshine percentage, wind speed, rainfall, frost, and thawing actions on the performance of pavement. In the course of development, stochastic processes and random methods are employed to analyze past climatological data, and to estimate and predict the effects of the environment on the performance of pavement with specified confidence levels. This paper describes a computerized method that has been developed to generate simulated rainfall patterns for use in pavement analysis and design. The method is both practical and useful because it meets several important criteria. It uses data that are readily available; it predicts realistic rainfall patterns; it permits analysts to select how severe a condition they wish to represent; and it is simple to use. The paper presents the method used to simulate the rainfall patterns; shows how the United States is divided into nine climatic regions and which cities have been selected as representative of those regions; and gives four examples of both the required input data and the resulting simulated rainfall patterns for a 95 percent confidence level. The model also includes the effect of freezing and thawing temperatures on the amount of rainfall that is available to infiltrate the pavement, and this is illustrated in one of the examples.

It is well known that pavement damage is caused mainly by traffic loads, unsuitable materials, and environment. The effects of the first two factors on the performance of pavements can be estimated for design purposes by empirical or mechanistic methods (*1*). However, an estimation of the effects of environmental factors, especially of the effects of rainfall on the performance of pavements, is not adequate.

At present, only the worst conditions are employed in existing design methods. For example, current test procedures still recommend that the modulus of subgrade reaction for rigid pavement design be determined under saturated conditions (*2*), even though the new AASHTO Design Guide (*3*) recommends the testing of materials for actual site conditions, and not for the worst conditions.

An integrated model that is being developed under contract to the FHWA combines three different completed environmental effects models: the CMS Model (*4*), CRREL Model (*5*), and the TAMU ID Model (*6*). It will be a comprehensive model that predicts the effects of air, temperature, sunshine percentage, wind speed, rainfall, frost, and thawing actions on the performance of pavement. In the course of the development, stochastic processes and random methods are employed to analyze past climatological data, and to estimate and predict the effects of the environment on the performance of pavement with specified confidence levels.

A computerized method has been developed to generate simulated rainfall patterns for use in pavement analysis and design. The method is both practical and useful because it meets several important criteria. It uses data that are readily available; it predicts realistic rainfall patterns; it permits analysts to select how severe a condition they wish to represent; and it is simple to use.

The paper presents the method used to simulate the rainfall patterns; shows how the United States is divided into nine climatic regions and which cities have been selected as representative of those regions; and gives four examples of both the required input data and the resulting simulated rainfall patterns for a 95 percent confidence level. The model also includes the effect of freezing and thawing temperatures on the amount of rainfall that is available to infiltrate the pavement, and this is illustrated in one of the examples.

RAINFALL GENERATOR

It is impossible to generate truly random sequences of wet days and amounts of rainfall for estimating future rainfall effects by using a deterministic algorithm. Nevertheless, it is possible to produce by deterministic means sequences of numbers that, to a degree acceptable for predictive purposes, possess the attributes of randomness.

Statistical rainfall data are available from the National Climatic Data Center (*7*). In estimating rainfall amounts and sequences, these statistical data are typically used together with Monte Carlo methods and the simulation of random processes to produce samples automatically from the prescribed statistical distributions of rainfall. This paper describes the use of the uniform type of pseudorandom number and multiplicative congruential theories (*8*) to predict these rainfall patterns.

The form of the generator is

$$X_n = CX_{n-1} (\text{mod } M) \tag{1}$$

which means "X_n is congruent to CX_{n-1} modulo M." That is,

$$CX_{n-1} = Q_n M + X_n \tag{2}$$

where Q_n equals a largest integer not exceeding CX_{n-1}/M.

Texas Transportation Institute, Texas A&M University, College Station, Tex. 77843.

The congruential relation (1) may be rewritten as a difference equation as follows:

$$X_n = X_0 C^n \pmod{M} \tag{3}$$

where

X_0 = seed,
M = modulus, usually $M = 2^b$,
C = a positive odd integer less than M excluding 1, and
b = the number of bits available in a computer word.

The development of the rainfall generator model includes the following considerations:

1. *Period of the Sequence of Wet Days*. The period of the sequence of wet days is the smallest integer d such that $X_{n+d} \equiv X_n \pmod{M}$ is in terms of the period of the sequence. The maximum possible least period 2^{b-2} is obtained when X_0 and C are selected from the set of least residues prime to 2^b and C is of form $8N + 3$ and $8N + 5$, where N is the number of items. Special care is taken to avoid a repetition of the dates on which rain falls for any particular month.
2. *Dates on Which Rain Falls*. Under some conditions, the same wet dates will appear when the same number of wet days occurs in different months. Certain measures are taken to prevent this kind of situation from occurring in the simulation.
3. *Type of Rainfall*. Rainfall is usually divided into two types: convective and frontal. Convective rainfall generally appears in a thunderstorm in the warm season and occurs sporadically. The precipitation in a frontal system is steady rainfall for several consecutive days because of a stream of warm moist air that originates in the warm sector, just ahead of a cold front.

The number of thunderstorms that occur in a month is employed as the criterion to distinguish convective rainfall from frontal rainfall. For the different climatic regions that were defined for highways, a different number of thunderstorms are used. Also, the number of days during which bunched (convective) or uniform (frontal) rain falls are distinguished for each month in a given region.

4. *Freeze-Thaw Period*. In accordance with actual highway conditions, it is assumed that the infiltration of rainfall will stop during the cold season when the average monthly air temperature is less than 30°F. The equivalent amount of moisture of the snow that falls during the cold season will infiltrate into the pavement during the first half month of the thawing period when the average monthly air temperature rises from below 30°F to above 30°F.

CONFIDENCE LEVELS

The most recent statistical rainfall data that are available for 30-yr periods are from 1957–1986 (*7*). Normal distributions of rainfall are assumed to apply for any particular month, and average values and standard deviations are determined from the historical data. In considering a severe case of rainfall, we are interested only in estimating the maximum rainfall and, because of this, the one-tailed confidence limit is employed.

$$P\left[\mu > \bar{x} + Z_\alpha \frac{s}{(N)^{1/2}}\right] = 1 - \alpha \tag{4}$$

Therefore

$$\mu = \bar{x} + \frac{s}{(N)^{1/2}} Z_\alpha \tag{5}$$

where

$\bar{x}$ = the mean monthly rainfall,
μ = the maximum rainfall to be considered in a particular month,
Z_α = the normal variate corresponding to a confidence level of $(1 - \alpha)$,
s = the standard deviation of the monthly rainfall, and
N = the number of years represented in the sample.

For design purposes, a computer program has been written so that the user selects a specific confidence level based on the pavement type, the degree of importance of the pavement, and the requirements of the user. In general, a confidence level of 0.95 is employed automatically as a default when the input confidence level is left blank.

SAMPLES

For highway technology, the climatic zones are defined as shown on Table 1 (*9*). Four of nine regions are chosen for rainfall random testing. The representative cities for each region are:

New York City	I-A
San Francisco, California	I-C
Fargo, North Dakota	II-A
Dallas, Texas	II-C

These cities are located across the United States and represent distinctively different climatic regions (Figure 1). The average values and standard deviations of rainfall for the four cities are shown in Table 2 (*7*). A confidence level of 0.95 is used in generating the simulated rainfall, the results of which are shown in Tables 3–6.

In Fargo, North Dakota, the rainfall simulation program indicates that the pavement will be frozen from January through March and again from November through December. The equivalent snow melt is 0.27 in. per day for two weeks during the thawing period.

In Dallas, Texas, no periods of snow on the ground were simulated, and peak monthly rainfall occurs in April and May. In May, a total of 5.76 in. of rain fell, compared with an average of 4.76 in. for that month, the difference reflecting the higher level of confidence specified.

In San Francisco, there is a single wet season from November through March, with no periods during which frozen conditions prevent infiltration into pavement.

In New York, New York, once more, no frozen period is found in this simulation. The number of days of rainfall each month are fairly uniform throughout the year.

The simulated results appear to be reasonable and produce realistic patterns of wet days and total rainfall within a month. The program has been written so that if actual historical rainfall and snowfall data are unavailable, the designer can estimate and analyze the local rainfall information by inputting the number of the climatic region and the confidence level required. Typical statistical data for each of the six larger

TABLE 1 CLIMATIC ZONES ARE DEFINED FOR HIGHWAY TECHNOLOGY

Moisture Region		Temperature Region		
		A	B	C
Potential of Moisture Being Present in Pavement Structure During Typical Year		Severe Winters High Potential for Frost Pentration to Appreciable Depths Into Subgrade	Freeze-Thaw Cycles in Pavement Surface and Base Occasional Moderate Freezing of Subgrade	Low Temperature Not a Problem High Temperature Stability Should Considered
I	High	I-A	I-B	I-C
II	Moderate Seasonally Variable	II-A	II-B	II-C
III	Low	III-A	III-B	III-C

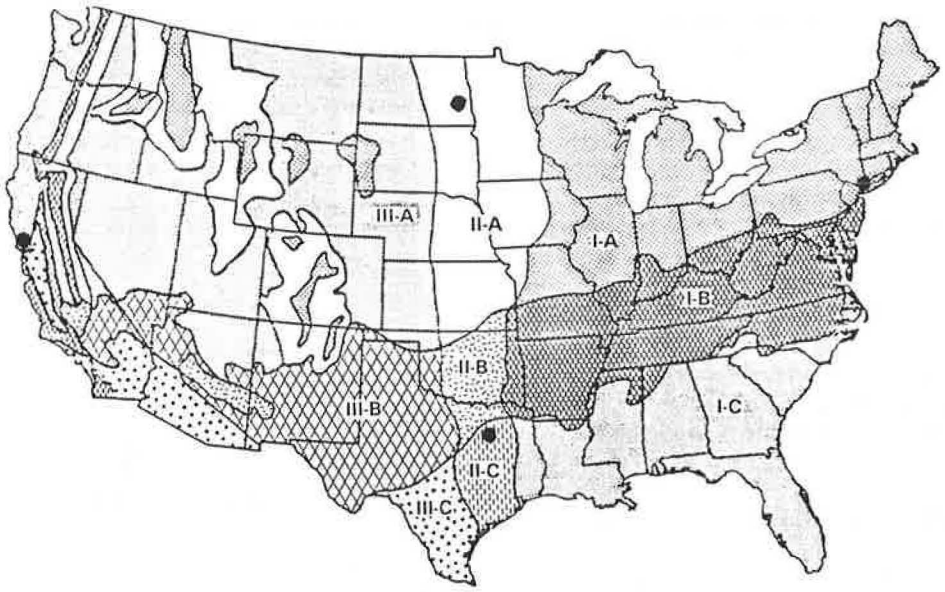

FIGURE 1 Environmental regions and the locations of rainfall samples.

TABLE 2 RAINFALL DATA BASE FOR FOUR CITIES (1957–1986)

	Jan.	Feb.	March	April	May	June	July	Aug.	Sept.	Oct.	Nov.	Dec.
New York, NY												
Ave. Amount (in)	3.07	3.26	3.60	3.85	3.40	3.39	3.65	3.45	3.46	2.76	3.61	3.68
Stndev.	1.89	1.53	1.65	2.09	1.75	1.95	2.34	1.94	2.15	1.46	2.22	1.82
Ave. Wet Days	10	10	11	11	11	10	11	9	8	8	10	11
Stndev.	3.12	2.56	3.40	1.53	4.08	3.11	9.36	3.11	3.18	2.09	3.77	2.56
No. of Thunderstorms	0	0	1	2	3	3	4	5	2	1	0	0
Stndev.	0.32	0.45	1.26	1.19	1.20	1.98	2.16	1.36	1.27	0.98	0.74	0.49
San Francisco, CA												
Ave. Amount (in)	4.53	3.67	3.15	1.57	0.28	0.10	0.03	0.05	0.27	1.23	2.85	3.06
Stndev.	2.82	2.83	2.35	1.69	0.69	0.20	0.08	0.13	0.47	1.66	2.33	1.62
Ave. Wet Days	10	10	11	6	2	1	1	1	1	4	8	9
Stndev.	4.03	4.02	4.04	4.82	2.87	0.59	0.26	1.14	1.76	2.43	4.59	5.03
No. of Thunderstorms	1	1	0	0	0	0	0	0	0	0	0	0
Stndev.	0.37	0.87	0.89	0.59	0.42	0.19	0.26	0.53	0.67	0.49	0.59	0.42
Fargo, ND												
Ave. Amount (in)	0.56	0.41	0.92	1.98	2.37	3.08	3.12	2.31	1.83	1.78	0.78	0.61
Stndev.	0.44	0.37	0.62	1.36	1.57	1.80	1.76	1.54	1.35	1.68	0.85	0.39
Ave. Wet Days	8	7	7	21	10	11	10	11	8	7	5	8
Stndev.	3.85	2.44	3.61	2.41	2.34	2.05	2.77	13.44	3.54	3.12	2.73	2.35
No. of Thunderstorms	0	0	0	1	4	7	9	7	3	1	0	0
Stundev.	0.00	0.26	0.72	1.60	1.76	2.61	2.02	1.82	2.07	1.11	0.26	0.26
Dallas, TX												
Ave. Amount (in)	1.67	2.11	3.07	4.25	4.76	3.00	2.14	2.16	3.54	4.20	2.41	2.26
Studev.	1.22	1.29	2.00	3.50	3.34	2.15	2.05	1.67	2.53	3.35	1.52	2.13
Ave. Wet Days	6	7	8	8	9	6	5	5	7	6	6	6
Studev.	4.14	2.24	2.64	3.20	3.28	3.36	2.68	2.12	2.80	3.86	3.26	3.13
No. of Thunderstorms	1	2	4	6	7	6	4	4	3	3	2	1
Studev.	0.83	0.96	1.93	2.05	2.70	2.37	2.65	2.25	1.68	1.17	1.47	0.74

TABLE 3 RAINFALL ESTIMATION FOR FARGO, N.D. (1957–1986), $1 - \alpha = 0.95$, II-A

January	1	8	11	12	13	18	22	30	
	0.00	0.00	0.00	0.00	0.00	0.00	0.00	0.00	
February	1	2	5	8	13	17	18		
	0.00	0.00	0.00	0.00	0.00	0.00	0.00		
March	1	2	4	5	10	13	15		
	0.00	0.00	0.00	0.00	0.00	0.00	0.00		
April	1	2	3	4	5	6	7	8	9
	0.67	0.28	0.27	0.27	0.27	0.27	0.27	0.27	0.27
	10	11	12	13	14	15	18	21	23
	0.57	0.76	0.27	0.27	0.27	0.27	0.46	0.20	0.36
	27	28							
	0.16	0.01							
May	8	10	14	16	18	22	23	27	
	0.23	0.20	0.43	0.34	0.40	0.26	0.15	0.40	
	28	30							
	0.12	0.31							
June	8	10	13	16	17	18	19	23	26
	0.14	0.47	0.18	0.30	0.47	0.40	0.51	0.23	0.28
	27	29							
	0.33	0.31							
July	1	2	3	4	8	12	14	25	
	0.74	0.08	0.12	0.02	0.85	0.42	0.23	0.36	
	26	29							
	0.06	0.76							
August	8	10	14	16	18	20	22	23	27
	0.28	0.11	0.35	0.13	0.23	0.36	0.30	0.38	0.18
	28	30							
	0.21	0.25							
September	2	7	8	12	18	19	21	22	
	0.04	0.44	0.39	0.25	0.43	0.36	0.16	0.17	
October	2	4	8	9	26	28	29		
	0.08	0.62	0.63	0.57	0.16	0.19	0.04		
November	1	12	13	14	19				
	0.00	0.00	0.00	0.00	0.00				
December	2	6	9	15	23	26	27	28	
	0.00	0.00	0.00	0.00	0.00	0.00	0.00	0.00	

TABLE 4 RAINFALL ESTIMATION FOR DALLAS, TEX. (1957–1986), $1 - \alpha = 0.95$, II-C

January	14	16	17	22	25	28			
	0.27	0.36	0.24	0.27	0.47	0.43			
February	1	4	8	9	13	23	25		
	0.23	0.11	0.71	0.27	0.77	0.01	0.39		
March	1	3	4	6	7	18	23	28	
	0.03	0.73	0.27	0.17	1.15	0.25	0.11	0.97	
April	2	7	8	12	18	19	21	22	
	0.10	1.04	0.92	0.58	1.02	0.86	0.38	0.40	
May	1	2	10	12	18	22	24	28	29
	0.96	0.01	0.73	1.17	1.11	0.47	0.88	0.40	0.03
June	4	9	10	13	21	23			
	0.43	0.45	0.18	1.04	0.60	0.95			
July	3	8	22	24	28				
	0.79	0.26	0.09	0.71	0.91				
August	5	12	13	14	25				
	0.53	0.18	0.45	0.54	0.97				
September	2	3	4	6	16	23	26		
	0.32	0.84	1.42	0.14	0.11	0.24	1.22		
October	1	4	19	25	30	31			
	0.17	1.44	1.19	0.06	1.46	0.89			
November	9	14	15	16	19	27			
	0.78	0.53	0.41	0.26	0.46	0.42			
December	3	5	8	12	18	22			
	0.95	0.35	0.20	0.77	0.12	0.51			

climatic regions have been developed by averaging the data from two cities within each region. The remaining three regions (i.e., II-B, II-C, and III-C) are represented by a single city, as shown in Table 7 and Figure 2. These data will be used in simulating data that are not available within a given region.

The program is intended to be used in pavement design to provide the designer with a realistic set of weather conditions that are consistent with historical records and that are at a desired level of severity as specified by an input level of confidence.

These weather data then provide the moisture, temperature, solar radiation, cloud cover, and wind speed boundary conditions that are needed by the comprehensive computer program to produce for the designer temperature and moisture data with depth and corresponding layer moduli of a specified pavement as they vary through the seasons. The designer may then determine by further calculations whether the pavement will be able to withstand the expected traffic. The entire process depends on a realistic simulation of the weather conditions; the simulation of rainfall has proven to be the most difficult. This paper reports the development of a successful and simple model of rainfall patterns that is sufficiently realistic for pavement design purposes.

CONCLUSION

The amount of rainfall and the dates when it falls are important for the analysis and design of pavements, catchment, and other engineering structures. The rainfall model described here produces simulated sequences of wet days based on weather data from the past several decades.The model is concerned not only with the type of rainfall, to match the convective or frontal precipitation each month, but also with the snowfall-thawing period in considering the infiltration and drainage of moisture into the pavement. The example problems show that this model is fairly realistic and close to in situ highway conditions. It is recommended for use by pavement designers.

ACKNOWLEDGMENT

The results reported in this paper were obtained as part of an ongoing research project on verification and extension of previously developed pavement analysis and drainage models sponsored by the Federal Highway Administration. The authors also acknowledge the contribution of John F. Griffiths in discussion and analysis of weather data.

TABLE 5 RAINFALL ESTIMATION FOR SAN FRANCISCO, CALIF. (1957–1986), $1 - \alpha = 0.95$, I-C

January	8	10	14	16	18	22	23	27	
	0.44	0.38	0.81	0.64	0.76	0.48	0.28	0.75	
	28	30							
	0.23	0.59							
February	1	2	3	4	7	11	13	22	
	0.92	0.10	0.15	0.03	1.06	0.52	0.29	0.45	
	23	26							
	0.08	0.94							
March	1	10	12	15	19	21	23	24	
	0.39	0.44	0.28	0.19	0.46	0.22	0.35	0.55	
	25	28	29						
	0.54	0.01	0.43						
April	5	9	10	21	23	29			
	0.19	0.21	0.63	0.49	0.11	0.45			
May	18	24							
	0.29	0.21							
June	27								
	0.16								
July	4								
	0.06								
August	10								
	0.09								
September	16								
	0.41								
October	4	17	29	30					
	0.36	0.63	0.65	0.09					
November	1	8	11	12	13	17	21	29	
	0.04	0.67	0.94	0.37	0.40	0.55	0.34	0.25	
December	3	5	12	15	16	17	22	25	28
	0.71	0.30	0.37	0.54	0.42	0.39	0.08	0.63	0.13

TABLE 6 RAINFALL ESTIMATION FOR NEW YORK CITY (1957–1986), $1 - \alpha = 0.95$, I-A

January	1	2	12	14	17	21	24	25	
	0.52	0.05	0.64	0.01	0.44	0.29	0.56	0.25	
	26	30							
	0.35	0.54							
February	2	3	6	9	10	19	21	22	
	0.08	0.70	0.49	0.56	0.54	0.06	0.22	0.65	
	25	27							
	0.27	0.15							
March	8	10	14	16	17	18	20	23	
	0.16	0.53	0.20	0.34	0.54	0.45	0.57	0.27	
	27	28	30						
	0.31	0.38	0.35						
April	8	10	13	16	17	19	21	23	
	0.45	0.18	0.57	0.22	0.37	0.58	0.49	0.62	
	26	27	29						
	0.29	0.34	0.41						
May	1	3	4	8	11	13	14	15	
	0.11	0.64	0.41	0.10	0.23	0.04	0.53	0.46	
	17	20	21						
	0.35	0.40	0.65						
June	4	5	9	10	11	22	26	27	
	0.08	0.51	0.21	0.20	0.69	0.24	0.12	0.64	
	29	30							
	0.60	0.68							
July	2	6	8	9	11	17	23	27	
	0.38	0.04	0.69	0.61	0.64	0.13	0.25	0.70	
	28	30	31						
	0.20	0.21	0.51						
August	1	2	10	12	18	22	24	28	29
	0.67	0.01	0.51	0.82	0.78	0.33	0.62	0.28	0.02
September	1	3	4	6	7	17	23	27	
	0.03	0.81	0.30	0.19	1.28	0.28	1.12	1.08	
October	2	7	8	12	18	20	22	23	
	0.06	0.63	0.56	0.35	0.61	0.52	0.23	0.24	
November	1	3	6	9	11	22	23	27	
	0.62	0.60	0.07	0.24	0.72	0.29	0.17	0.75	
	28	30							
	0.02	0.80							
December	1	2	10	12	15	18	19	23	
	0.35	0.23	0.58	0.28	0.44	0.69	0.67	0.01	
	24	28	29						
	0.53	0.42	0.03						

TABLE 7 SELECTED CITIES FOR EACH ENVIRONMENTAL REGION

Moisture Region	Temperature Region		
	A	B	C
I	New York, NY Chicago, IL	Washington, D.C. Cincinnati, OH	San Francisco, CA Atlanta, GA
II	Fargo, ND Lincoln, NE	Oklahoma City, OK	Dallas, TX
III	Reno, NV Billings, MT	Las Vegas, NV San Angelo, TX	San Antonio, TX

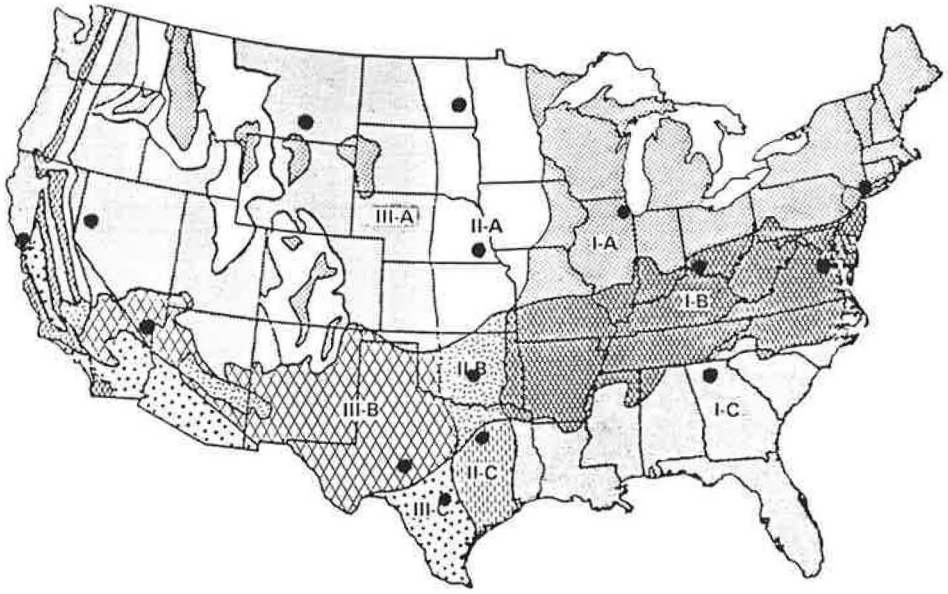

FIGURE 2 Locations of selected cities for each environmental region.

REFERENCES

1. *Interim Guide for Design of Pavement Structures*, rev. ed. AASHTO, Washington, D.C., 1981, chap. III.
2. E. J. Yoder and M. W. Witzack. *Principles of Pavement Design*, 2nd ed. John Wiley and Sons, New York, 1975.
3. *Guide for Design of Pavement Structures*. AASHTO, Washington, D.C., 1986.
4. B. J. Dempsey, W. A. Herlache, and A. J. Patal. *The Climatic-Materials-Structural Pavement Analysis Program*. University of Illinois, Urbana, 1985.
5. G. L. Guyman, R. L. Berg, T. C. Johnson, and T. V. Hromadka. *Mathematical Model of Frost Heave and Thaw Settlement in Pavements*. U.S. Army Engineer Cold Regions Research Lab (CRREL), Hanover, N.H. 1986.
6. S. J. Liu and R. L. Lytton. *Environmental Effects on Pavements—Drainage Manual*. Texas Transportation Institute, College Station, 1985.
7. *Local Climatological Data*. Weather Bureau, U.S. Department of Commerce.
8. C. Brian. *Techniques in Operational Research*, Vol. 2: *Models, Search and Randomization*. John Wiley & Sons, New York, 1981.
9. S. H. Carpenter, M. I. Darter, and B. J. Dempsey. *A Pavement Moisture Accelerated Distress (MAD) Identification System*. Report FHWA/RD-81/680, Final Report Vol. 2. FHWA, U.S. Department of Transportation, Sept. 1981.

Publication of this paper sponsored by Committee on Environmental Factors Except Frost.